Evaluation of the Regenerative Potential of Osteoarthritic Chondrocytes for Cartilage Tissue Engineering

by

Ciara Davis

A dissertation submitted in partial fulfillment
of the requirements for the degree of
Doctor of Philosophy
(Biomedical Engineering)
in the University of Michigan
2023

Doctoral Committee:

Professor Rhima Coleman, Chair
Professor Susan Brooks
Clinical Associate Professor John Grant
Professor Megan Killian

Ciara Davis

ciaradav@umich.edu

ORCID iD: 0000-0003-2321-5007

Dedication

To my family: Deena, Harry and Trey Davis who have been supporting me since I began this journey in 2017.

Acknowledgements

I would first like to acknowledge my thesis advisor Dr. Rhima Coleman. I am beyond grateful for you taking a chance on me in 2019. Thank you for believing in me and being a great mentor.

I would also like to think my thesis committee members, Dr. Megan Killian, Dr. Susan Brooks and Dr. John Grant for their time, dedication and insight towards this thesis project.

Thank you to all the members of my lab. Dr. Tiana Wong, Dr. Gurcharan Kaur and Dr. Yue Qin, Dr. Ryan Rosario and Sunny Karnan this would not have been possible without your support and teamwork throughout the years.

I also want to thank Dr. Ovijit Chaudhuri from Stanford for providing me with the first biomedical engineering research experience and encouragement. Carl Wales, my mentor at NASA Goddard who has been an incredible mentor and introduced me to satellites.

Finally, I would like to thank the Meyerhoff Scholars program at the University of Maryland Baltimore country for guidance during my undergraduate years and the continues support in my PhD program.

Table of Contents

List of Tables

List of Figures

List of Appendices

Abstract

Focal defects in articular cartilage and other traumatic joint injuries trigger destructive pathways including inflammation, oxidative stress and increased expression of catabolic enzymes that often lead to post-traumatic osteoarthritis (PTOA). These pathways promote phenotypic changes characteristic of chondrocyte hypertrophy and senescence[1]. Senescence and hypertrophy are major phenotypic shifts seen in aging and OA and share similar markers such as expression of metalloproteinases (MMPs) that drive matrix degradation as well as an altered response growth factors that have been shown to be anabolic in healthy chondrocytes[1,2,3,4]. The term “chondrosenescence” was recently coined to describe this phenotype which is driven by inflammation, joint trauma, aging and other mechanical and chemical stimuli[5]. Accordingly, using aged or OA chondrocytes, which exhibit features of chondrosenescence, in clinically approved treatments for focal defect repair will yield subpar production of structural macromolecules and, therefore, subpar cartilage regeneration. Understanding the process of chondrosenescence will improve cartilage tissue engineered from these cells.

This thesis focuses on the role of RUNX2 (Runt-related transcription factor 2), a transcription factor (TF) that drives chondrocyte hypertrophy during endochondral ossification. Specifically, we suppress RUNX2 in OA cells and investigate its role in the development of the chondrosenescent phenotype.

We investigated the role of RUNX2 in two ways. First we defined the differences between young, healthy chondrocytes and aged/OA chondrocytes when regenerated *in vitro*. We found that OA cells have regeneration potential and produce cartilage matrix, limited by the upregulation of RUNX2 through multiple pathways. Next, we investigate the matrix production of OA cells when RUNX2 is suppressed using our previously developed cell regulation gene circuit. We found that high levels of RUNX2 suppression increases chondrogenic gene expression and increases cartilage matrix production. Finally, we developed an *in vitro* model of chondrosenescence to investigate that lead to the development of this phenotype. We show that our model leads to chondrosenescence and that multiple pathways are responsible for this development.

Overall, this dissertation explores methodologies to enhance cartilage matrix production in aged/OA chondrocytes including suppressing RUNX2 and investigating other potential targets for suppression.

Chapter 1 Introduction

1.1 Background

Articular (hyaline) cartilage is the connective tissue that covers the end of long bones[1]. It provides a smooth, low friction surface and redistributes mechanical loads during joint movement[2–5]. The cartilage extra cellular matrix (ECM) is responsible for the unique mechanical properties of this tissue. Cartilage ECM is deposited by chondrocytes and is composed of type II collagen and aggrecan as shown in Figure 1-1. Collagen type II forms a dense fibril network that provides tensile strength to the tissue that prevents cartilage swelling and tensile loads that arise during daily activity[6]. Aggrecan contains sulfated glycosaminoglycan (sGAG) side chains. These side chains are highly negatively charged and attract water molecules into cartilage, which provides compressive strength to the tissue[7,8]. The mechanical properties of the ECM protect healthy chondrocytes from mechanical stress[7,8].

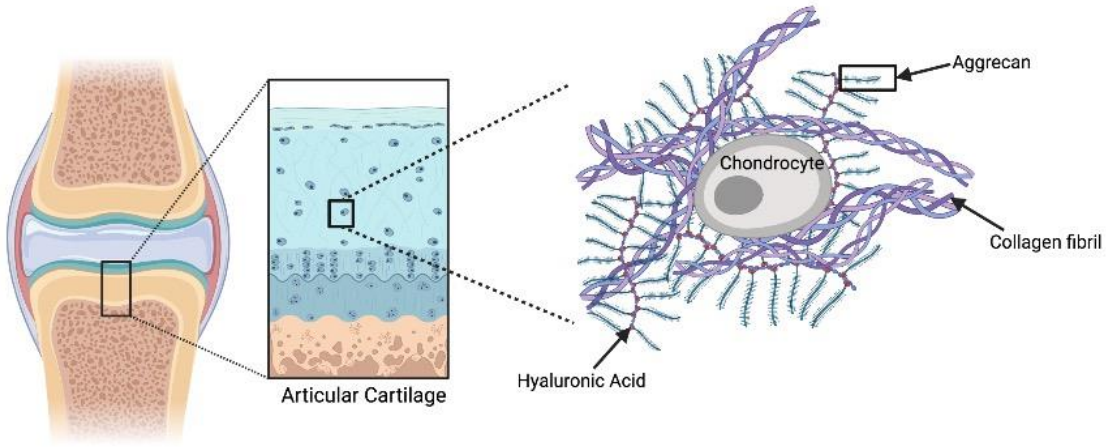

Figure 1-1: Schematic of articular cartilage matrix. Articular cartilage is a connective tissue (left) and at the cellular level the main cell type, chondrocytes, are surrounded by an ECM composed of collagen and aggrecan. Created with BioRender.com

Traumatic joint injuries, like ligamental tears, can often also result in cartilage defects. These defects are not reparable because cartilage is avascular and cannot access progenitor cells and nutrients necessary to facilitate healing[9–12]**.** These defects are often undetected and this disruption in the tissue integrity leads to high loads on the remaining healthy tissue. This increase in tissue stress causes chondrocytes to produce inflammatory cytokines such as IL-1β (interleukin-1 beta)[13,14] and TNFα (tumor necrosis factor alpha)[13,15] which further induce the expression of matrix degrading enzymes[15–18]. Long term inflammation and mechanical overload accelerate the deterioration of the remaining healthy cartilage, eventually leading to post traumatic osteoarthritis (PTOA)[19–21]. PTOA affects over 5.6 million people within the United States[19,20]

1.2 Current Treatment Options

The current treatment options for clinical repair of cartilage defects include microfracture, osteochondral transplantation and autologous chondrocyte implantation (ACI). There are benefits and drawbacks associated with each procedure but overall, none of these options fully restore cartilage function[22].

Microfracture is the most commonly performed procedure for small cartilage defects[22–24]. The repair process involves debridement of the cartilage from the defect area followed by perforation of the underlying subchondral bone to allow bone marrow and blood to be released into the injury site. This initiates the repair process by bone marrow mesenchymal stem cells (MSCs) and eventually forms cartilaginous tissues[25]. This procedure is minimally invasive with short recovery time[26–29]. However, this method is generally only effective in small defects (<2 cm^2) and younger patients[24]. In addition, the recruited MSCs form fibrocartilage instead of hyaline cartilage[22,30–32]**.** Fibrocartilage is not

as stiff as hyaline cartilage and does not have sufficient mechanical properties to resist the high compressive loads of the knee joint[33,34]. This affects the long term effectiveness of this treatment, leading to degradation of the repair tissue and onset of PTOA[24,25,33,35].

Osteochondral transplantation uses tissue grafts from healthy cartilage to repair surgical defects[22,36,37]. These grafts can be autografts or allografts. For autographs, a tissue plug made up of cartilage and the underlying subchondral bone is taken from a low weight-bearing area of the patients knee before being implanted in the defect site[22].This method restores most of the mechanical function but limitations include insufficient donor tissues, donor site morbidity and damages to the harvested grafts[38]. For larger defects (<3 cm^2) allografts are typically used[36]. Allografts have risks including disease transmission and host immune responses and cell death in the graft because most donor tissues are not freshly harvested[39,40].

Autologous chondrocyte implantation (ACI) is a treatment for large cartilage defects[33,41,42]. ACI is a two-step procedure that starts with harvesting healthy chondrocytes from the low weight-bearing region of the patient's cartilage. The harvested chondrocytes are then expanded *in vitro* before being injected back into the chondral defect underneath a periosteal patch in a second surgery[22,43].

Recently, matrix-induced autologous chondrocyte implantation has been used to avoid complications associated with the use of the periosteal patch[44,45]. In this method, cells are seeded on a membrane made of collagen I/III before being implanted back into the defect site[46]**.** The limitations of these procedures are that it includes multiple invasive procedures and requires *in vitro* monolayer expansion[47]**.** Studies have shown that monolayer expansion of chondrocytes leads to dedifferentiation[48]. ACI has good clinical

results in young patients after 1-11 years but increasing patient age decreases the effectiveness of these ACI procedures[49–51]. In addition, ACI shows subpar repair in joints showing signs of OA[52–54].

1.3 Tissue Engineering Based Cartilage Repair

To overcome the issues with the clinical repair strategies outlined above, tissue engineering solutions have been proposed to create new cartilage tissues with the key structural macromolecules (type II collagen and aggrecan). This includes the use of other cell types, scaffolds and biomolecular/biochemical stimuli[55–57], which are three essential components of tissue engineering and a combination of the three contributes to the functional success of engineered cartilage tissues.

Adult mesenchymal stem cells (MSC) are a cell alternative to articular chondrocytes for cartilage tissue engineering . These cells can differentiate into chondrocytes and can be harvested from various tissues[58–60]. MSC-derived chondrocytes (MdChs) produce cartilage matrix proteins[61–63]. Studies have used many different factors to stimulate matrix production by MdChs including growth factors[59,64–67]**,** scaffolds[68–71], and mechanical stimuli[37,55,72]. Despite all of the various techniques investigated, MdChs do not have a stable chondrogenic phenotype[55,59,73]. When growth factors are used to induce chondrogenesis of MSCs, they follow the endochondral ossification pathway and begin to express hypertrophy-associated markers not expressed in primary chondrocytes[74–77]. This hypertrophy leads to neocartilage degradation and compromises the integrity of engineered tissue[78–80].

The focus of this work is on the use of articular chondrocytes in cartilage repair. Primary articular chondrocytes are the gold standard for cartilage tissue engineering[22] and have been approved by the FDA to repair articular cartilage. ACI has demonstrated 60% to 90% good-excellent clinical outcomes after 1 to 11 years in young patients (15 to 50 years of age) with large defects and moderate symptoms[54,81,82]**.** Since 1994[43], ACI has evolved from a scaffold free implantation to the membrane-based delivery in MACI. The matrix assisted ACI (MACI) procedure shows benefits over classic ACI, including improved clinical outcomes in early OA patients.[83–85] For both procedures, maintaining robust hyaline tissue synthesis by isolated chondrocytes is an ongoing challenge.[86] **Overall, improvements to these methods still do not overcome the problems associated with the availability and expansion of articular chondrocytes or the decrease of cartilage matrix deposition by aged and OA chondrocytes**, which limits the success of tissue-engineered cartilage products.

1.3.1 Genetic Engineering in Cartilage Tissue Regeneration

Intracellular regulators of chondrocyte hypertrophy can be directly targeted and silenced using RNA interference (RNAi). RNAi of a gene induces its loss of function by stimulating targeted degradation of suppressing mRNA translation[87–89]. Three types of RNA molecules are commonly used to facilitate RNAi; short interfering RNAs (siRNAs), microRNAs (miRNAs), and the artificial short hairpin RNAs (shRNAs). Both siRNA[90] and shRNA[91–93] have been used in osteoarthritic chondrocytes to investigate their chondrogenic abilities. Long term inhibition of genes is difficult with siRNA because it can be transient[87]. Lentiviral delivered shRNA is seen as a solution to this problem because

it integrates into the genome and can be passed onto daughter cells[87]. During RNAi, shRNA is processed into siRNA that induces silencing of the target sequence.

Our lab has engineered a synthetic gene circuit that suppresses translation of RUNX2 through a synthetically established intracellular feedback mechanism. The feedback loop is activated by intracellular RUNX2, making the circuit phenotype-specific and the regulation of RUNX2 cell autonomous **(Figure 1-3)**. This circuit utilizes two well characterized elements: a Col10a1 basal promotor and cis-enhancers that facilitate RUNX2 binding to the Col10a1 promotor[94,95]. Binding of RUNX2 to the promotor induces transcription of short hairpin RNA for RUNX2 (shRUNX2) that targets RUNX2 mRNA, establishing a negative feedback loop. Kaur et. al have shown that the use of this gene circuit improves MdCH cartilage matrix accumulation[96].

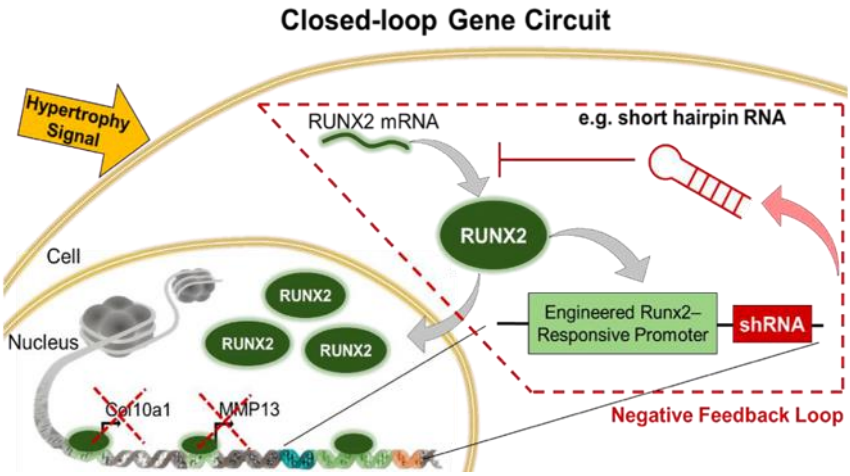

Figure 1-2: Closed loop gene circuit mechanism When intracellular RUNX2 binds to the Col10a1-like promoter, the gene circuit is activated driving expression of shRNA for RUNX2. The shRNA binds to the mRNA inhibiting translation of RUNX2. The suppression of RUNX2 decreases the expression of type X collagen, MMP13, ADAMTS5.

1.4 Challenges in Tissue Engineering Based Repair

The aged and OA phenotypes may explain the subpar cartilage repair seen in aged patients when they undergo ACI[53]. Investigations targeted at tuning exogenous cues to

regulate chondrocyte phenotype have predominantly been conducted using fetal or juvenile chondrocytes and we are finding that the response of aged and OA chondrocytes to these cues are not equivalent to their younger counterparts[97]. For example, supplementing chondrocytes with TGF-β increases matrix production. This effect occurs through SMAD2/3 signaling which upregulates collagen II and aggrecan. However, in aged and OA chondrocytes TGF-β signaling is altered and instead drives chondrocyte hypertrophy[98]. The ***objective*** of this work is to improve cartilage tissue regenerative outcomes using aged chondrocytes by addressing the two major phenotypes identified in aging and OA.

1.4.1 Aging leads to chondrosenescence

Inflammaging, defined as chronic low-level inflammation, is thought to be a driving force behind age-related pathologies such as diabetes mellitus[99–101] atherosclerosis[102] and OA progression[103]. The exact cause of inflammaging is unknown but is thought to be due to accumulation of misplaced and misfolded molecules from damaged cells[104,105]. These molecules can be a source of constant stress leading to activation of the innate immune response. As we age, disposal of these molecules decreases due to decreased autophagy[106,107], which is necessary for normal chondrocyte function[108]. Decreased autophagy and increased inflammation can lead to a senescent-like phenotype, dubbed “chondrosenescence”, resulting in increased OA severity[109].

Inflammaging increases the number of chondrosenescent cells in the joint. This is because senescent and senescent-like cells secrete pro-inflammatory cytokines and matrix degrading enzymes and chemokines, which are characteristic of the senescence associated secretory phenotype (SASP)[110] . Key cytokines known to contribute to OA

progression, such as TNF-α and IL-1β, have also been identified as cytokines involved in inflammaging[103,111–113]. IL-1β has been shown to upregulate the transcription factor RUNX2 in chondrocytes and RUNX2 upregulates pathways that lead to chondrocyte hypertrophy[101-105] and matrix catabolism[79]. These inflammatory cytokines also activate the NF-κB and MAPK pathways—both of which are abnormally activated in OA chondrocytes— leading to matrix degradation[78, 79] and shifts in chondrocyte phenotype[79]. NF-κB is also the major signaling pathway that stimulates the appearance of the SASP[115]. This phenotype exhibits markers that are also involved in the progression of the hypertrophic phenotype seen in OA such as RUNX2 and MMP13[116].

1.4.2 Osteoarthritis leads to hypertrophy in articular chondrocytes

Chondrocyte hypertrophy is a major marker in OA progression[117,118]. Hypertrophic differentiation naturally occurs during a endochondral ossification, a multi-step process that occurs during limb development[74–76,119]. During limb development, cells condense prior to early chondrogenesis, proliferation, hypertrophic maturation, calcification and blood vessel invasion before differentiating into bone[119].

Hypertrophy is a critical step in endochondral ossification that prepares for the mineral deposition in cartilage matrix shown in Figure 1-2[120]. This process is driven by the master transcription factor RUNX2 (runt-related transcription factor 2)[121–125]. RUNX2 upregulates collagen type X[94,95] and MMP13[126,127] during hypertrophy. MMP13 degrades both aggrecan[128] and type II collagen[129]. These are the two major components of cartilage ECM and this increased degradation leads to a decrease in the mechanical strength of cartilage. Previous works shows that inhibiting RUNX2 can delay this process. Transgenic mice expressing conditional knockout of RUNX2 exhibit impaired endochondral

ossification, marked by delayed chondrocyte maturation and less absorption of articular cartilage[130–132].

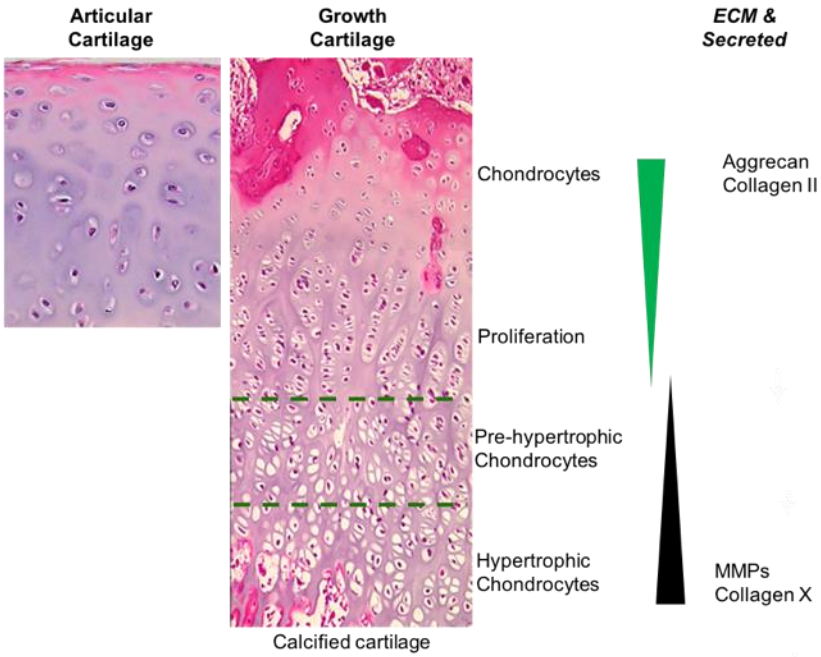

Figure 1-3: H&E staining of articular cartilage and growth cartilage. The OA phenotype follows the formation of growth cartilage. Chondrocytes become hypertrophic leading to decreased collagen and aggrecan production and increased expression of MMPs and other hypertrophic factors.

1.5 Project Goals and Hypothesis

This work was accomplished by first developing a method for chondrocyte redifferentiation that resulted in matrix production of both young and OA chondrocytes. RUNX2 was then suppressed in OA chondrocytes using our previously established cell-autonomous shRUNX2 gene circuit to evaluate matrix accumulation. Finally, the evolution of the chondrosenescent phenotype was investigated by creating an *in vitro* model that simulated aging and inflammaging. We hypothesize that targeting RUNX2 in aged and OA chondrocytes will improve ECM production and reduce ECM turnover and that RUNX2 has a role in chondrosenescence. We will investigate this hypothesis in the following aims:

Aim 1: Investigate the role of RUNX2 in young and aged/OA chondrocytes during 3D redifferentiation culture.

Hypertrophy and senescence share similar markers and processes. RUNX2 increases the expression of matrix degrading enzymes and decreases expression of cartilage structural macromolecules during OA[6,7]. Chondrocytes expressing RUNX2 have shown a senescent like phenotype[178,20], indicating a role for RUNX2 in chondrocyte senescence. The purpose of this study was to investigate the role of RUNX2 in the ECM production of aged/OA chondrocytes in a scaffold-free, 3D environment.

Aim 2: Determine the effect of RUNX2 suppression on matrix production of chondrocytes isolated from low grade OA tissue.

RUNX2 drives chondrocyte hypertrophy, a major maker of OA progression. Our lab previously developed a cell-autonomous gene circuit that drives the expression of shRNA for RUNX2 (shRUNX2). Kaur et. al has shown that the use of this gene circuit improves MdCh cartilage matrix accumulation[96]. The purpose of this study was to determine if RUNX2 suppression increases the accumulation of cartilage matrix macromolecules by increasing expression of articular cartilage markers and inhibiting the expression of matrix metalloproteinases in OA cells.

Aim 3: Determine the effect of low-level inflammatory stimulus on the inflammaged phenotype of chondrocytes.

Chondrosenescence is the product of exposure to maintained levels of low-grade inflammation as cells age. Researchers directly investigate chondrosenescence using cells from aged patients, but these cells only show the final phenotype[133,134]. An *in vitro* model of chondrosenescence would allow us to study the progression and regulators of

this phenotype. We investigated the combination of simulated aging (monolayer expansion) and inflammaging (IL-1β treatment) on young HACs induced a chondrosenescent phenotype. The purpose of this study was to induce biomarker profiles and ECM production levels similar to that of inflammaged HACs isolated from aged/OA patient samples in an *in vitro* model of chondrosenescence.

Chapter 2 Regeneration Potential of Osteoarthritic Cells is Decreased by RUNX2

2.1 Introduction

Strategies to repair cartilage defects in aged patients using autologous cells is still a significant clinical challenge[52,135–137]. The incidences of focal defects that require clinical regeneration strategies to delay osteoarthritis (OA) and prevent joint replacement increase with our aging population[135,136,138]. FDA approved methods for defect repair using autologous cells, such as autologous chondrocyte implantation (ACI), provide good clinical outcomes in young patients, but have subpar results using cells from older patients and/or joints showing signs of OA[52,137]. This is attributed to the slowed synthesis of cartilage structural macromolecules vital to the mechanical strength of articular cartilage—collagen II, aggrecan and sulfated glycosaminoglycans (sGAGs).[139] Allogenic transplants from young donors are limited by lack of donor tissue, indicating a need to focus on improving cartilage tissue engineering outcomes using autologous chondrocytes in OA patients.

ACI has demonstrated 60% to 90% good-excellent clinical outcomes after 1 to 11 years in young patients (15 to 50 years of age) with large defects and moderate symptoms.[54,81,82] The matrix assisted ACI (MACI) procedure shows benefits over classic ACI, including improved clinical outcomes in early OA patients.[83–85] For both procedures, maintaining robust hyaline tissue synthesis by isolated chondrocytes is an ongoing challenge.[86]

Procedures using autologous cells require extensive 2D monolayer expansion to acquire a large number of cells. This is known to lead to the dedifferentiation of articular chondrocytes and contributes to the difficulty in regenerating cartilage[140,141]. Researchers have used various methods to stop the dedifferentiation including growth factors, low density cultures and altering the cell environment[81,142–144]. Coupled with 3D redifferentiation techniques, including scaffold and scaffold-free cultures, researchers have shown that chondrocytes can accumulate matrix *in vitro*, typically involving a growth factor regimen or biomaterial design.

Investigations targeted at tuning exogenous cues to regulate chondrocyte phenotype have predominantly been conducted using fetal or juvenile chondrocytes and the response of aged chondrocytes to these cues are not equivalent to their younger counterparts. For example, the anabolic effects of TGF-β through the binding to ALK5 seen in young articular chondrocytes is decreased in OA chondrocytes **(Figure 2-1)**[145,146]. This is due to increased binding to the ALK1 receptor increasing the expression of RUNX2 leading to cartilage matrix degradation. Thus, there is still a need to demonstrate that these techniques are successful with cells isolated from aged patients or patients with OA.

In this study, matrix production in chondrocytes isolated from young, healthy patients was compared to cells isolated from cartilage showing early signs of OA (grades 1 and 2). First, the scaffold-free pellet culture model was optimized for articular chondrocytes. Second, the phenotypic and genotypic differences in neo-cartilage

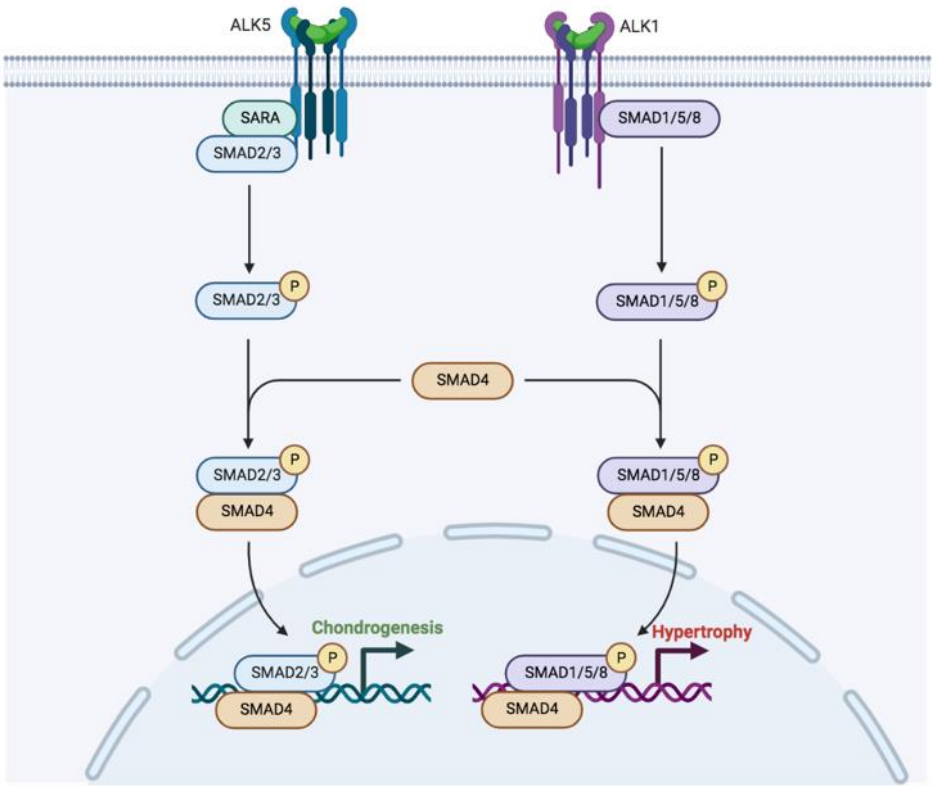

Figure 2-1: Schematic of the TGF-β pathway. TGF-β can act through ALK1 and ALK5 and lead to chondrogenesis of chondrocyte hypertrophy. Created in BioRender.com.

formation between these 2 cell populations after monolayer expansion was compared to determine the sensitivity of the cells to this process. This work shows that OA cells produce cartilage matrix but at a lower level compared to young cells. In addition, the differences in response to anabolic grow factors *in vitro* were highlighted and it was shown that these differences are driven by the RUNX2 pathway.

2.2 Methods

2.2.1 Young Cell Source

HACs in the age range of 30±10 years were purchased from StemBioSys. HACs were plated at 20,000 cells/cm^2 and cultured in growth media containing low-glucose DMEM (Gibco), 10% fetal bovine serum (FBS) (Invitrogen), 1% antibiotic-antimycotic

(Invitrogen), 1 ng/ml transforming growth factor beta (TGFβ1) (Shenandoah), 5 ng/ml fibroblast growth factor (FGF-2) (Shenandoah) and 10 ng/ml platelet derived growth factor (PDGF-BB) (Shenandoah) at 37 °C, 5% CO_2.[147,148] HACs were trypsinized and sub-cultured every three days. Population doublings were calculated by: PD = 3.32[log (final cell #) – log (initial cell #). Age and sex of donors: M,24; M,19; F,20.

2.2.2 OA Cell Source

De-identified distal ends of femurs from patients undergoing total knee replacement were obtained from 6 patients. Patient sex and age were provided and cartilage of OA grades 1 and 2 were identified and tissue was then harvested from condylar regions of femur of OA grade 1 or 2, shown in **Figure 1-2**. Chondrocytes were isolated by mincing cartilage and digesting with 0.1% collagenase II (Worthington) for 16 hours in Ham's F12 (Gibco) medium with 5% FBS. OA cells were plated and sub-cultured as described in *Young Cell Source*. Age and sex of donors: F,63; M,71; F,73.

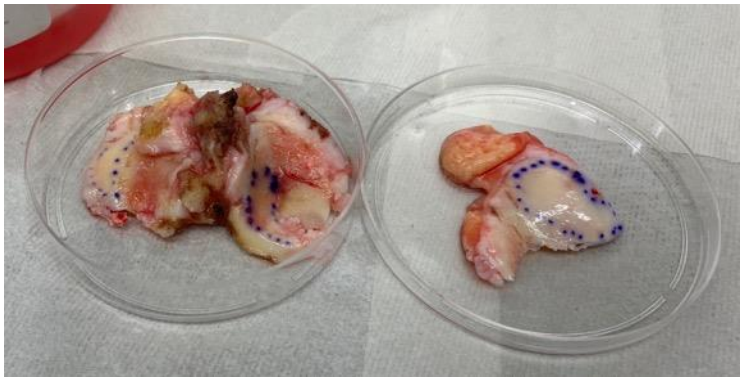

Figure 2-2: OA patient samples. Tissue from OA patients. OA grades of 1 and 2 are outlines with blue pen and tissue was only harvested from these regions.

2.2.3 Scaffold-free Culture

Pellets were created by adding $0.25x10^6$ cells suspended in redifferentiation media to wells of U-bottom, 96-well plates (Fisher). Plates were spun down at 1000x*g* for 5 minutes and allowed to condense for 3 days. Redifferentiation media contained high-glucose DMEM (Invitrogen), 1.25 mg/mL bovine serum albumin (BSA) (Fisher), 1mM sodium pyruvate (Invitrogen), 10^{-7} M dexamethasone (Sigma), 50 μg/ml ascorbic 2-phosphate (Sigma), 40 μg/ml L-proline (Sigma), 10 ng/ml TGFβ1, 1% ITS+ Premix (Corning), 1% antibiotic-antimycotic[148,149]**.** Cultures were maintained for 28 days and media was changed every other day. A schematic representing the experimental outline is shown below.

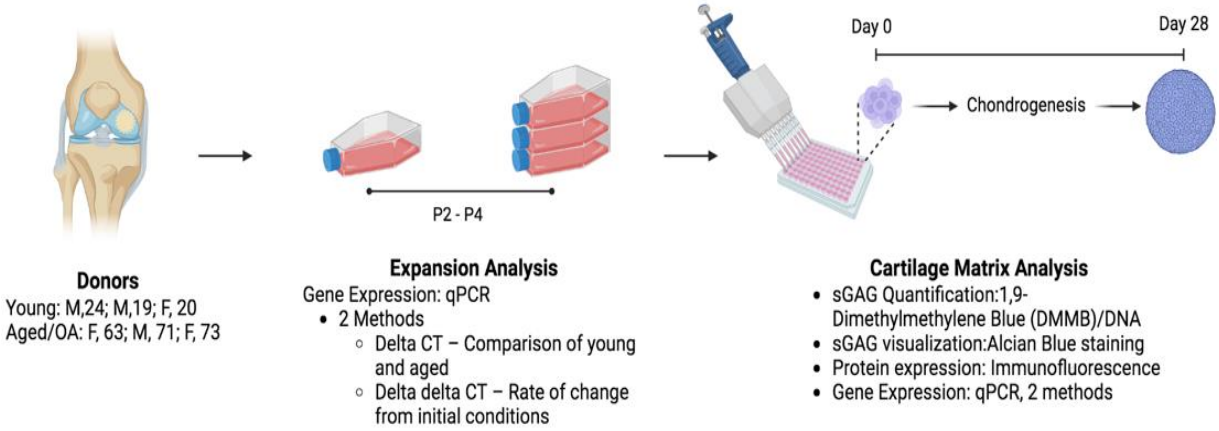

Figure 2-3: Redifferentiation of human articular chondrocytes. Young and aged/OA chondrocytes were expanded to passage 4 and then placed redifferentiation in 3D pellet culture for 28 days.

2.2.4 Histological Analysis

Pellets were washed twice with PBS and fixed with 10% neutral buffered formalin at room temperature for 30 minutes. Fixed pellets were washed with PBS followed by 70% ethanol. Pellets were dehydrated with an ethanol-xylene series prior to paraffin embedding and sectioning. Sections were deparaffinized and stained with Alcian Blue (1% in 3% Acetic Acid, Poly Scientific) and counterstained with Nuclear Fast Red

(Electron Microscopy Sciences) to evaluate proteoglycan accumulation. For immunofluorescence, sections underwent antigen retrieval (BD Pharmingen) and blocking prior to primary antibodies incubation for aggrecan (1:500 dilution in 10% goat serum in 0.1% Triton X100 in TBS), collagen type II (1:100) (Abcam), collagen type X (1:100), RUNX2 (1:100), or MMP13 (1:200), phospho-smad3 (1:100), phospho-smad5 (1:100) , alk1, alk5, (Abclonal), overnight at 4°C. Histological slides were incubated with Goat anti-Rabbit Alexa Fluor™ Plus 488 secondary antibody (Fisher) for 1 hour at room temperature Sections were counterstained with DAPI (Life Technologies) for 5 minutes at room temperature.

2.2.5 Production of Structural Macromolecules

Pellets were harvested, frozen at -80°C and digested in 0.3 units/ml papain (Sigma) in a buffer of L-cysteine hydrochloride (Sigma), Ethylenediaminetetraacetic acid (EDTA) (Sigma), and sodium phosphate dibasic (Sigma) buffer solution at 65°C for 16 hours. Cartilage matrix accumulation was measured using the 1,9-dimethylmethylene blue (DMMB) assay as previously described[56,150,151]. A standard curve was generated using known concentrations of chondroitin-6-sulfate (Sigma) in duplicate and samples were run in triplicate. DMMB dye was added to each well and absorbance was measured using a Synergy H1 plate reader at wavelengths 525nm and 595nm.

Matrix production was normalized by DNA content as determined using the PicoGreen assay (Thermo Fisher). A standard curve was generated according to the manufacturers instructions using λ DNA in duplicate and samples were run in triplicate. The plate was incubated for 5 minutes at room temperature in the PicoGreen-Tris dye

solution and fluorescence was measured using a Synergy H1 plate reader at excitation wavelength 498nm and emission wavelength 528nm.

2.2.6 Gene Expression

Analysis of gene expression was performed as previously described [56,151,152]**.** After experiment completion, pellets were washed with PBS and flash frozen in liquid nitrogen and stored at -80°C until processing. Briefly, pellets were homogenized using TRI Reagent RT (Molecular Research Center). Following homogenization, bromoanisol was added for phase separation and RNA was precipitated using isopropanol. Purified RNA was resuspended in Ultrapure DI water and concentration was quantified using a Thermo NanoDrop 2000. RNA purity was assessed using the A_{260}/A_{280} and A_{260}/A_{230} ratios measured by the NanoDrop. Values greater than 1.7 were considered suitable for downstream applications[153].

Following RNA extractions, cDNA was synthesized using High-Capacity cDNA Reverse Transcription Kit (Life Technologies) using 1μg RNA/sample according to the manufacturer's protocol. Gene expression was analyzed using Fast SYBR Green PCR Master Mix (Life Technologies) on Applied Biosystems 7500 Fast qPCR machine. Primer sequences are listed below in Table 2-1. The mean cycle threshold of housekeeping genes *GUS* and *TBP* (*HK*) was used to determine the fold change of gene expression levels using both the ΔCT and $\Delta\Delta CT$ methods. For the ΔCT method, relative expression levels were calculated as $\Delta CT = CT_{Gene\ of\ interest} - CT_{Housekeeping}$ and fold change was calculated as $2^{-\Delta CT}$. Relative expression levels for the ΔΔCT method were calculated as $\Delta\Delta CT = \Delta CT_{Day\ 28} - \Delta CT_{Day\ 0}$ and fold changes was calculated as $2^{-\Delta\Delta CT}$.

Table 2-1:Primer sequences for qPCR gene expression analysis

Gene	Forward	Reverse
ACAN	GGAGTGGATCGTGACCCAAG	AGTAGGAAGGATCCCTGGCA
COL2A1	CTCCAATGGCAACCCTGGAC	CAGAGGGACCGTCATCTCCA
RUNX2	CCGGAATGCCTCTGCTGTTA	AGCTTCTGTCTGTGCCTTCTGG
COL10A1	GAACTCCCAGCACGCAGAATC	TGTTGGGTAGTGGGCCTTTT
MMP13	TTGCAGAGCGCTACCTGAGA	CCCCGCATCTTGGCTTTTTC
SOX9	GCTCTGGAGACTTCTGAACGA	CCGTTCTTCACCGACTTCCT
COL1A1	GATCTGCGTCTGCGACAAC	GGCAGTTCTTGGTCTCGTCA
TBP	GTGGGGAGCTGTGATGTGAA	TGCTCTGACTTTAGCACCTGT
GUSB	GACTGAACAGTCACCGACGA	ACTTGGCTACTGAGTGGGGA

Abbreviations: ACAN, aggrecan; COL2A1, collagen type II; RUNX2, runt-related transcription factor 2; COL10A1, collagen type X; MMP13, matrix metalloproteinase 13; SOX9, SRY-Box transcription factor 9; COL1A1, collagen type I; IL6, interleukin 6; NFKB, nuclear factor kappa B; TBP, tata binding protein; GUS, glucuronidase beta

2.2.7 Statistical analysis

All data is presented as mean ± standard deviation (SD). Each point on a graph represents a donor. All statistical analysis was performed using GraphPad Prism 8.3 software (GraphPad). One-way nested ANOVA was used with Šídák multiple comparison post-hoc test. P-value <0.05 was considered statistically significant.

2.3 Results

During expansion, there was a decrease in the expression of chondrogenic redifferentiation markers in both young and aged/OA HACs. **Figure 2-4** shows gene expression of both populations at each passage during monolayer expansion. Expansion led to an increase in fibroblastic marker *COL1A1* in both populations – indicating the dedifferentiation often seen in HACs during monolayer expansion. *RUNX2* expression was higher in aged cells but expression remained constant in both populations during expansion. *SOX9* and *ACAN* were expressed at higher levels in young cells. Expression of both *COL2A1* and *COL10A1* remained constant as passage number increased.

MMP13 expression varied among donors but lowest expression was observed at passage 3 for both populations.

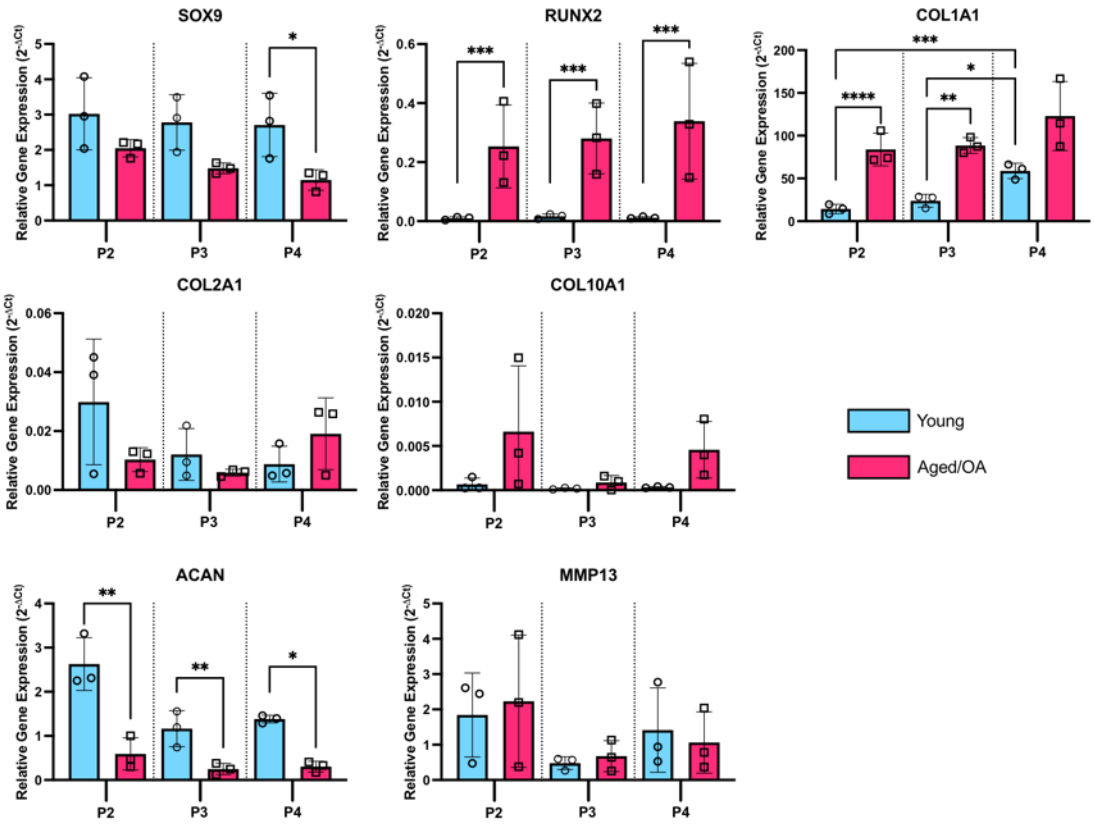

Figure 2-4: Gene expression during monolayer expansion. Gene expression of chondrogenic (left) and hypertrophic (center) genes during 4 monolayer passages. Expression is normalized to housekeeping genes at each passage. Data is presented as mean ± SD. Each point represents a different donor (n=3 for young and aged). (* – p<0.05, ** – p<0.005, *** – p<0.001, **** – p<.0001)

Figure 2-5 shows the change in expression at passage 4 compared to the initial plating at passage 2. Overall, expression of hypertrophic markers (*COL1A1, COL10A*1 and *RUNX2*) increased in both young and aged cells. The degree of differentiation was similar in both populations and shows that they behaved the same when undergoing monolayer expansion.

Before examining all donors, the scaffold-free culture model for HACs had to be optimized. One donor from each population (M, 19 and F, 63) were condensed into pellets

after 4 passages in monolayer and exposed to redifferentiation media of various formulations. The common components of the basal media (BM) include high-glucose DMEM, BSA, sodium pyruvate, dexamethasone, ascorbic 2-phosphate, and ITS+.

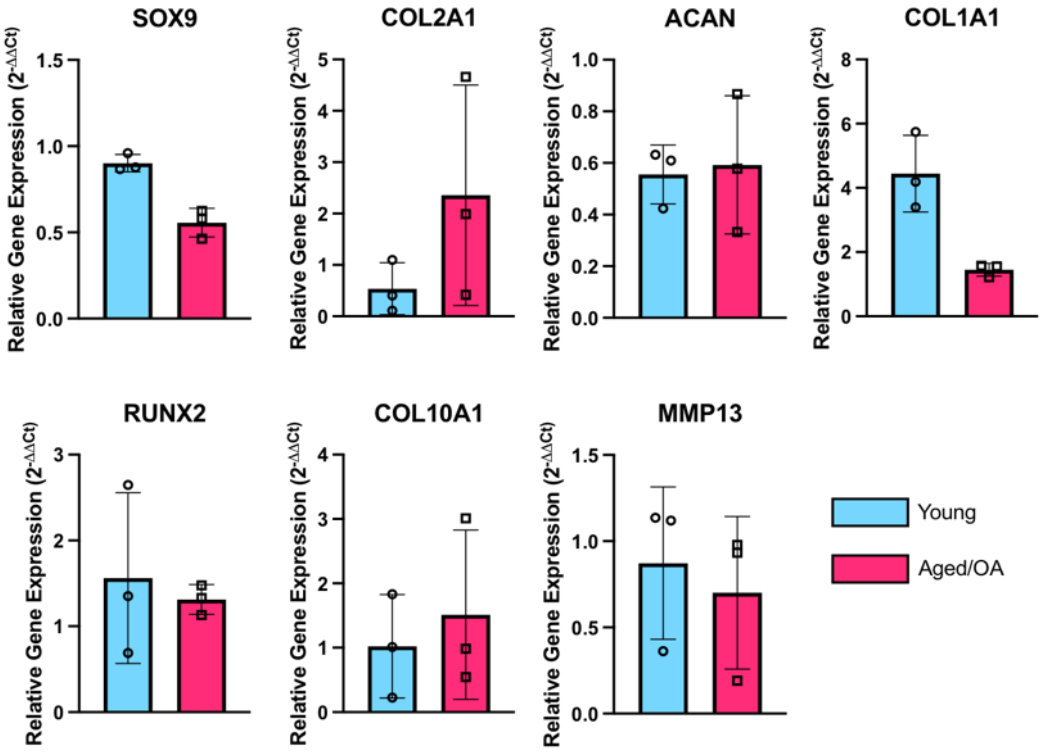

Figure 2-5: Gene expression at passage 4 relative to passage 2 for young and aged chondrocytes. Gene expression of chondrogenic (top) and hypertrophic (bottom) genes after 4 monolayer passages. Expression is normalized to housekeeping genes and passage 2. Data is presented as mean ± SD. Each point represents a different donor (n=3 for young and aged).

Under these conditions low matrix production was observed by both donors **(Appendix A).** When supplemented with TGF-β1, a growth factor known to stimulate matrix production in chondrocytes, and L-proline, a component of collagen, the cells exhibited a more articular cartilage-like phenotype with round cells in large lacunae and increased sGAG content in the center of the pellets. Total sGAG in media supplemented with L-proline and TGF-β1 increased by 85.9% in young chondrocytes and 62.1% in aged chondrocytes when compared to basal media.

Based on these results, the media supplemented with L-proline and TGF-β1 was used in all future studies. **Figure 2-6** shows the difference in matrix accumulation between young and OA chondrocytes On average, young cells had higher matrix accumulation compared to OA cells. Alcian blue staining shows higher accumulation of sGAG by young cells.

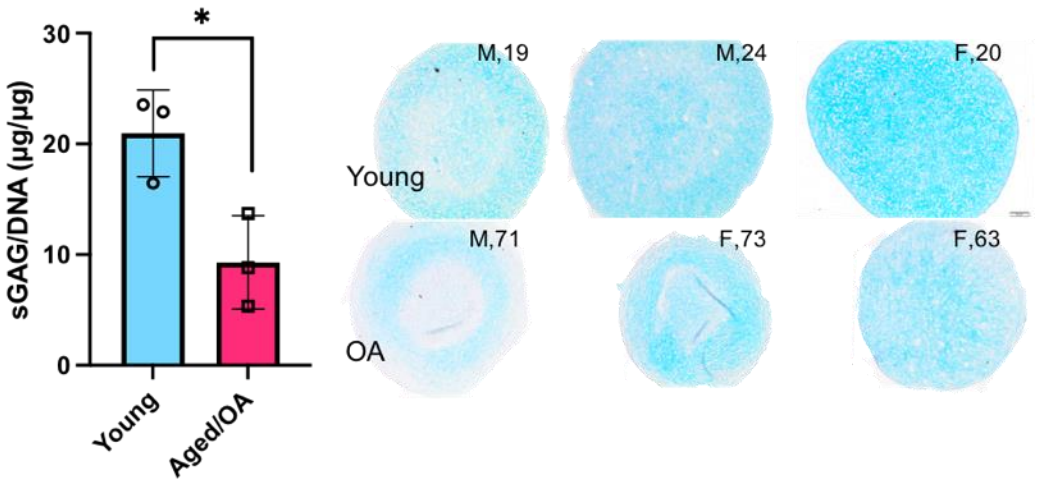

Figure 2-6: Matrix accumulation in young and OA cells.(a) sGAG quantification of young and OA cells across three donors for each population. Data is presented as mean ± SD. Each point represents a different donor (n=3 for young and aged). (*=p<.05) (b) Alcian blue staining of pellets at day 28 of pellet culture. Scale = 50µm

Gene expression analysis after 28 days of redifferentiation culture showed upregulation of chondrogenic markers in both populations. Expression of *COL2A1* was significantly higher in young cells compared to OA cells **(Figure 2-7)**. Upregulation of fibroblastic marker *COL1A1* occurred in both populations but was higher in OA cells. Upregulation of hypertrophic genes (*RUNX2, COL10A1* and *MMP13*) only occurred in OA cells.

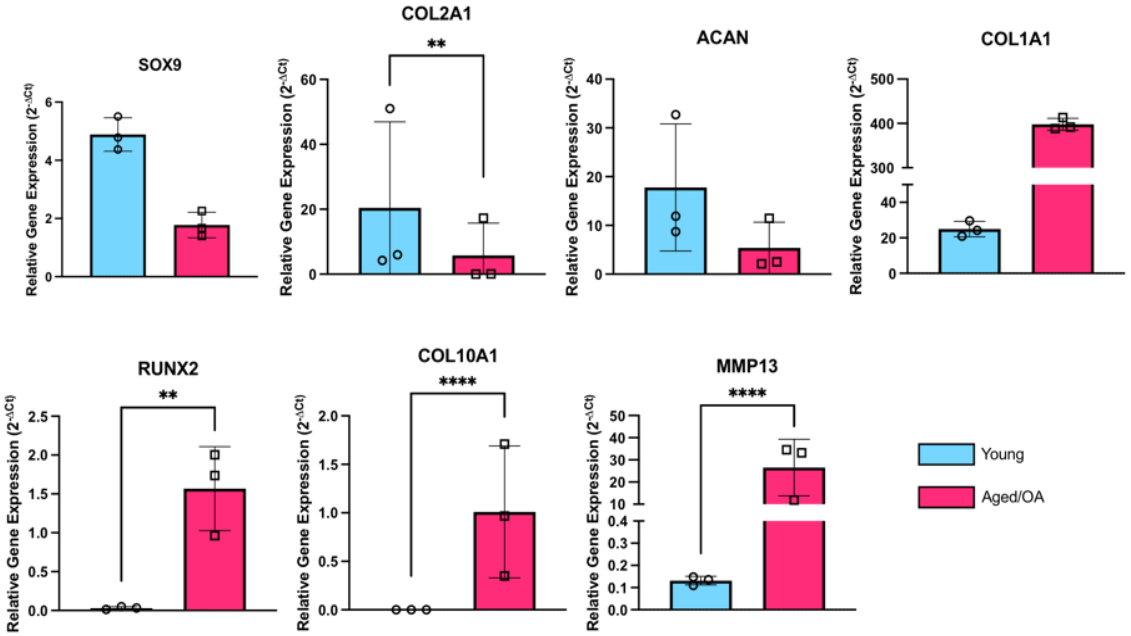

Figure 2-7:Gene expression after redifferentiation. Gene expression of chondrogenic (top) and hypertrophic (bottom) genes after redifferentiation. Expression is normalized to housekeeping genes at day 28. Data is presented as mean ± SD. Each point represents a different donor (n=3 for young and aged). (** = p<0.005, ***=p<0.001, ****=p<.0001)

Figure 2-8 shows the change in expression at day 28 compared to the cells before initiating chondrogenesis at day 0. Upregulation of *RUNX2* was seen in both populations but at a higher level in OA cells. Both downstream targets of *RUNX2, COL10A1* and *MMP13* were significantly upregulated in OA cells compared to young cells. *ACAN* and *SOX9* were upregulated in both populations at a similar level. Upregulation of *COL2A1* was significantly higher in young cells compared to OA cells.

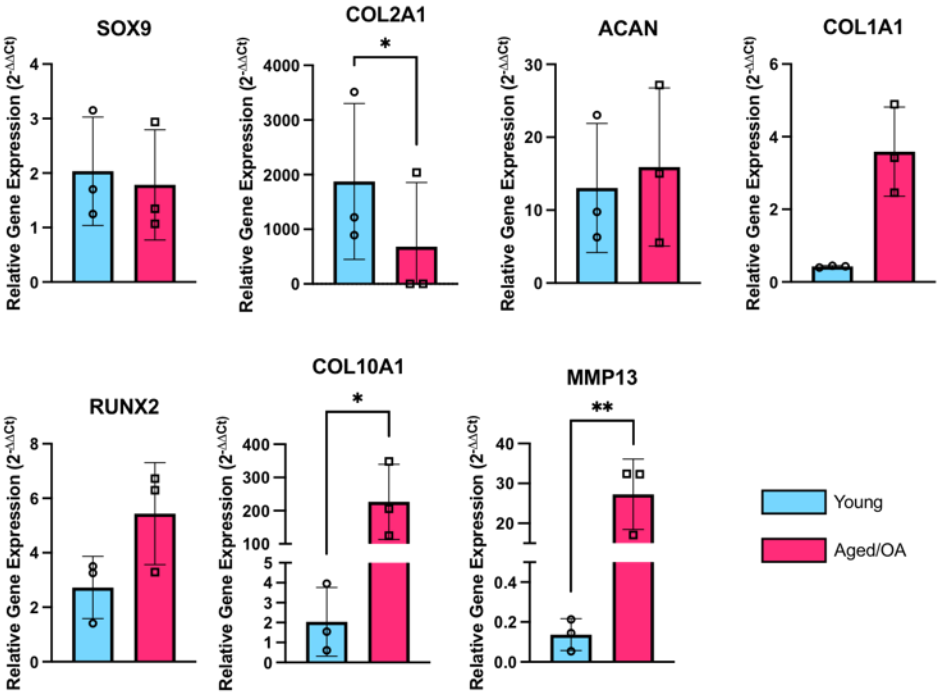

Figure 2-8: Gene expression after redifferentiation for young and aged chondrocytes. Gene expression of chondrogenic (top) and hypertrophic (bottom) genes after 28 days of redifferentiation. Expression is normalized to housekeeping genes and day 0 of culture. Data is presented as mean ± SD. Each point represents a different donor (n=3 for young and aged). (* = $p<0.05$, ** = $p<0.005$)

Gene expression showed increased levels of *COL2A1* in young cells and protein expression appears to show higher COLII protein expression. *ACAN* expression increased in both young and aged populations at a similar rate, but protein expression shows higher expression in young cells **(Figure 2-9)** after redifferentiation.

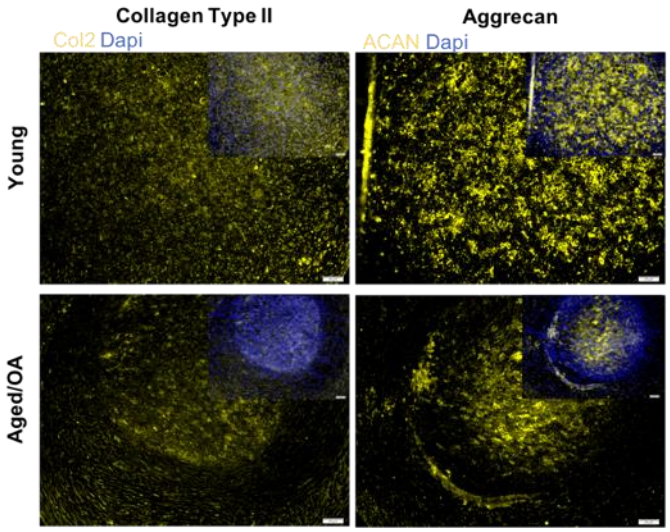

Figure 2-9: Protein expression of chondrogenic markers. Protein expression of chondrogenic markers in young and OA cells. Insets contain merged images with counterstain DAPI (blue). Yellow indicates protein. Scale = 20μm

Gene expression showed upregulation of *RUNX2* and its target genes *COL10A1* and *MMP13* in OA cells. Immunofluorescence shows higher protein expression of RUNX2 and COL10 in OA cells compared to young cells which have little to no protein expression. Interestingly, protein expression of MMP13 appears similar between young and aged cells when gene expression shows significant higher expression by OA cells **(Figure 2-10).**

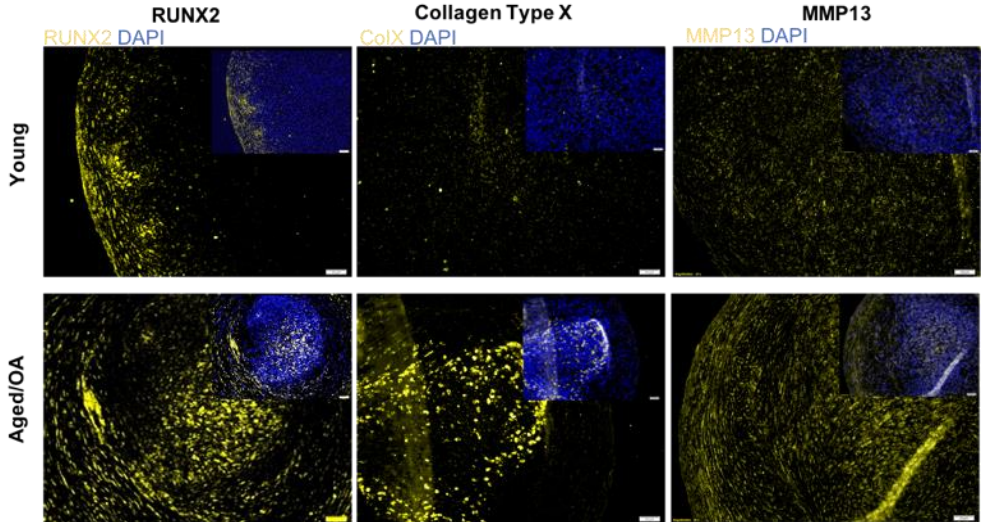

Figure 2-10: Protein expression of hypertrophic markers. Protein expression of hypertrophic markers in young and OA cells. Insets contain merged images with counterstain DAPI (blue). Yellow indicates protein. Scale = 20μm.

The response to TGFβ was probed by looking at the ALK1 and ALK5 receptors and their downstream effectors, SMAD5 and SMAD3. ALK5 and SMAD3 promote the anabolic effects of TGFβ in HACs and protein expression shows that ALK5 and phosphorylated SMAD3 are present in both young and OA cells. Young cells express both throughout the pellets where OA cells have only small highlighted sections of expression **(Figure 2-11)**. ALK1 and SMAD5 promote hypertrophy in chondrocytes and protein expression shows that ALK1 is expressed in both populations but at a higher level in OA cells. Phosphorylated SMAD5 is present in OA cells and OA cells had little to no expression in SMAD3. **(Figure 2-11)**.

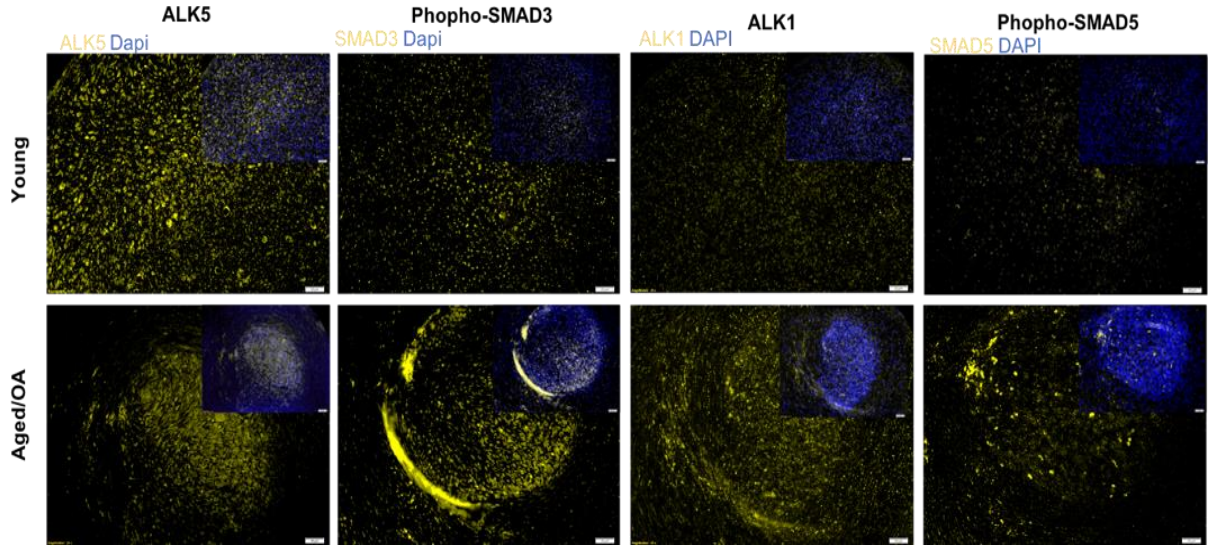

Figure 2-11: Protein expression of TGFβ pathway markers. Protein expression of markers involved in the TGFβ pathway in young and OA cells. Insets contain merged images with counterstain DAPI (blue). Yellow indicates protein. Scale = 20μm.

2.4 Discussion

Improving cartilage regeneration using aged/OA cells is a challenge in clinical applications. There are known differences between young cells and aged/OA cells and investigating the mechanisms behind them is necessary to improve regenerative outcomes. We show that young and aged HACs dedifferentiate is a similar pattern (increased expression of fibroblastic markers and decreased expression of chondrocyte genes) when expanded in monolayer. We show that redifferentiation culture leads to higher matrix production in young cells compared to OA cells. In addition, redifferentiation leads to increased hypertrophic gene expression in OA cells but not young cells. Finally, we show that both the chondrogenic and hypertrophic TGFβ pathways are active in OA cells. This data suggests aged/OA cells are capable of cartilage regeneration similar to that of young cells if RUNX2 and other pathways are targeted simultaneously.

Dedifferentiation of HACs during monolayer expansion leads to a decrease in chondrogenic gene expression and is listed as one of the factors that leads to poor cartilage regeneration *in vitro* [140,141,148,154,155]. However, Barbero et al. demonstrated that the addition of growth factors PDGFBB, TGFβ1and FGF-2[97,148] increased HAC proliferation and maximized the redifferentiation potential of HACs. Here, the use of these growth factors resulted in similar proliferation rates between young and aged cells and a similar decrease in chondrogenic gene expression indicating that the effect is consistent across age groups **(Appendix B)**. The balance between redifferentiation potential and acquiring a large cell number is important in clinical autologous procedures in order to shorten time between surgeries and improve patient outcomes.[147,156,157]

The added growth factors are often combined with low glucose media to slow the rapid decrease in chondrogenic gene expression and retain chondrogenic potential[149,158,159]. Here we show dedifferentiation of both populations but at higher levels in aged cells. This could be due to the phenotype acquired before the cells are isolated but also due to FGF which has been shown to induce a hypertrophic phenotype in non-OA chondrocytes during expansion[119]. Our results show increased hypertrophic gene expression in OA cells but a more fibroblastic phenotype associated with chondrocyte dedifferentiation in young cells.[90,160] This demonstrates the differing responses to growth factors between young and aged cells.

Literature indicates that aged/OA cells have decreased gene expression, matrix production and responses to anabolic growth factors when redifferentiated in vitro.[158,161] In this study we saw lower matrix production in OA cells compared to young cells after redifferentiation. Gene expression in OA cells remained more hypertrophic compared to young cells after redifferentiation. High levels of *ACAN* have been observed in normal (non-OA) age-matched chondrocytes, OA and late chondrogenesis of MSCs[51,52,139,162]**.** In this study, we saw levels of *ACAN* in OA cells that were similar to young cells which could explain the matrix production measured in OA cells.

RUNX2 leads to degradation of cartilage matrix through upregulation of collagen degrading enzymes like MMP13[78]**.** The upregulation of both of these genes occurs during OA progression[163,164] and this is seen in the present study in OA cells after redifferentiation. Coupled with the low *COL2A1* gene expression and decreased matrix production the data shows that OA cells do produce cartilage matrix macromolecules but

the robustness of this response may be limited by the upregulation of RUNX2 and its target genes.

Chondrogenic media contained TGFβ1 which stimulates chondrocyte matrix production in vitro. Age and OA lead to the dysregulation of the TGFβ pathway such that there is an increase in the ALK1 to ALK5 ratio.[91,145,165–167] ALK5 mediates the anabolic effects of TGFβ while ALK1 promotes hypertrophy and MMP-13 expression. The upregulation of MMP13 and RUNX2 in OA cells could be due to the exogenous TGFβ1 in the media and result in the lower matrix production by OA cells that we see in this study.

Dehne et. al showed that age-matched normal and non-OA chondrocytes have comparable matrix production.[168] All donors were over 40, which is the age where clinicians start to see increased incidence of OA and where researchers start to see a decrease in the ability to make matrix, or chondrogenic potential.[169–171]. This indicates that age may not be the biggest factor and that the hypertrophic phenotype seen in OA have a larger influence on matrix production. Mazor et. al showed that cells from early OA grades produce hyaline cartilage furthering the evidence shown here and by others that OA cells retain chondrogenic potential under the right conditions.[133,158,159,172]

RUNX2 has diverse roles in chondrocyte proliferation and has been shown to be necessary for matrix production. In the present study, we saw upregulation of RUNX2 gene expression in young cells showing that RUNX2 is upregulated in this population. However, expression of downstream genes COL10A1 and MMP13 was still low indicating that the RUNX2 levels did not lead to an increase in hypertrophic gene expression. RUNX2 is also responsible for driving the hypertrophic phenotype seen in OA cells making it an ideal target for suppression in OA cells. However, previous work has shown

that a total knockout lead to low matrix production and a decrease in chondrogenic gene expression in an ATDC5 model[96]. Combined with the data in this study, this indicates that a low level of RUNX2 expression is present in all populations but a high level results in lower matrix production and low chondrogenic gene expression that we see in OA cells.

2.5 Conclusion

Our data highlights the distinct responses of young and aged/OA chondrocytes *in vitro*. Though donor variability has a significant outcome on matrix production in both young and OA populations[173–175], our data shows that overall OA cells upregulate hypertrophic genes and produce less cartilage matrix compared to young cells. We also showed that both populations can proliferate quickly and achieve the high cell numbers necessary for clinical autologous procedures and that aged/OA cells can be candidates for these procedures in the future.

Chapter 3 RUNX2 Suppression Increases Matrix Accumulation of Osteoarthritic Chondrocytes

3.1 Introduction

Strategies to repair cartilage defects in aged patients using autologous cells is still a significant unmet clinical need. This is due to the fact that incidences of focal defects that require clinical regeneration strategies to delay osteoarthritis (OA) and prevent joint replacement increase with our aging population[138]. FDA approved methods using autologous cells, such as autologous chondrocyte implantation (ACI), provides good clinical outcomes in young patients, but have subpar results in older patients and joints showing signs of OA[52,54,81]. This is attributed to the slow synthesis of cartilage structural macromolecules vital to the mechanical strength of articular cartilage – collagen II, aggrecan and sulfated glycosaminoglycans (sGAGs)[176]. Allogenic transplants from younger to aged donors are limited by donor site morbidity and lack of donor tissue, indicating a need to shift focus onto improving cartilage tissue engineering outcomes using chondrocytes from an aged population.

Chondrocyte hypertrophy is a major marker in OA progression[117,118]. Hypertrophic differentiation naturally occurs during a developmental process known as endochondral ossification (EO) and is regulated by the transcription factor, RUNX2[78]. RUNX2 decreases expression of cartilage structural macromolecules, collagen II and aggrecan, and increases expression of collagen type X. RUNX2 also induces the expression of matrix degrading enzymes such as MMP13 and ADAMTS4/5, compromising the mechanical

integrity of the tissue[78]. Liao et al. showed that OA progression was slowed with aggrecan-targeted knockout of RUNX2 in articular chondrocytes[132]. This indicates that targeting RUNX2 may attenuate hypertrophic differentiation seen in OA.

In addition to hypertrophy, articular cartilage undergoes age-related changes including decreased tensile strength, surface fibrillation and a reduction in chondrocyte density and proliferation[114]. These changes compromise the strength of the tissue and can lead to structural defects. Collectively, these age-related changes of articular chondrocyte function is called chondrosenescence. Chondrosenescence affects the functional phenotype of chondrocytes and is intimately linked with inflammaging (low-level inflammation that occurs during aging)[103,177]. Chondrocytes expressing RUNX2 have shown a senescent like phenotype characterized by flattened morphology and β-galactosidase expression, indicating a role for RUNX2 in chondrocyte senescence[179].. Accordingly, RUNX genes may play a central role in regulating the cell cycle in response to stress signals, such as the chronic inflammatory environment of the joint[179]. RUNX2 presents itself as an ideal target to attenuate both major phenotypes seen in OA.

Genetic reprogramming has been utilized in cartilage tissue engineering to delay hypertrophic maturation[96,180]. Gene silencing through RNA interference (RNAi) allows integration with the genome and can provide long-term inhibition of genes[87]. Our lab previously developed a cell-autonomous gene circuit that drives the expression of short hairpin RNA for RUNX2 (shRUNX2) when intracellular RUNX2 expression is increased. This system is tunable through the implementation of varying amounts of cis enhancers upstream of the basal promoter. Kaur et al have shown that the use of this gene circuit improves mesenchymal stem cell (MSC) cartilage matrix accumulation[96]. However, this

gene circuit has not been yet been evaluated in OA cells. The purpose of this study was to evaluate RUNX2 suppression using this gene circuit in improving cartilage regeneration outcomes in OA cells.

3.2 Methods

3.2.1 Circuit Assembly

The gene circuit was created as previously described[96]. A Tet-on inducible system was modified from the pINDUCER plasmid originally developed by Meerbrey et al. to synthesize tet-on-Luc-mir30-shRUNX2[181]. The shRNA sequence for RUNX2 was selected from the Hannon-Elledge libraries (RNAi Codex). The COL10A1 basal promotor (-220 to 110 bp) and its cis-enhancer (-4296 to -4147 bp)[94,95] were synthesized by Integrated DNA Technologies using gBlocks Gene Fragments service and assembled into pLenti-CMVtight-Egfp-Puro vector. The Tet-on promotor was then replaced with the engineered COL10A1 promotor. The engineered COL10A1 promotor was synthesized with 1 or 3-cis enhancers using the Gibson Assembly method to produce 1cis-Luc-mir30-shRUNX2 and 3cis-Luc-mir30-shRUNX2 **(Figure 1-1)**. Scramble controls were synthesized similarly by using the same backbone and scrambling the shRUNX2 sequence to create a non-specific oligonucleotide sequence which doesn't target any genes. Lentivirus were produced by the University of Michigan Vector Core.

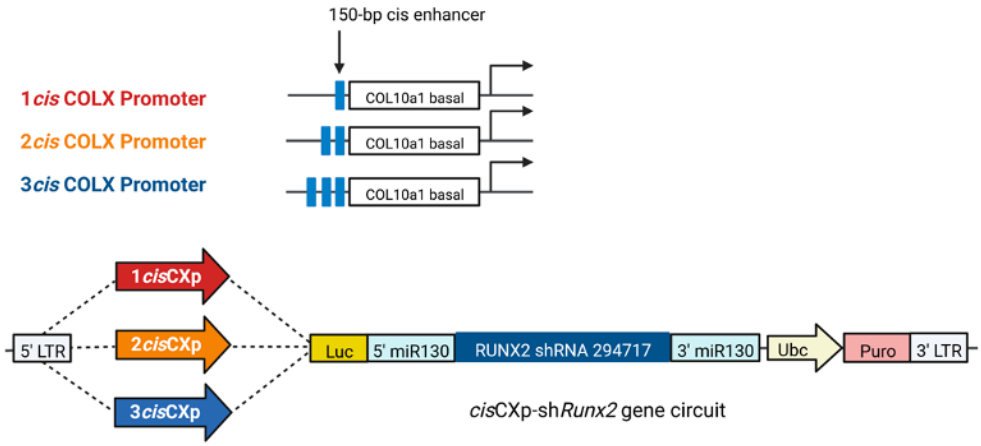

Figure 3-1: Map of RUNX2 suppressing gene circuits made of either 1, 2 or 3 cis-enhancer sequences.COL10a1 basal promoter provides chondrocyte specificity and number of cis enhancers provide tunability of the circuit to RUNX2 concentration. Luciferase provides reporter activity and miRNA30 sequences flanking the shRNA (or Scramble) help in post transcriptional processing of shRNA. Downstream of Ubc constitutive promoter, there is puromycin selection marker.

3.2.2 Lentiviral Transduction

In a 6-well plate, $1x10^5$ cells were exposed to lentiviral supernatant at moieties of infection (MOI) = 5 in the presence of 5 µg/ml polybrene (Sigma) without antibiotics for 24 hours[96]. Cells were then selected using 2 µg/ml puromycin (Sigma) for 48 hours. Cells were then expanded further.

3.2.3 OA Cell Source

De-identified distal ends of femurs from patients undergoing total knee replacement were obtained from one patient. Patient sex and age were provided and cartilage of OA grades 1 and 2 were identified by our collaborator, Dr. John Grant. and tissue was harvested from condylar regions of femur of OA grade 1 or 2 shown in **Figure 1-2**. Chondrocytes were isolated by mincing cartilage and digesting with 0.1% collagenase II (Worthington) for 16 hours in Ham's F12 (Gibco) medium with 5% FBS. Cells were plated at 20,000 cells/cm^2 and cultured in growth media containing low-

glucose DMEM (Gibco), 10% fetal bovine serum (FBS) (Invitrogen), 1% antibiotic-antimycotic (Invitrogen), 1 ng/ml transforming growth factor beta (TGFβ1) (Shenandoah), 5 ng/ml fibroblast growth factor (FGF-2) (Shenandoah) and 10 ng/ml platelet derived growth factor (PDGF-BB) (Shenandoah) at 37 °C, 5% CO_2.[147,148] HACs were trypsinized and sub-cultured every three days. Population doublings were calculated by: PD = 3.32[log (final cell #) – log (initial cell #).

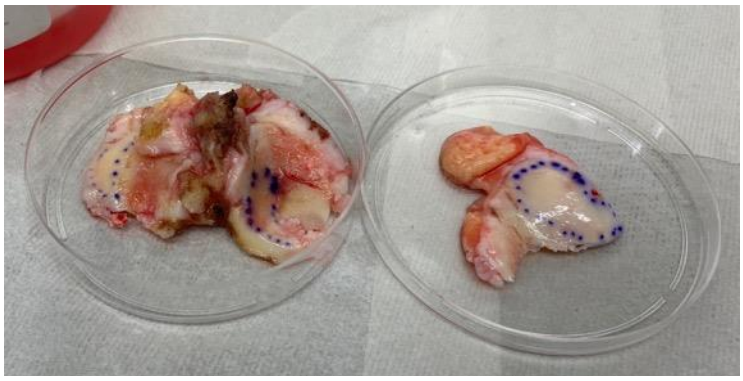

Figure 3-2: OA patient samples. Tissue from OA patients. OA grades of 1 and 2 are outlines with blue pen and tissue was only harvested from these regions.

3.2.4 Scaffold-free Culture

Pellets were created by adding $0.25x10^6$ cells suspended in redifferentiation media to wells of U-bottom, 96-well plates (Fisher). Plates were spun down at 1000x*g* and allowed to condense for 3 days. Redifferentiation media contained high-glucose DMEM, 1.25 mg/mL bovine serum albumin (BSA) (Fisher), 1mM sodium pyruvate (Invitrogen),10^{-7} M dexamethasone (Sigma), 50 μg/ml ascorbic 2-phosphate (Sigma), 40 μg/ml L-proline (Sigma), 10 ng/ml TGFβ1, 1% ITS+ Premix (Corning), 1% antibiotic-antimycotic. [148,149] Cultures were maintained for 28 days and media was changed every other day. An experimental design is shown in Figure 1.1, the experiment was repeated three times with the same donor.

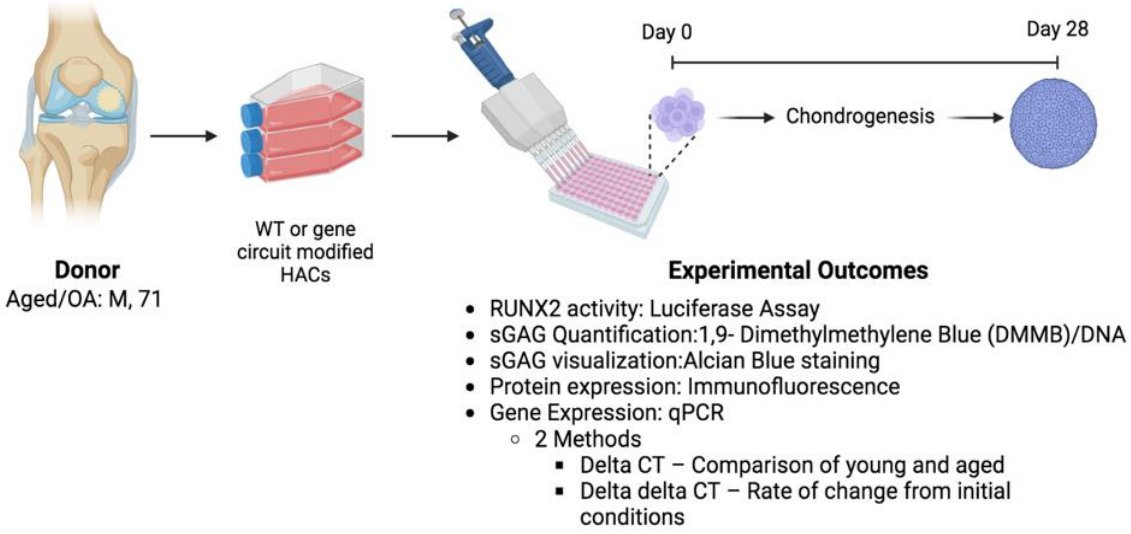

Figure 3-3: Experimental design. An aged/OA donor was transduced with shRUNX2 gene circuits and the corresponding scramble circuits. Then modified and wildtype cells were then placed into redifferentiation media in 3D pellet culture for 28 days.

3.2.5 Luciferase Assay

Luciferase activity was measured at every media change. Chondrogenic media was replenished 6 hours before the assay. D-Luciferin (BioVision) was added to the media at a final concentration of 150 μg/mL and incubated for 20 minutes at 37 °C. Luminescence was measured using a Synergy H1 plate reader (BioTek). Chondrogenic media was replenished after readings.

3.2.6 Histological Analysis

Pellets were washed twice with PBS and fixed with 10% neutral buffered formalin at room temperature for 30 minutes. Fixed pellets were washed with PBS followed by 70% ethanol. Pellets were dehydrated with an ethanol-xylene series prior to paraffin embedding and sectioning. Sections were deparaffinized and stained with Alcian Blue (1% in 3% Acetic Acid, Poly Scientific) and counterstained with Nuclear Fast Red

(Electron Microscopy Sciences) to evaluate proteoglycan accumulation. For immunofluorescence, sections underwent antigen retrieval (BD Pharmingen) and blocking prior to primary antibodies incubation for aggrecan (1:500 dilution in 10% goat serum in 0.1% Triton X100 in TBS), collagen type II (1:100) (Abcam), collagen type X (1:100), RUNX2 (1:100), or MMP13 (1:200), phospho-smad3 (1:100), phospho-smad5 (1:100) , alk1, alk5, (Abclonal), overnight at 4°C. Histological slides were incubated with Goat anti-Rabbit Alexa Fluor™ Plus 488 secondary antibody (Fisher) for 1 hour at room temperature Sections were counterstained with DAPI (Life Technologies) for 5 minutes at room temperature.

3.2.7 Production of Structural Macromolecules

Pellets were harvested, frozen at -80°C and digested in 0.3 units/ml papain (Sigma) in a buffer of L-cysteine hydrochloride (Sigma), ethylenediaminetetraacetic acid (EDTA) (Sigma), and sodium phosphate dibasic (Sigma) buffer solution at 65°C for 16 hours. Cartilage matrix accumulation was measured using the 1,9-dimethylmethylene blue (DMMB) assay as previously described[56,150,151]. A standard curve was generated using known concentrations of chondroitin-6-sulfate (Sigma) in duplicate and samples were run in triplicate. DMMB dye was added to each well and absorbance was measured using a Synergy H1 plate reader at wavelengths 525nm and 595nm.

Matrix production was normalized by DNA content as determined using the PicoGreen assay (Thermo Fisher). A standard curve was generated according to the manufacturers instructions using λ DNA in duplicate and samples were run in triplicate. The plate was incubated for 5 minutes at room temperature in the PicoGreen-Tris dye

solution and fluorescence was measured using a Synergy H1 plate reader at excitation wavelength 498nm and emission wavelength 528nm.

3.2.8 Gene Expression

Analysis of gene expression was performed as previously described [56,151,152]**.** After experiment completion, pellets were washed with PBS and flash frozen in liquid nitrogen and stored at -80°C until processing. Briefly, pellets were homogenized in TRI Reagent RT (Molecular Research Center). Following homogenization, bromoanisol was added for phase separation and RNA was precipitated using isopropanol. Purified RNA was resuspended in Ultrapure DI water and concentration was quantified using a Thermo NanoDrop 2000. RNA purity was assessed using the A_{260}/A_{280} and A_{260}/A_{230} ratios measured by the NanoDrop. Values greater than 1.7 were considered suitable for downstream applications[153].

Following RNA extractions, cDNA was synthesized using High-Capacity cDNA Reverse Transcription Kit (Life Technologies) using 1μg RNA/sample according to the manufacturer's protocol. Gene expression was analyzed using Fast SYBR Green PCR Master Mix (Life Technologies) on Applied Biosystems 7500 Fast qPCR machine. Primer sequences are listed below in Table 2-1. The mean cycle threshold of housekeeping genes *GUS* and *TBP* (*HK*) was used to determine the fold change of gene expression levels using both the ΔCT and $\Delta\Delta CT$ methods. For the ΔCT method, relative expression levels were calculated as $\Delta CT = CT_{Gene\ of\ interest} - CT_{Housekeeping}$ and fold change was calculated as $2^{-\Delta CT}$. Relative expression levels for the ΔΔCT method were calculated as $\Delta\Delta CT = \Delta CT_{Day\ 28} - \Delta CT_{Day\ 0}$ and fold changes was calculated as $2^{-\Delta\Delta CT}$.

Table 3-1: Primer sequences for qPCR gene expression analysis

Gene	Forward	Reverse
ACAN	GGAGTGGATCGTGACCCAAG	AGTAGGAAGGATCCCTGGCA
COL2A1	CTCCAATGGCAACCCTGGAC	CAGAGGGACCGTCATCTCCA
RUNX2	CCGGAATGCCTCTGCTGTTA	AGCTTCTGTCTGTGCCTTCTGG
COL10A1	GAACTCCCAGCACGCAGAATC	TGTTGGGTAGTGGGCCTTTT
MMP13	TTGCAGAGCGCTACCTGAGA	CCCCGCATCTTGGCTTTTTC
COL1A1	GATCTGCGTCTGCGACAAC	GGCAGTTCTTGGTCTCGTCA
SOX9	GCTCTGGAGACTTCTGAACGA	CCGTTCTTCACCGACTTCCT
TBP	GTGGGGAGCTGTGATGTGAA	TGCTCTGACTTTAGCACCTGT
GUS	GACTGAACAGTCACCGACGA	ACTTGGCTACTGAGTGGGGA

Abbreviations: ACAN, aggrecan; COL2A1, collagen type II; RUNX2, runt-related transcription factor 2; COL10A1, collagen type X; MMP13, matrix metalloproteinase 13; SOX9, SRY-Box transcription factor 9; COL1A1, collagen type I; IL6, interleukin 6; NFKB, nuclear factor kappa B; TBP, tata binding protein; GUS, glucuronidase beta

3.2.9 Statistical analysis

All data is presented as mean ± standard deviation (SD). Each point on a graph represents an experiment. All statistical analysis was performed using GraphPad Prism 8.3 software (GraphPad). One-way ANOVA was used with Šídák multiple comparison post-hoc test. P-value <0.05 was considered statistically significant.

3.3 Results

To measure the level of RUNX2 activity suppression achieved by each gene circuit, the luciferase activity of containing shRUNX2 was compared to its respective scrambled control (1-cis or 3-cis). The luciferase assay shows that the 3-cis shRUNX2 suppresses RUNX2 activity to a greater extent than the 1-cis shRUNX2 gene circuit **(Figure 3-4)**. We observed a peak at day 11 where the suppression levels of the 1-cis and 3-cis gene circuits were 78% and 92% respectively. Hence, we labelled 1-cis-shRUNX2 as low

suppression and 3-cis-shRUNX2 as high suppression for the rest of this study. RUNX2 activity was the highest in the first 3 days of chondrogenic culture – indicating that OA chondrocytes are expressing high levels of RUNX2 during expansion and in the early process of redifferentiation.

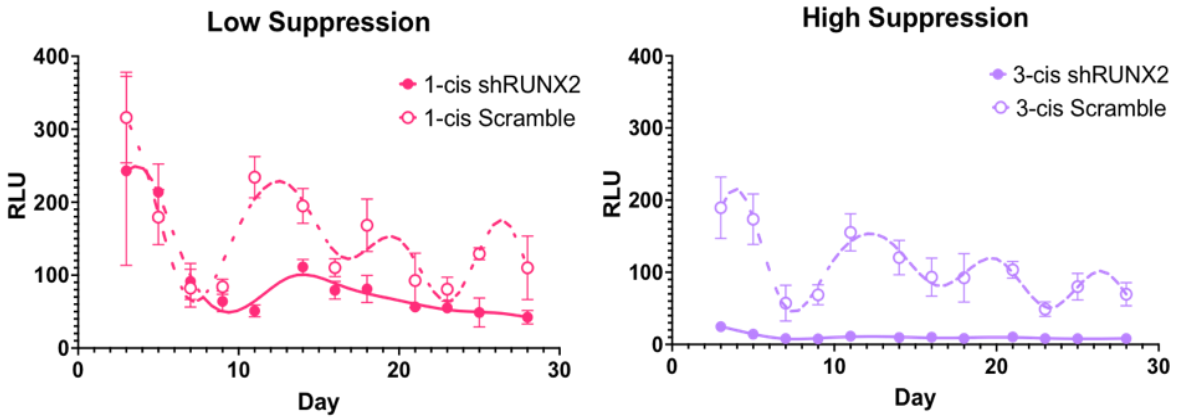

Figure 3-4: Luciferase activity of low and high suppressing RUNX2 gene circuits. Scramble (white-filled) show RUNX2 activity and is higher than the shRUNX2 circuits (solid-filled). Data shown is from one experiment. Other experiments can be found in Appendix E.

Alcian blue staining shows more robust staining throughout the pellet in the high suppressing group compared to both wildtype and low suppressing. Scramble pellets for both suppression levels showed a phenotype with more cells in round lacunae compared to wildtype cells **(Figure 3-5a)**. Genetically modified cells had higher matrix accumulation compared to wildtype cells. Matrix accumulation of both scramble groups was similar to wildtype cells **(Figure 3-5b).**

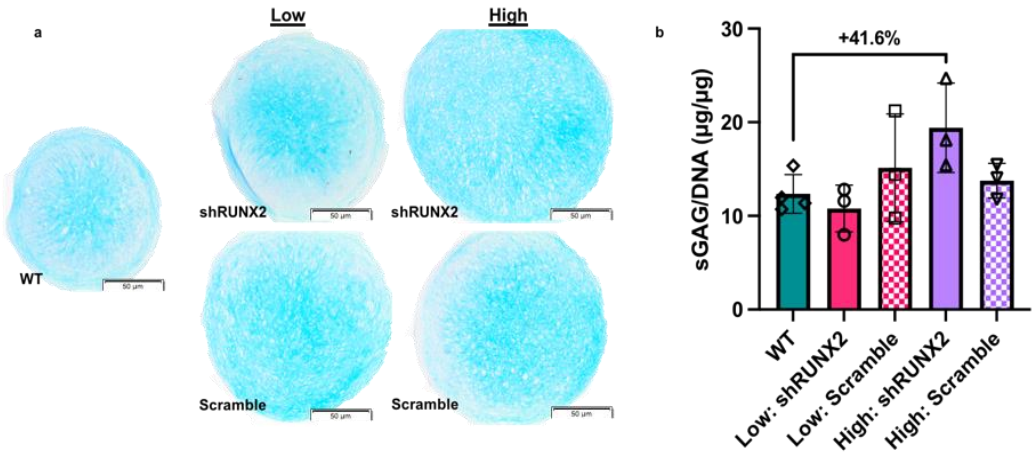

Figure 3-5: Matrix accumulation of genetically modified OA cells. (a) Alcian blue staining of wildtype and modified pellets at day 28 of pellet culture. Scale = 50m (b) sGAG quantification of modified and WT cells. Data is presented as mean SD. Each point represents a different experiment (n=3). Percent difference is identified.

Figure 3-6 shows gene expression analysis after 28 days of redifferentiation. Expression of *SOX9*, *ACAN* and *COL1A1* was similar between WT and all levels of RUNX2 suppression when compared to housekeeping genes.

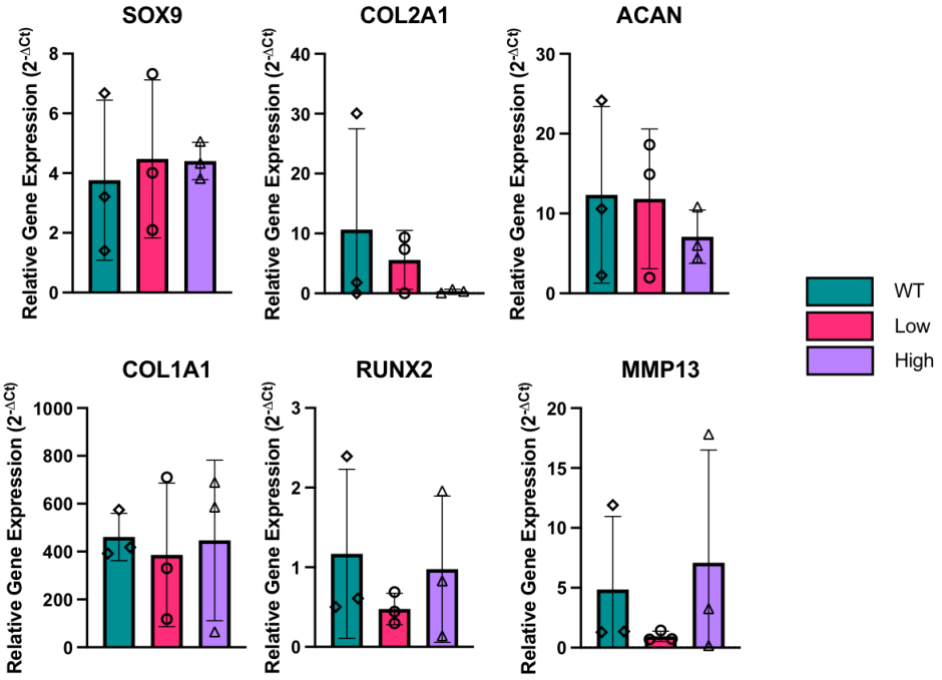

Figure 3-6: Gene expression after redifferentiation. Gene expression of chondrogenic (top) and hypertrophic (bottom) genes after redifferentiation. Expression is normalized to housekeeping genes at day 28. Data is presented as mean SD. Each point represents a different experiment (n=3).

Figure 3-7 shows gene expression analysis compared to the cells before initiating chondrogenesis at day 0. Expression of *SOX9*, *ACAN* and *COL1A1* was similar between WT and all levels of RUNX2 suppression. Cells with low suppressing circuits showed higher *COL2A1* expression compared to both WT and high suppressing circuits. Both circuits expressed *RUNX2* at a lower level compare to WT cells. However, the high suppressing group expressed *MMP13* and *COL10A1* at a higher level than WT and low suppressing cells.

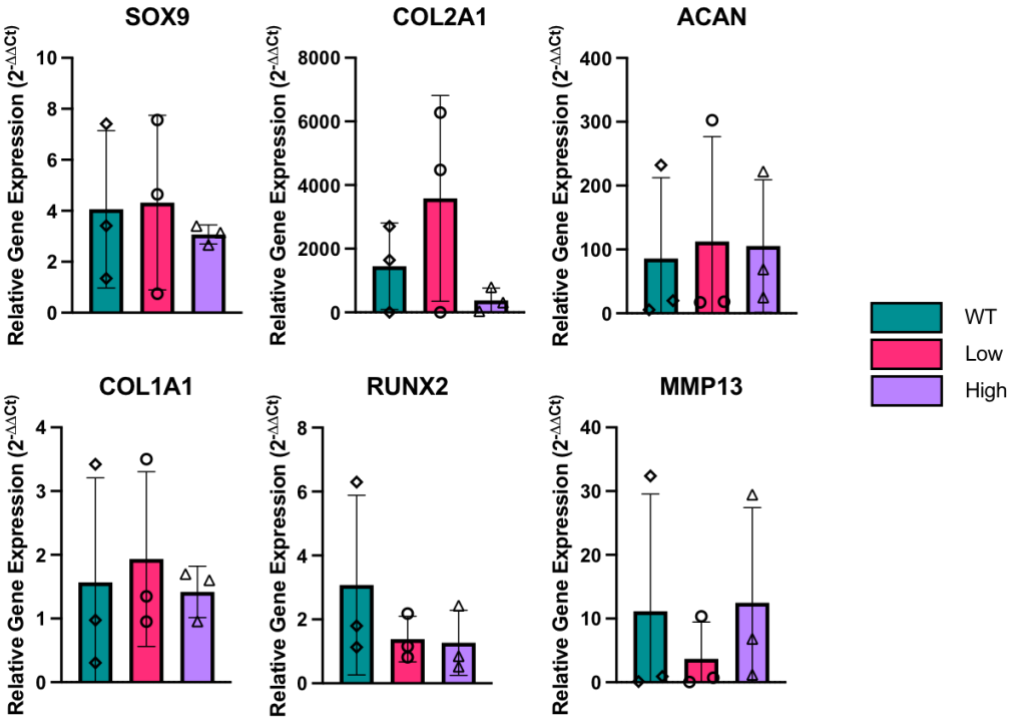

Figure 3-7: Gene expression after redifferentiation compared to day 0. Gene expression of chondrogenic (top) and hypertrophic (bottom) genes after 28 days of redifferentiation. Expression is normalized to housekeeping genes and day 0 of culture. Data is presented as mean SD. Each point represents a different experiment (n=3).

Protein expression of chondrogenic markers shows increasing aggrecan and collagen type II protein expression with increasing RUNX2 suppression levels. **(Figure 3-8)**.

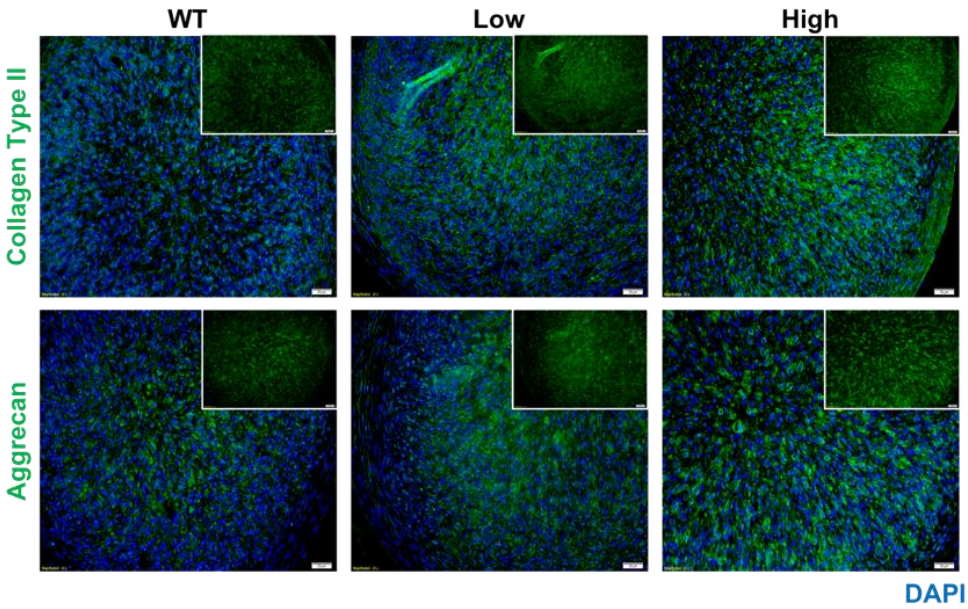

Figure 3-8: Protein expression of chondrogenic proteins. Aggrecan and collagen type II (green) immunofluorescence to visualize protein expression. Scale = 50μm. Insets contain images without DAPI counterstain.

Protein expression of hypertrophic genes shows that RUNX2 expression appears to be higher in WT cells compared to RUNX2 suppressing cells **(Figure 3-9)**. The downstream targets of RUNX2, collagen type X and MMP13, appear to be higher expression in WT cells.

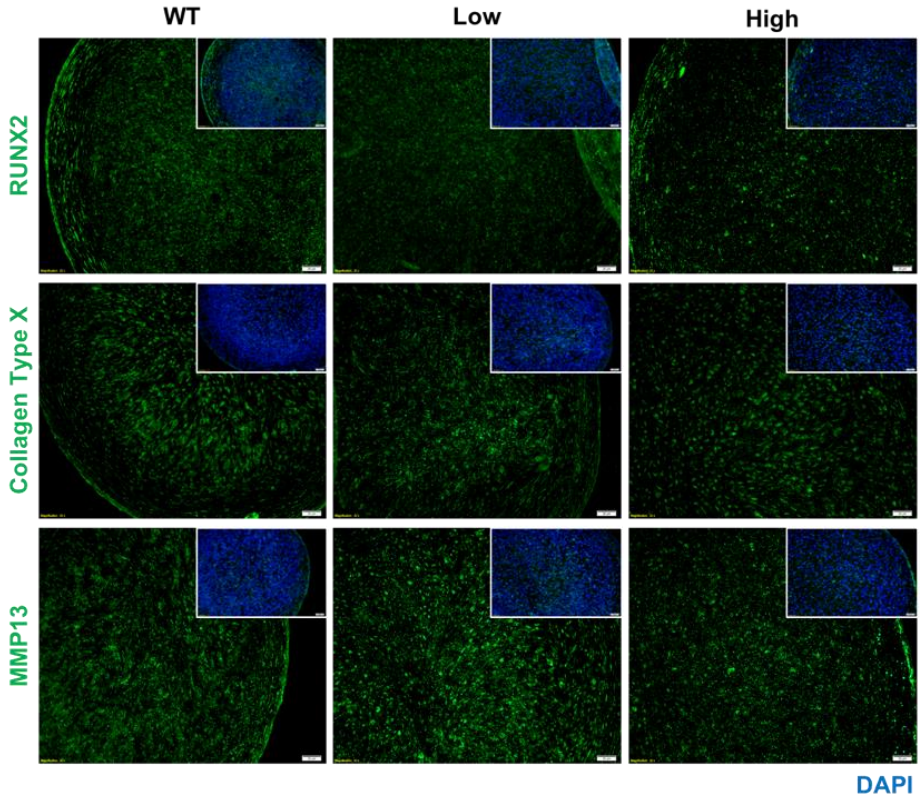

Figure 3-9: Protein expression of hypertrophic proteins. RUNX2, Collagen X and MMP13 (green) immunofluorescence to visualize protein expression. Scale = 50μm. Insets contain images merged with DAPI counterstain.

The response to TGFβ was probed by looking at the ALK1 and ALK5 receptors and their downstream effectors, SMAD5 and SMAD3. ALK5 and SMAD3 promote the anabolic TGFβ pathway in chondrocytes and protein expression shows that ALK5 and phosphorylated SMAD3 are present in all conditions. **(Figure 3-10)**.

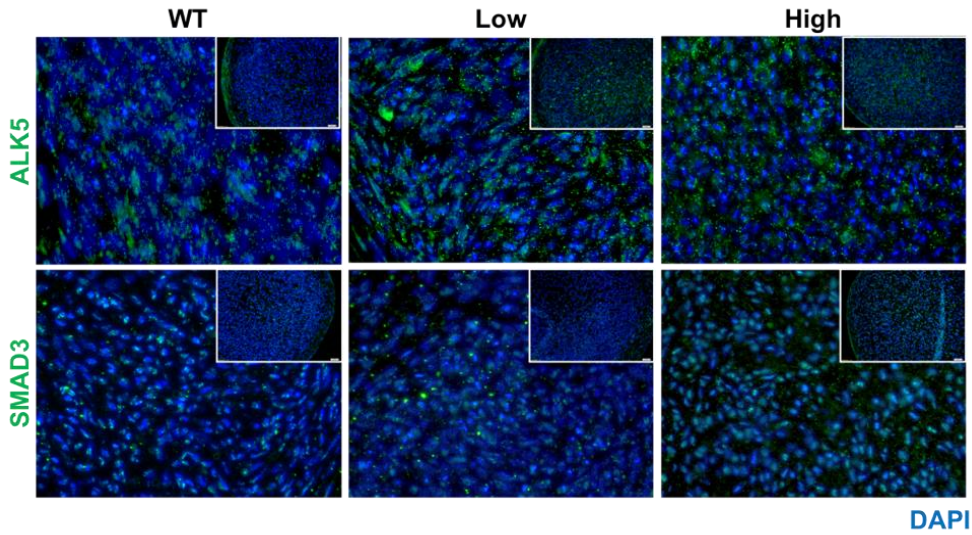

Figure 3-10: Protein expression of chondrogenic TGFβ pathway markers. Protein expression of markers involved in the chondrogenic TGFβ pathway. Images are zoomed in from the insets (Inset Scale = 20μm). Green indicates protein and blue indicates nuclear counterstain (DAPI).

ALK1 and SMAD5 mediate the non-anabolic TGFβ pathway the in chondrocytes and protein expression and OA cells show a shift in the ratio of TGFβ receptors, including an apparent increase in levels of ALK1 compared to young cells. WT cells appears to have higher expression of both ALK1 and SMAD5 compared to RUNX2 suppressing cells **(Figure 3-11)**.

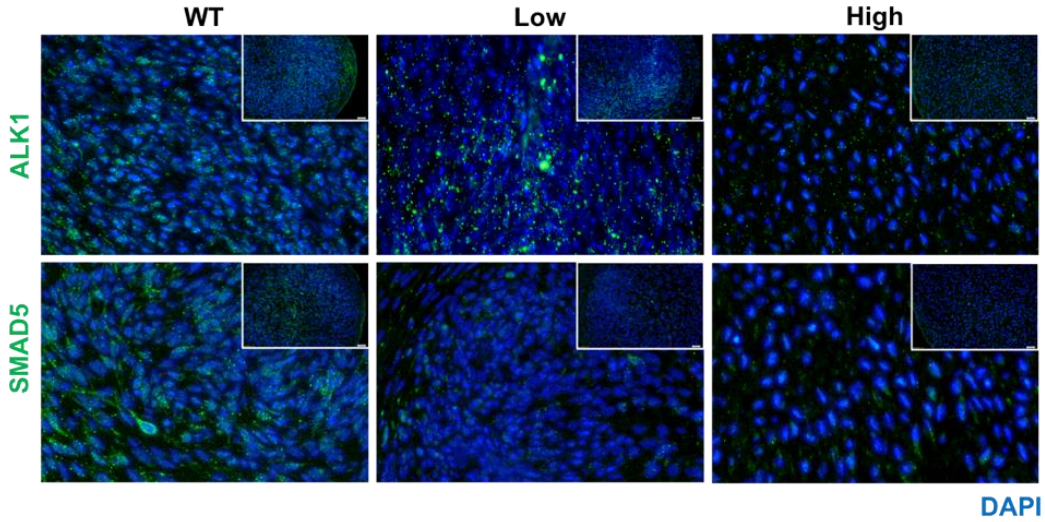

Figure 3-11: Protein expression of hypertrophic TGFβ pathway markers. Protein expression of markers involved in the hypertrophic TGFβ pathway. Images are zoomed in from the insets (Inset Scale = 20μm). Green indicates protein and blue indicates nuclear counterstain (DAPI).

3.4 Discussion

Improving cartilage regeneration in aged patients is a long-standing goal in clinical cartilage repair strategies. RUNX2 drives hypertrophy, a major marker in OA progression, and makes it an ideal target for suppression to improve cartilage regeneration in OA cells[117,118]. However, we and others have shown that RUNX2 is necessary for chondrogenesis and that constitutive suppression of RUNX2 inhibits chondrogenesis[96]. In this study we show that auto-regulated RUNX2 suppression via our gene circuits does not inhibit redifferentiation of OA cells. In addition, we show that a low and high level of RUNX2 suppression changes OA chondrocyte phenotype after redifferentiation (increased sGAG staining and cells in lacunae) and that high suppression improves matrix production in OA cells.

OA chondrocytes produce cartilage matrix but at a lower level compared to young cells[133,158,159,172,182,183]. In this study, we see that the matrix production by OA cells increases with high levels of RUNX2 suppression by the 3-cis circuits. In addition, we show that, in the presence of anabolic growth factors, OA cells maintain matrix production when modified with RUNX2 suppressing gene circuits[158,161].

RUNX2 overexpression leads to an increase in the expression of its target genes MMP13 and COL10A1 and this is also observed in the OA phenotype [184,185]**.** Both levels of RUNX2 suppression led to a decrease in *RUNX2* gene expression but we only observed a decrease in the downstream genes in the low suppressing circuits.

Overall, chondrogenic gene expression was similar between WT and RUNX2 suppressing cells. This indicates that the suppression had little effect on the chondrogenic genotype in OA cells. However, protein expression does indicate that the high suppressing circuit had increased expression of collagen type II and aggrecan as well as decreased expression of RUNX2 compared to both WT and low suppressing cells.

Protein expression analysis through IF appears to show that RUNX2 suppression increased expression of ALK5/SMAD3 and decreased expression of ALK1/SMAD5. Normally, OA chondrocytes are associated with an increase in ALK1 expression associated with an increase in MMP13 expression which can lead to cartilage matrix degradation[91]. RUNX2 is also a key target of the ALK1/SMAD5 TGFβ signaling pathway[186]. TGFβ1 activates both SMAD3 and SMAD5 in OA chondrocytes[187]; SMAD3 inhibits RUNX2 while SMAD5 cooperates with RUNX2 to regulate osteogenic gene expression[188]. The reduction of ALK1 can lead to the reduction of SMAD5 activity which will decrease osteogenic gene expression. The increase in ALK5 expression increases

SMAD3 activity. This could lead to additional suppression of RUNX2 which could be why we see increased staining of SMAD3 and decreased RUNX2 activity in high suppressing cells compared to low suppressing and wildtypes.

There does not seem to be a significant difference in genotype between wild type and RUNX2 suppressing cells. This study suggests that both levels of RUNX2 suppression led to decreased gene expression of *RUNX2* but chondrogenic gene expression was not significantly different with RUNX2 suppression. This study does show that high levels of RUNX2 result in increased matrix accumulation but the lack of significant differences suggests that a higher sample size and additional measures are needed to improve gene expression and matrix accumulation in OA cells. In addition, earlier timepoints should also be evaluated to see if there were more obvious genetic differences before day 28 of culture. Therefore, future studies should incorporate other factors that impact OA cell phenotype including the inflammatory joint environment[189–191]; other target for suppression such as MMP13[93,192], Ihh[193], Sox4[194] and VEGF[93] and other factors such as DNA methylation[195], kinases[92] and micro RNAs[196].

3.5 Conclusion

Clinical application of autologous cartilage repair strategies is dependent on the ability of OA HACs to increase production of cartilage extracellular matrix. In this study, we demonstrate the applicability of synthetic biology tools like auto-regulated gene circuits to improve OA phenotype and increase cartilage matrix production. Our results exhibit that auto-regulated gene circuits are a valid approach to suppress RUNX2 and other targets without the need for exogenous cues that can have potential off-target effects.

Chapter 4 High Level of Expansion Combined with IL-1β Treatment Leads to the Development of a Chondrosenescent Phenotype

4.1 Introduction

There are a number of risk factors for OA including joint malalignment, obesity and joint injury—but the most prominent risk factor for OA development is aging[197] . Inflammaging, defined as chronic low-level inflammation, is thought to be a driving force behind age-related pathologies such as diabetes mellitus[99–101] atherosclerosis[102] and OA progression[103]. The exact cause of inflammaging is unknown but is thought to be due to accumulation of misplaced and misfolded molecules from damaged cells[104,105]. These molecules can be a source of constant stress leading to activation of the innate immune response. As we age, disposal of these molecules decreases due to decreased autophagy[106,107] which is necessary for normal chondrocyte function[108].

Decreased autophagy and increased inflammation can lead to a senescent-like phenotype, dubbed “chondrosenescence”, resulting in increased OA severity[109]. These cells secrete pro-inflammatory cytokines and matrix degrading enzymes and chemokines, which are characteristic of the senescence associated secretory phenotype (SASP)[110] **(Figure 4-1)**.

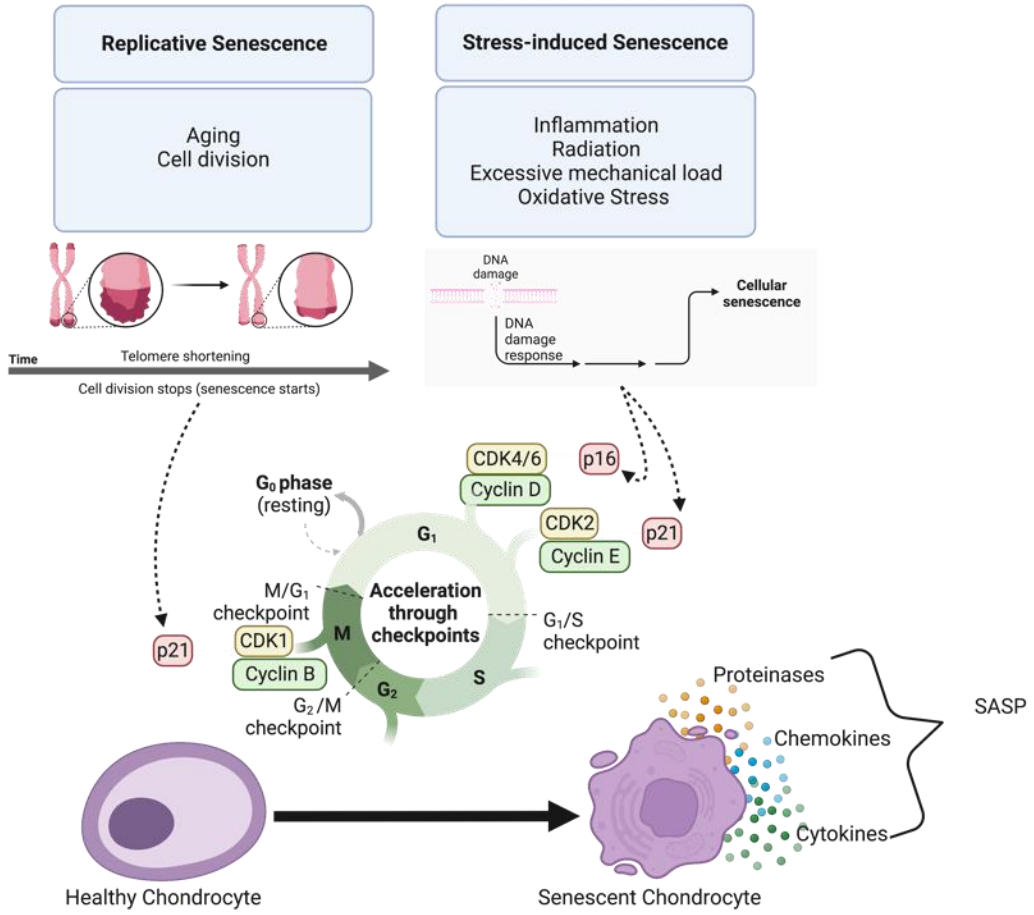

Figure 4-1: Types of chondrosenescence. Senescence can be replicative (left) or stress-induced (right) in chondrocytes. Both lead to growth arrest and take a healthy chondrocyte to a senescent chondrocyte.

Key cytokines known to contribute to OA progression, such as TNF-α and IL-1β, have also been identified as cytokines involved in inflammaging[103,111–113]. IL-1β has been shown to upregulate the transcription factor RUNX2 through the NF-κB pathway in chondrocytes and RUNX2 upregulates pathways that lead to matrix catabolism[79]. Based on this evidence, our scientific premise is that inflammaging leads to the development of chondrosenescence through the RUNX2 pathway. However, the RUNX2-specific pathways that mediate the emergence of the chondrosenescent phenotype is currently unknown.

Chondrosenescence is typically studied using cells from aged patients[133,198], but these cells only show the final phenotype **(Figure 4-2)**. Other models used to investigate the etiology of this phenotype *in vitro* include extensive monolayer expansion, treatment with catabolic stresses including oxidative stress[199], high levels of inflammatory cytokines (10 ng/ml)[200,201], and irradiation[202]. While these models have uncovered some key insights into the biology of senescent cells, there is the need for a model of chondrosenescence that will allow us to study the progression of this phenotype using physiologically relevant inflammatory cytokine concentrations on actively "aging" cells.

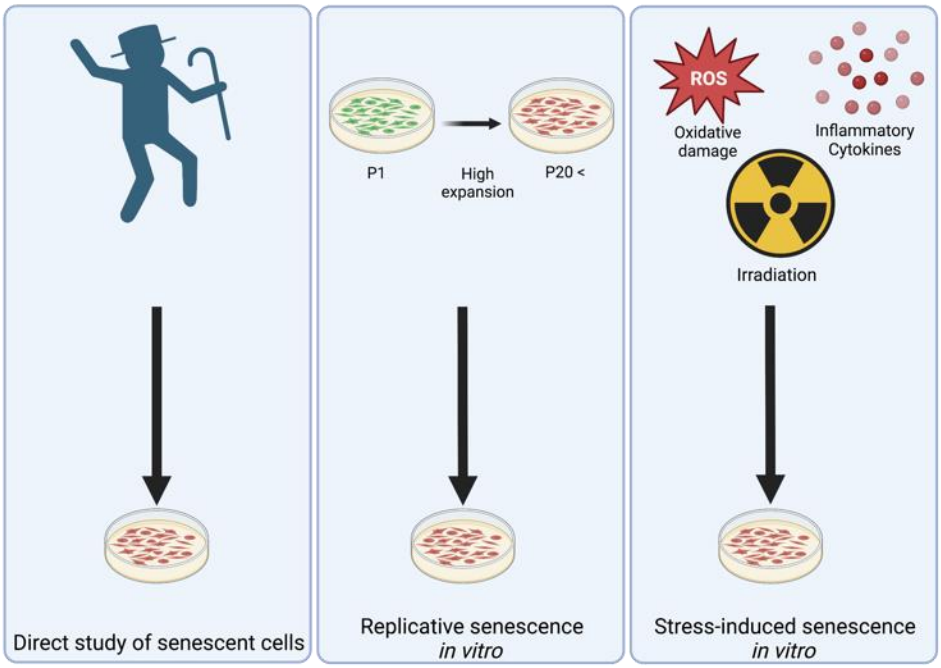

Figure 4-2: Current senescence models. Researchers can induce senescence in multiple ways but a model combining high expansion and inflammatory treatment allows for study on "aging" cells.

Using both simulated DNA damage as a model of cell aging (monolayer expansion) and low-level inflammation (1 ng/mL of IL-1β), we sought to create an in vitro model that replicates the phenotype of chondrosenescence found in patient samples. We hypothesize that treatment of chondrocytes from young patients with inflammatory

cytokines during extensive monolayer expansion will induce biomarker profiles and ECM production levels similar to that of inflammaged human articular chondrocytes (HACs) isolated from aged/OA patient samples. We show that this combined stimulation increased expression of chondrosenescent markers and lowered matrix production upon redifferentiation compared to cells that were expanded without IL-1β, producing a chondrosenescent phenotype.

4.2 Methods

4.2.1 Chondrosenescence Model:

HACs from two young donors (M,19 and M,24) were purchased from StemBioSys. Cells were plated at a density of 20,000 cells/cm^2 in 12-well plates and cultured in growth media containing low- glucose DMEM, 10% FBS, 1% antibiotic-antimycotic, 1ng/ml TGFβ1, 5 ng/ml FGF-2 and 10 ng/ml PDGF-BB[147,148] at 37 °C and 5% CO_2. Cells were expanded with or without the presence of 1ng/mL IL-1β. HACs were sub-cultured every three days and population doublings calculated using: PD = 3.32[log (final cell #) – log (initial cell #)]. Young HACs expanded to passage 4 served as positive controls.

4.2.2 SA-β-gal Expression[98]

Senescence associate beta-galactosidase (SA-β-gal) was assessed through histology (Cell Signaling, 9860). Briefly, cells were fixed and then incubated with β-Gal staining solution for 24-48 hours at 37 °C with no CO_2 as the assay is pH sensitive. SA-β-Gal positive cells (blue) versus total cells were counted in 5 brightfield images in each of 3 samples to calculate the percent of positive cells. Area

of blue staining was calculated using ImageJ.

4.2.3 RNA Sequencing

Total cellular RNA of pooled samples (n=2) was isolated using the RNAeasy kit (Qiagen) for mRNA sequencing. Library construction and sequencing was performed by LC Sciences. Poly(A) RNA sequencing library was prepared following Illumina's TruSeq-stranded-mRNA sample preparation protocol. RNA integrity was checked with Agilent Technologies 2100 Bioanalyzer. Poly(A) tail-containing mRNAs were purified using oligo-(dT)magnetic beads with two rounds of purification. After purification, poly(A) RNA was fragmented using divalent cation buffer in elevated temperature. Quality control analysis and quantification of the sequencing library were performed using Agilent Technologies 2100 Bioanalyzer High Sensitivity DNA Chip. Paired-ended sequencing was performed on Illumina's NovaSeq 6000sequencing system. Firstly, Cutadapt and perl scripts in house were used to remove the reads thatcontained adaptor contamination, low quality bases and undetermined bases[203]. Then sequence quality was verified using FastQC. HISAT2 was used to map reads to the genome of homosapiens[204]. The mapped reads of each sample were assembled using StringTie[205]. Then, all transcriptomes were merged to reconstruct a comprehensive transcriptome using perl scripts and gff compare. Matrix count files were uploaded to the pcaExplorer Shiny application[206] for principle component analysis to identify outliers in data. After these outliers are removed, count files of data from two experimental conditions and their associated conditional matrix files were input into theDESeq2[207] R package version 1.33.452 to identify differentially-expressed genes (DEGs, padj <0.05, based on Wald test with BH-adjustment) between conditions by calculating FPKM: (FPKM = [total_exon_fragments / mapped_reads (millions) ×

exon_length (kB)). Various combinations of conditions will be compared using this method. Lowly-expressed genes (row sums < 10) were removed prior to running the DESeq function. Gene IDs and log 2-fold change values from DESeq results were input into the Panther Classification System[208,209] to compute differential gene ontologies (GOs). GOs were identified according to the Panther statistical enrichment test with the GO biological process complete annotation set. Select GOs from this analysis were represented in figures generated with other R packages.

4.2.4 Monolayer Histological Analysis:

Wells were washed twice with PBS and fixed with 10% neutral buffered formalin at room temperature for 30 minutes. For immunofluorescence, samples were permeabilized (0.5% Triton X100 in PBS) and underwent blocking prior to primary antibody incubation for RUNX2 (1:100 in 10% goat serum in 0.05% Tween in PBS), γH2AX (1:100)m p21 (1:100), p16 (1:100), SOX9 (1:100) and MMP13 (1:200) (Abclonal) overnight at 4◦C. Wells were incubated with secondary antibodies for 1 hour at room temperature. Wells were counterstained with phalloidin (Thermo) for 30 minutes at room temperature and then with DAPI (Life Technologies) for 5 minutes at room temperature. Images were taken on an Olympus microscope.

4.2.5 Scaffold-free Culture:

Pellets were created by adding $0.25x10^6$ cells suspended in redifferentiation media to wells of U-bottom, 96-well plates (Fisher). Plates were spun down at 1000x*g* and allowed to condense for 3 days. Redifferentiation media contained high-glucose DMEM, 1.25 mg/mL bovine serum albumin (BSA) (Fisher), 1mM sodium pyruvate

(Invitrogen),10^{-7} M dexamethasone (Sigma), 50 μg/ml ascorbic 2-phosphate (Sigma), 40 μg/ml L-proline (Sigma), 10 ng/ml TGFβ1, 1% ITS+ Premix (Corning), 1% antibiotic-antimycotic. [148,149] Cultures were maintained for 28 days and media was changed every other day.

4.2.6 Pellet Histological Analysis:

Pellets were washed twice with PBS and fixed with 10% neutral buffered formalin at room temperature for 30 minutes. Fixed pellets were washed with PBS followed by 70% ethanol. Pellets were dehydrated with an ethanol-xylene series prior to paraffin embedding and sectioning. Sections were deparaffinized and stained with Alcian Blue (1% in 3% Acetic Acid, Poly Scientific) and counterstained with Nuclear Fast Red (Electron Microscopy Sciences) to evaluate proteoglycan accumulation.

4.2.7 Production of structural macromolecules:

Pellets were harvested, frozen at -80°C and digested in 0.3 units/ml papain (Sigma) in a buffer of L-cysteine hydrochloride (Sigma), Ethylenediaminetetraacetic acid (EDTA) (Sigma), and sodium phosphate dibasic (Sigma) buffer solution at 65°C for 16 hours. Cartilage matrix accumulation was measured using the 1,9-dimethylmethylene blue (DMMB) assay as previously described[56,150,151]. A standard curve was generated using known concentrations of chondroitin-6-sulfate (Sigma) in duplicate and samples were run in triplicate. DMMB dye was added to each well and absorbance was measured using a Synergy H1 plate reader at wavelengths 525nm and 595nm.

Matrix production was normalized by DNA content as determined using the PicoGreen assay (Thermo Fisher). A standard curve was generated according to the

manufacturers instructions using λ DNA in duplicate and samples were run in triplicate. The plate was incubated for 5 minutes at room temperature in the PicoGreen-Tris dye solution and fluorescence was measured using a Synergy H1 plate reader at excitation wavelength 498nm and emission wavelength 528nm.

4.2.8 qPCR Analysis

Analysis of gene expression was performed as previously described [56,151,152]**.** After experiment completion, pellets were washed with PBS and flash frozen in liquid nitrogen and stored at -80°C until processing. Briefly, pellets were homogenized in TRI Reagent RT (Molecular Research Center). Following homogenization, bromoanisol was added for phase separation and RNA was precipitated using isopropanol. Purified RNA was resuspended in Ultrapure DI water and concentration was quantified using a Thermo NanoDrop 2000. RNA purity was assessed using the A_{260}/A_{280} and A_{260}/A_{230} ratios measured by the NanoDrop. Values greater than 1.7 were considered suitable for downstream applications[153].

Following RNA extractions, cDNA was synthesized using High-Capacity cDNA Reverse Transcription Kit (Life Technologies) using 1μg RNA/sample according to the manufacturer's protocol. Gene expression was analyzed using Fast SYBR Green PCR Master Mix (Life Technologies) on Applied Biosystems 7500 Fast qPCR machine. Primer sequences are listed below in Table 2-1. The mean cycle threshold of housekeeping genes *GUS* and *TBP* (*HK*) was used to determine the fold change of gene expression levels using both the ΔCT and $\Delta\Delta CT$ methods. For the ΔCT method, relative expression levels were calculated as $\Delta CT = CT_{Gene\ of\ interest} - CT_{Housekeeping}$ and fold change was

calculated as $2^{-\Delta CT}$. Relative expression levels for the ΔΔCT method were calculated as $\Delta\Delta CT = \Delta CT_{Day\ 28} - \Delta CT_{Day\ 0}$ and fold changes was calculated as $2^{-\Delta\Delta CT}$.

Table 4-1: Primer sequences for qPCR gene expression analysis

Gene	Forward	Reverse
ACAN	GGAGTGGATCGTGACCCAAG	AGTAGGAAGGATCCCTGGCA
COL2A1	CTCCAATGGCAACCCTGGAC	CAGAGGGACCGTCATCTCCA
RUNX2	CCGGAATGCCTCTGCTGTTA	AGCTTCTGTCTGTGCCTTCTGG
MMP13	TTGCAGAGCGCTACCTGAGA	CCCCGCATCTTGGCTTTTTC
COL1A1	GATCTGCGTCTGCGACAAC	GGCAGTTCTTGGTCTCGTCA
SOX9	GCTCTGGAGACTTCTGAACGA	CCGTTCTTCACCGACTTCCT
IL6	TTCGGTCCAGTTGCCTTCTC	TACATGTCTCCTTTCTCAGGGC
NFKB	GGCTACTCTGGCGCAGAAAT	CTGTACCCCCAGAGACCTCA
TBP	GTGGGGAGCTGTGATGTGAA	TGCTCTGACTTTAGCACCTGT
GUSB	GACTGAACAGTCACCGACGA	ACTTGGCTACTGAGTGGGGA

Abbreviations: ACAN, aggrecan; COL2A1, collagen type II; RUNX2, runt-related transcription factor 2; COL10A1, collagen type X; MMP13, matrix metalloproteinase 13; SOX9, SRY-Box transcription factor 9; COL1A1, collagen type I; IL6, interleukin 6; NFKB, nuclear factor kappa B; TBP, tata binding protein; GUS, glucuronidase beta

4.2.9 Statistical analysis

All data is presented as mean ± standard deviation (SD). All statistical analysis was performed using GraphPad Prism 8.3 software (GraphPad). One or two-way ANOVA was used with Tukey or Šídák multiple comparison post-hoc test. P-value <0.05 was considered statistically significant.

4.3 Results

Population doubling declines with extended passaging and that cells treated with IL-1β proliferate less than controls **(Figure 4-3a).** Quantification of β-gal staining showed an increase at passage 6 for samples treated with IL-1β and that the untreated samples

reach similar levels around passage 8 **(Figure 4-3b)**. **Figure 4-3c** shows representative SA-β-gal images at passage 8.

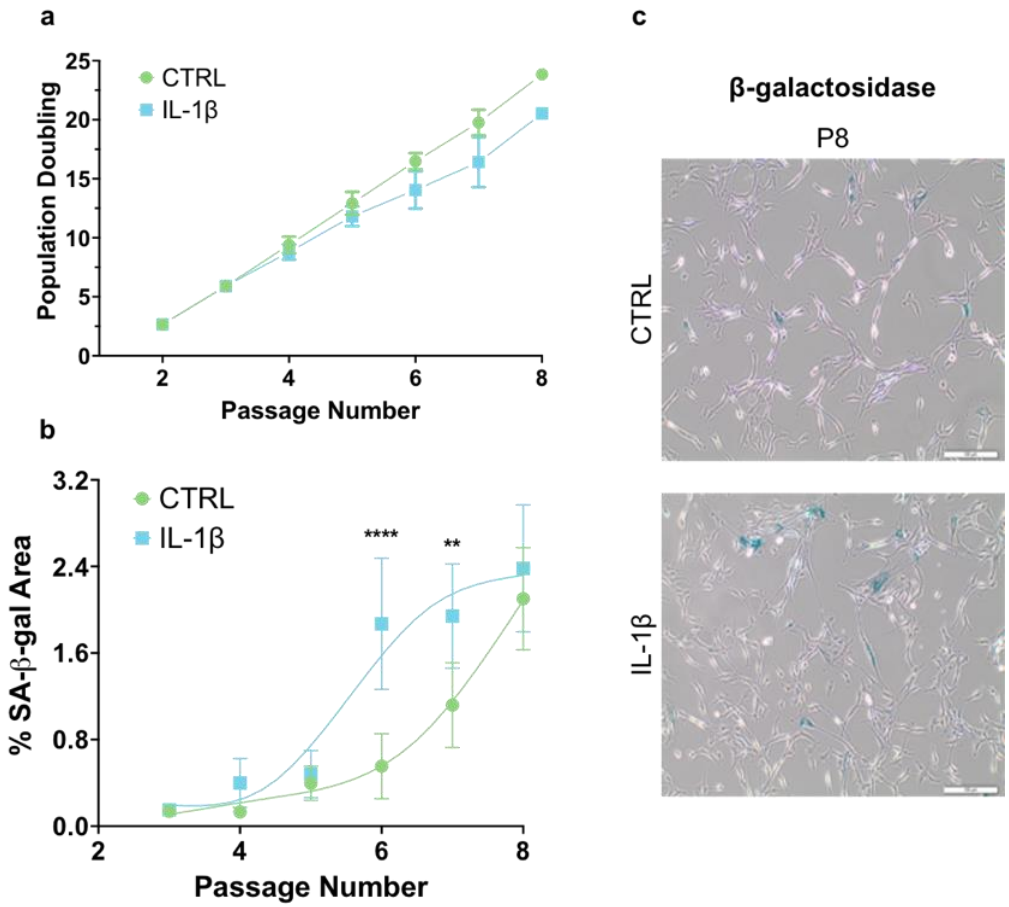

Figure 4-3: Proliferation and SA-β-gal during 8 passages. (a) Population doubling from two experiments. Data is presented as mean ± SD. (b) Quantification of SA-β-gal staining presented as % area. (c) SA-β-gal staining at passage 8. Statistics calculated using a two-way ANOVA with Šídák multiple comparison post-hoc test. ** = p<.002, **** = p< .0001

The SASP is a distinguishing feature of senescent cells. We used RNA-sequencing to evaluate expression of the SASP during expansion and treatment. Gene ontology analysis revealed downregulation of GO terms corresponding to DNA replication (purple) and upregulation of inflammatory response, chemotaxis and ECM disassembly (teal) in treated cells at passage 8 **(Figure 4-5a).** Moreover, at passage 8 we observed

significant upregulation in FPKM values of genes involved in chemotaxis, inflammation, and catabolic markers in both treated and untreated samples, but these levels were 2-3 orders of magnitude higher in IL-1β treated samples **(Figure 4-5b).** Expression of inflammatory and chemotaxis related SASP markers decreased as passage number increased in both populations. Selected markers are shown over time in **Figure 4-5c**.

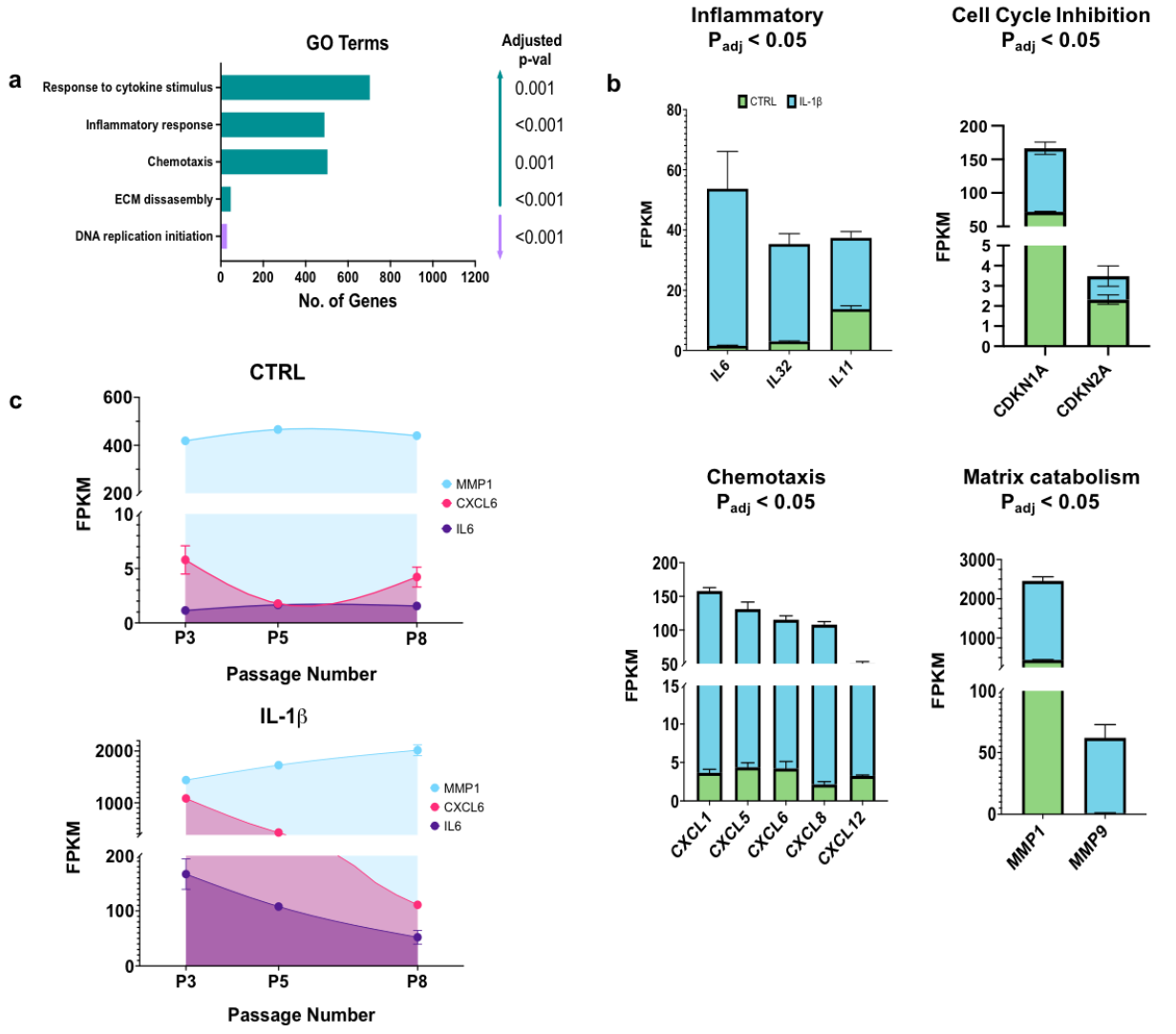

Figure 4-4: Inflammatory treatment increases expression of SASP markers. (a) Gene ontology analysis of treated and untreated cells at passage 8. (b) RNAseq FPKM analysis for expression of inflammatory response, chemotaxis, cell cycle inhibition and ECM disassembly in treated and untreated cells. CTRL = green, IL-1β = blue. (c) FPKM analysis over passage for selected SASP factors in treated and untreated cells.

At each passage, cells were put into pellets and redifferentiated for 28 days. **Figure 4-6a** shows sGAG production of both treated and non-treated cells and **Figure 4-6b** shows DNA amounts. We see that sGAG accumulation and DNA levels decreased in IL-1β treated cells with increasing passage. Levels of sGAG remained relatively similar with increasing passage but DNA levels dropped between passages 5 and 6. Alcian blue shows decreasing sGAG staining with passage number in both groups and decreased pellet size with IL-1β treatment **(Figure 4-6c)**.

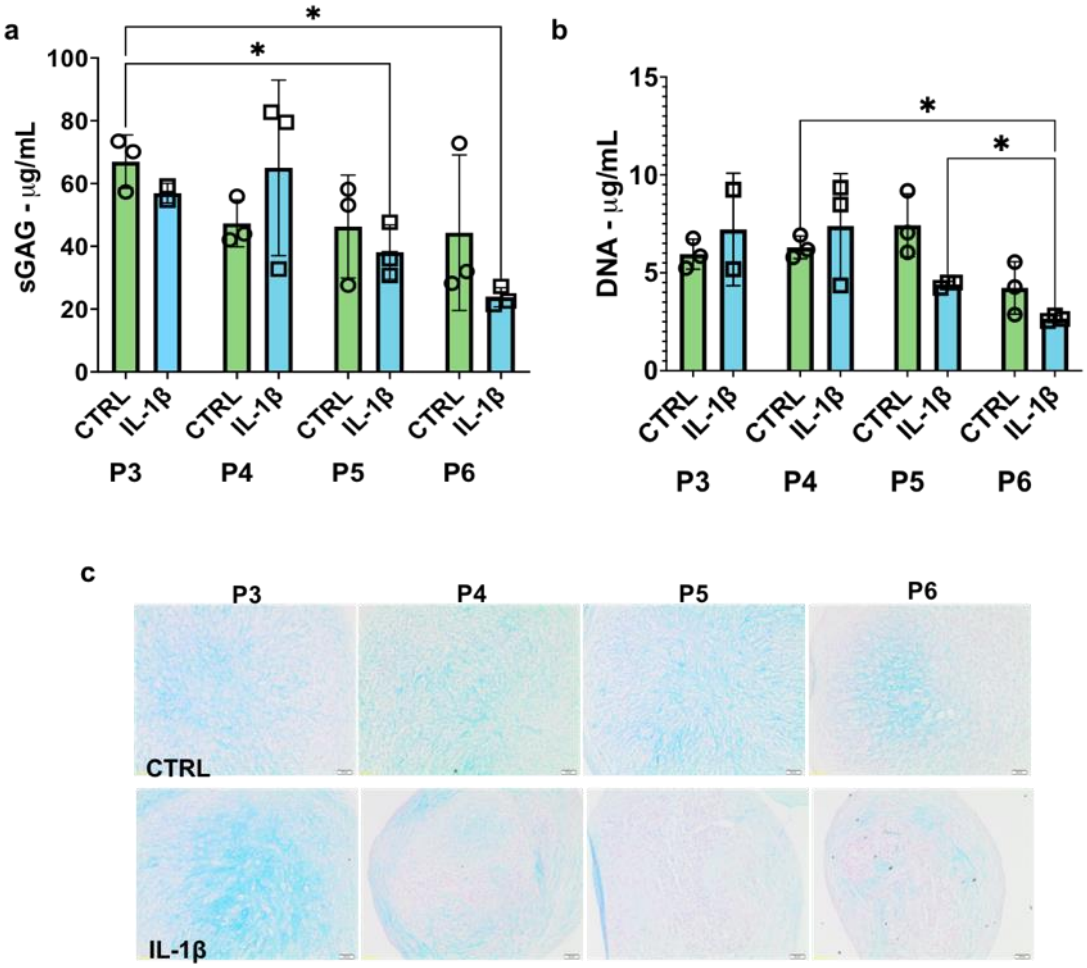

Figure 4-5: Matrix production and DNA content decreases with increasing passage number and IL-1β treatment. (a) sGAG content in pellets from each passage after 28 days of redifferentiation. (b) DNA content in treated and untreated samples after 28 days of redifferentiation. (c) Alcian blue staining of pellets after 28 days of redifferentiation. Scale = 20μm. Statistics calculated using a one-way ANOVA with Tukey multiple comparison post-hoc test. * = $p < 0.05$

Gene expression during expansion showed a decrease in *ACAN* expression with increasing passage number in both treated and untreated cells **(Figure 4-7)**. *SOX9* expression remained relatively constant in both populations.

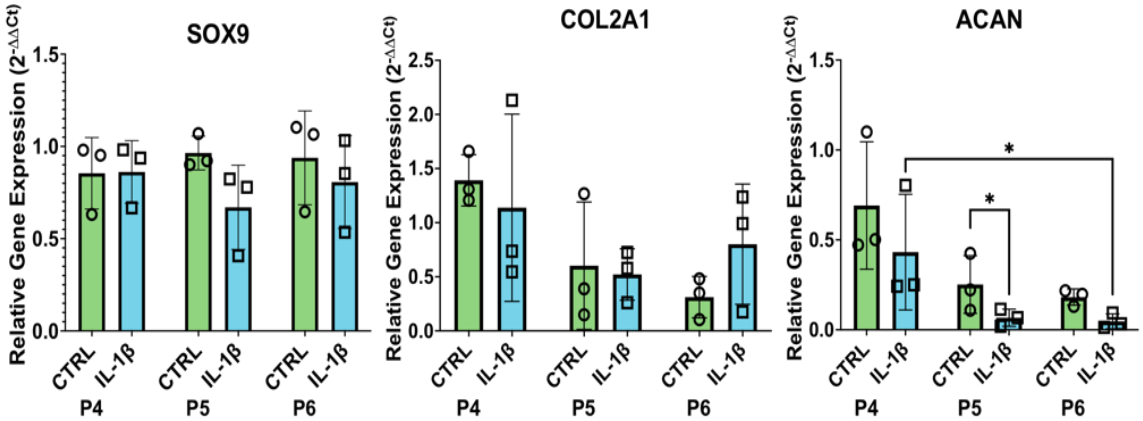

Figure 4-6: Chondrogenic gene expression decreases with increasing passage. Gene expression of chondrogenic genes in treated and untreated cells. Data is presented as mean ± SD. Each point represents a different experiment (n=3). Statistic was performed using a one-way ANOVA with Tukey post-hoc comparison. * = $p < 0.05$

Gene expression of *RUNX2* increased with increasing passage number in both populations but was more highly expressed in treated cells **(Figure 4-8)**. *MMP13* expression was elevated in treated cells but expression decreased over time while it remained constant in untreated cells.

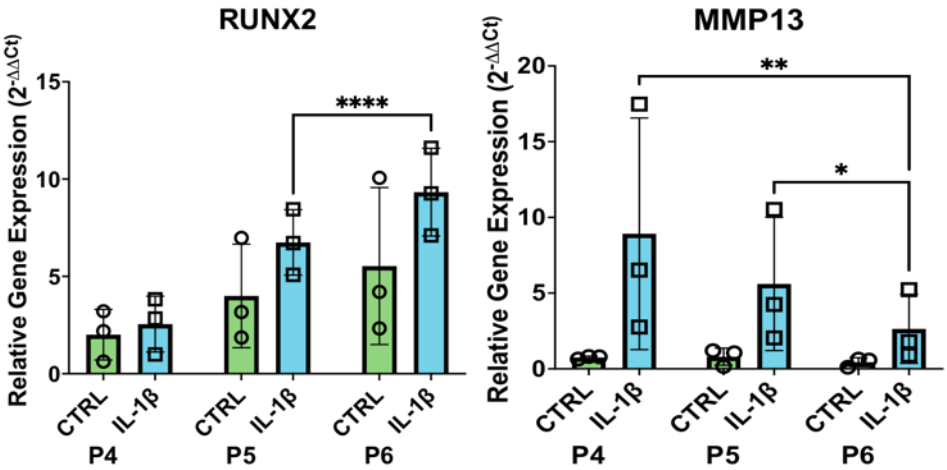

Figure 4-7: Hypertrophic gene expression elevated by IL-1β treatment. Gene expression of hypertrophic gene expression in treated and untreated cells. Data is presented as mean ± SD. Each point represents a different experiment (n=3). Statistic was performed using a one-way ANOVA with Tukey post-hoc comparison. * = $p < 0.05$

We looked at expression of NF-κB which is involved in the regulation of the SASP and IL-6 which was upregulated in our RNA sequencing data **(Figure 4-5b)** and is a major component of the SASP. Gene expression shows increased *NFKB* expression in IL-1β treated cells that remains elevated with extended passaging **(Figure 4-9)**. Expression of *IL6* was 3 orders of magnitude higher in treated cells, similar to the results at passage 8 in our sequencing data. Expression levels remained similar with extended passaging in both groups.

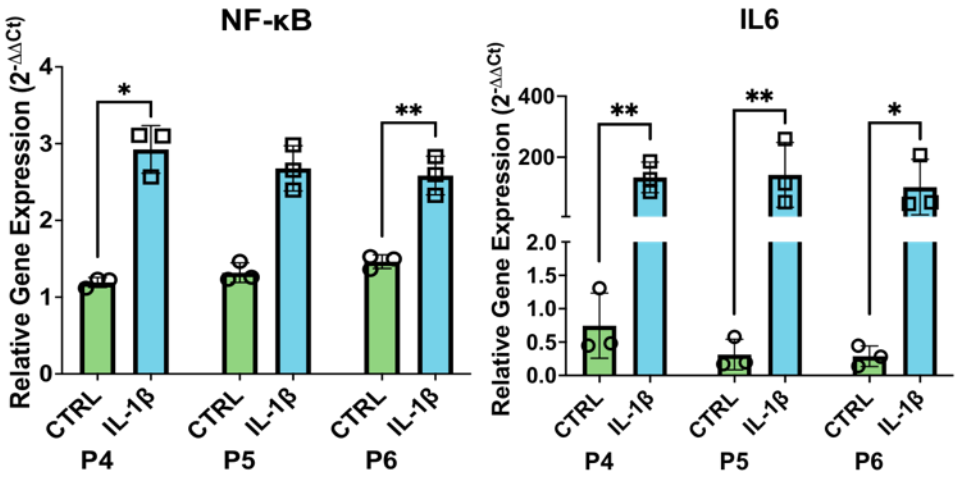

Figure 4-8: IL-1β treatment increases expression of SASP factors. Gene expression of two major SASP factors in treated and untreated cells. Data is presented as mean ± SD. Each point represents a different donor (n=2). Statistic was performed using a one-way ANOVA with Tukey post-hoc comparison. * = $p < 0.05$

To further explore SASP expression and probe for markers of DNA damage, we evaluated protein expression at each passage. When cells are no longer able to divide, the DNA damage response (DDR) occurs, leading upregulation of cell cycle inhibitors[210] such as CDKN1/2A, which leads to protein expression of p16 and p21. This response also leads to the formation of nuclear foci, which can be detected through staining of γ-H2AX, the phosphorylated form of histone H2AX[223–227]. Expression of γH2Ax appeared to remain

constant as passage number increased **(Figure 4-9a)**. P21 is a protein that promotes cell cycle arrest and protein expression of p21 is higher in untreated samples compared to treated samples **(Figure 4-9b)** and appears to decrease at passage 5 for both populations. P16 is another protein that promotes cell cycle arrest and protein expression of p16 increases as cells stop proliferating. At P4, the expression levels are similar between treated and untreated samples. As passage number increased, IL-1β treatment accelerates the expression of p16 (**Figure 4-9c).**

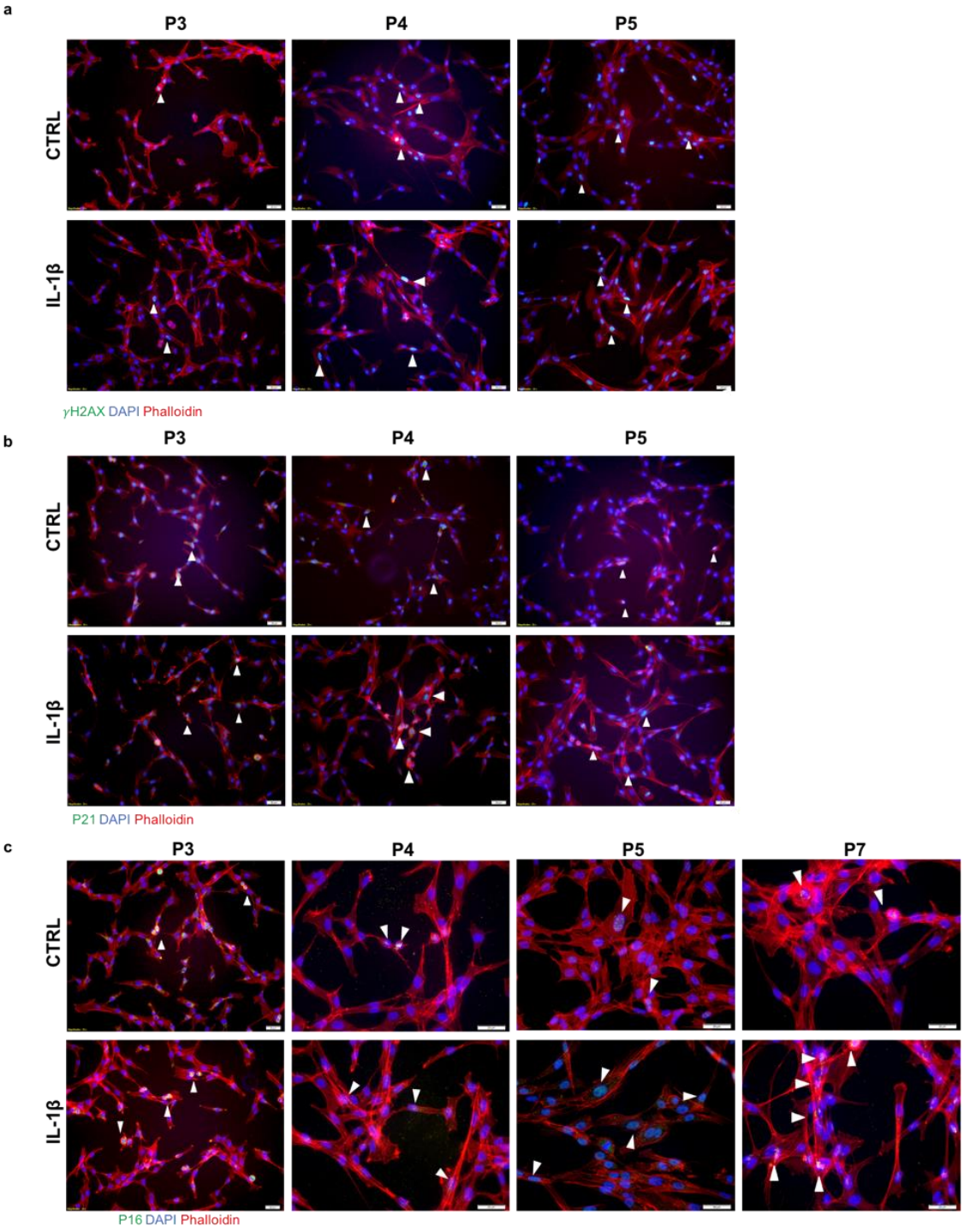

Figure 4-9: SASP expression. (a) γ-H2AX protein expression is similar between conditions (b) p21 protein expression is similar between conditions. (c) p16 protein expression increases with IL-1β treatment. Scale = 20μm

MMP13 is known to degrade cartilage matrix and is a part of the SASP. Expression increases with passage and treated and untreated samples have similar expression until passage 7 **(Figure 4-10a).** When we reach passage 7, IL-1β treatment increases MMP13 expression. RUNX2 expression changes depending on the time in the model **(Figure 4-10b)**. When we reach passage 7, we see that control cells show decreased expression and IL-1β treated samples have higher expression.

4.4 Discussion

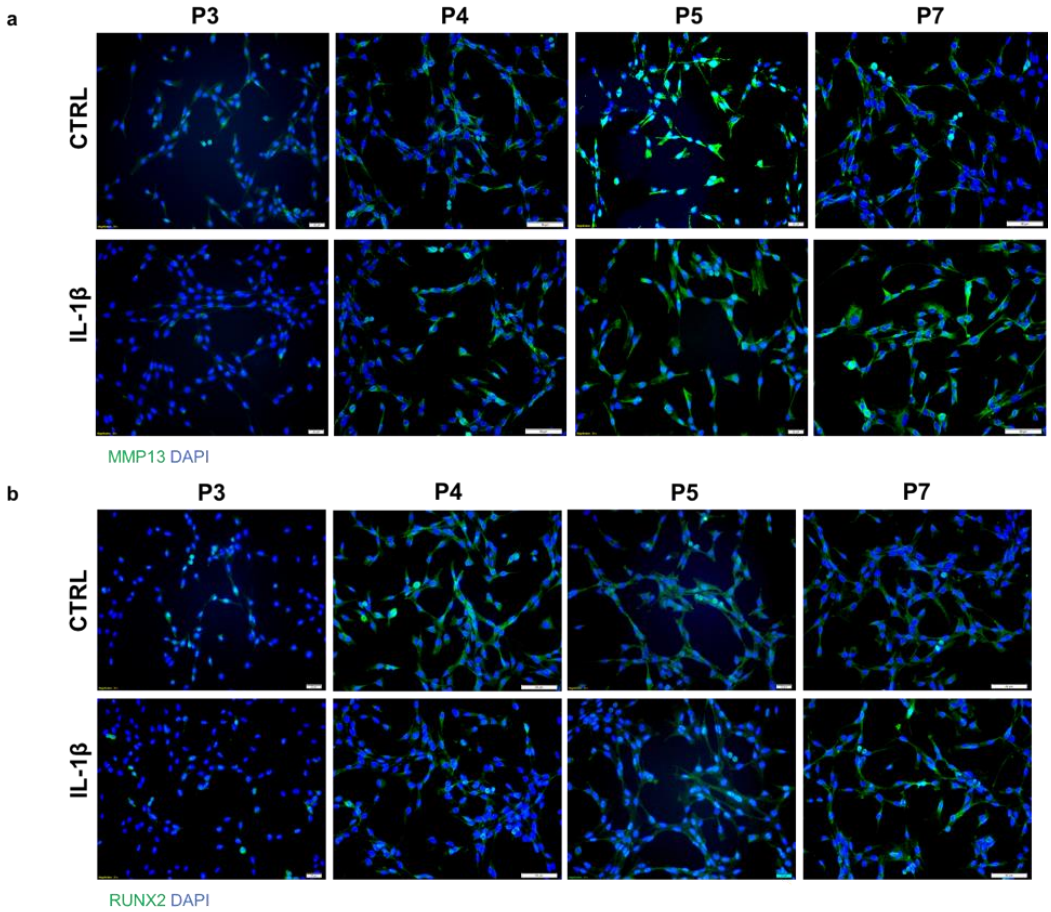

Figure 4-10: Hypertrophic and chondrosenescent markers. (a) MMP13 protein expression is similar between conditions until passage seven. (b) RUNX2 protein expression is higher in untreated samples until passage 7. Scale = 20μm

To improve cartilage regeneration in aged patients, researchers will need to target both major phenotypes seen in OA—hypertrophy and chondrosenescence.

Chondrosenescence can lead to an increase in OA severity[109] and increase the levels of inflammatory cytokines in the OA joint through the SASP[110]. The study of senescent cells is limited by the ability to study the progression of the phenotype clinically in patients. In this study we stimulated the process of chondrosenescence by combining DNA damage (aging) and inflammation (IL-1β) treatment on young cells. We show that this model increases expression of SASP factors in aging and inflamed cells. In addition, we show that this model reduces the redifferentiation potential of chondrocytes. This data suggests that the combination treatment leads to a chondrosenescent cell type that can give us more insight into the chondrosenescence process to improve cartilage repair strategies.

SA-β-gal is a biomarker for the increased lysosome activity or number that occurs in senescent cells[98,213–219]. Researchers have shown that OA chondrocytes express SA-β-gal, indicating that there are senescent cells present in this phenotype *in* vivo. Here we show that simulated DNA damage with and without IL-1β stimulus increases the activity of SA-β-gal and that IL-1β accelerates this activity. This data confirms that the higher inflammatory concentration given in this model (1ng/mL) is exacerbating this expression but a lower expression (0.001ng/mL), closer to the inflammation levels in the joint[220–227], should be explored to see if this trend continues.

Reduced proliferation is a feature observed in chondrosenescent cells[116,179,228,229]. Here, we see that untreated cells continue to proliferate at a steady rate even as we approach passage 8 (PD ~25). Media was supplemented with TGFβ, FGF and PDGFBB which are known to stimulate proliferation and could also explain why the untreated cells continue to proliferate. However, treatment with IL-1β lead to a decrease in proliferation showing that the inflammatory cytokine curbs the proliferation despite the media

additives. This is not surprising as IL1 inhibits proliferation induced by serum/TGFβ in chondrocytes[231–233] and has been shown to block the proliferative effects of PDGF[234]. This model could be improved by evaluated chondrocytes expanded without these growth factors to see if the treatment impacted the outcomes we see in this study.

There are two types of senescence referenced in literature: replicative and stress-induced premature senescence (SIPS). Replicative senescence acts through the p53/p21 pathway SIPS acts through the p38/p16 pathway[235,236]. Chondrosenescent cells have increased expression *p16*^{INK4A} [228,229,237] as well as secretion of pro-inflammatory cytokines and matrix degrading enzymes and chemokines that are characteristic of the SASP[5]. Here we show that IL-1β treatment increased expression of the genes that encode both p21 and p16 at passage 8 **(Figure 4-5b)**, CDKN1A and CDKN2A , respectively. There was similar expression of p16 and p21 protein until passage 7, when p16 levels drop in untreated cells. This data suggests that our model successfully induced both replicative and SIPS in chondrocytes. This more physiologically relevant as both aging and an inflammatory joint environment contribute to the OA phenotype[89,92–94].

The SASP is an important indication of chondrosenescence and many of these factors are also associated with chondrocyte hypertrophy which is the other major phenotype seen in OA. We observed increased RUNX2 and MMP13 gene and protein expression in our senescence model, indicating that the chondrosenescent phenotype involves upregulation of both of these markers similar to the hypertrophic phenotype seen in OA. MMP13 degrades cartilage matrix during hypertrophy and is also expressed in the SASP[200]. Previous studies have shown that chondrocytes expressing p16 also express increased MMP13[200]. MMP13 is known to decrease collagen type II and p21 is shown to

negatively correlate with collagen type II expression[243]. It is possible that increased MMP13 and p16 expression can lead to p21 expression through collagen type II degradation, making it a target for suppression in chondrosenescent cells.

P16 has been targeted in other studies. P16 was eliminated in an injury model but was not sufficient to prevent development of OA[245]. Baker et al. attempted to eliminate senescent cells with a tailored drug through the expression of a transgene that is only expressed in P16(Ink4a)-positive cells[246]. Our model shows that targeting p16 is a viable method as chondrosenescent cells express p16 at every passage. However, p16 is just one cell cycle inhibitor active in senescent cells and is associated with SIPS and our data indicates that p21 pathway, associated with replicative senescence, should also be targeted[235,236].

4.5 Conclusion

Based on our results, we can propose RUNX2 as another viable target to halt chondrocyte senescence and that silencing it may be able to attenuate the effects of chondrosenescent cells. We used 1 ng/mL of IL-1β and did not include the other cytokines seen in the joint for simplicity even though there are multiple inflammatory cytokines in the joint. Several clinical studies measuring the level of cytokines in aging and OA knee joints have identified that the range of concentrations of IL-1β is 0.001-0.3 ng/ml and TNF-α is 0.01-1 ng/ml[220–227]. This is an order of magnitude lower than the concentrations typically used in *in vitro* studies examine chondrocyte response to these factors[135,247–250]indicating a need to refine the model further to get even closer to what has been measured physiologically.

Chapter 5 Conclusions and Future Directions

5.1 Conclusions

Primary chondrocytes are the gold standard for cartilage tissue engineering[22] and are currently used in FDA-approved clinical strategies to repair articular cartilage. The age-related decline in chondrocyte function and the impact of osteoarthritis limits the success of tissue-engineered cartilage products. The goal of this dissertation was to investigate the aged and OA phenotypes and use cell-based methodologies to improve cartilage matrix accumulation.

In the second chapter, we explored the differences between chondrocytes from young and aged/OA donors when regenerated *in vitro*. Next, we investigated the matrix production of OA cells when RUNX2 is suppressed using our previously developed cell-regulated shRUNX2 gene circuit. Finally, we developed an *in vitro* model of chondrosenescence to investigate the pathways that lead to the development of this phenotype.

5.2 Summary

5.2.1 Aim 1: Regeneration Potential of Osteoarthritic Cells is Decreased by RUNX2

To improve regenerative outcomes in aged cells, we first investigated the differences between young cells and aged/OA cells. We observed that young and aged HACs dedifferentiate is a similar pattern when expanded in monolayer. When

redifferentiated, we observed that young cells show increased matrix production and chondrogenic gene expression but that the effect is the opposite in OA cells which show increased hypertrophic gene expression, including high levels of RUNX2. This data suggests aged/OA cells are capable of cartilage regeneration similar to that of young cells if RUNX2 and other pathways are targeted simultaneously.

Overall, we demonstrate that OA cells have regeneration potential but are limited by upregulation of hypertrophic pathways. Therefore, it is necessary to target strategies that can increase chondrogenic gene expression and improve matrix accumulation.

5.2.2 Aim 2: RUNX2 Suppression Increases Matrix Accumulation of Osteoarthritic Chondrocytes

Improving cartilage regeneration in aged patients is a long-standing goal in clinical cartilage repair strategies. RUNX2 drives hypertrophy, a major marker in OA progression, and makes it an ideal target for suppression to improve cartilage regeneration in OA cells[117,118]. In this aim we investigated the effect of varying levels of auto-regulated RUNX2 suppression on cartilage matrix accumulation by OA cells. We show that auto-regulated RUNX2 suppression via our gene circuits does not inhibit chondrogenesis in OA cells. In addition, we show that a low and high level of RUNX2 suppression improves OA chondrocyte phenotype and that high levels of suppression improve matrix production in OA cells.

However, chondrogenic expression does not significantly improves with RUNX2 suppressing circuits though the low suppressing circuit does decrease hypertrophic gene expression. This indicates that it may be necessary to combine RUNX2 suppression with suppression of other factors such as the NF-κB pathway, which is abnormally active in

OA chondrocytes[79]. We should also extend redifferentiation culture to see long term effects of RUNX2 suppression and investigate the effects of suppression in more donors to see if suppression levels are donor dependent.

5.2.3 Aim 3: High Level of Expansion Combined with IL-1β Treatment Leads to the Development of a Chondrosenescent Phenotype

Chondrosenescence can lead to an increase in OA severity[109] and increase the levels of inflammatory cytokines in the OA joint through the SASP[110]. In this aim, we combined aging (expansion) and inflammation (IL-1β) and studied the effect on the development of the chondrosenescent phenotype in young cells. We show that this model increases gene and protein expression of SASP factors and reduces the redifferentiation potential of chondrocytes. In addition, we demonstrate the overlap between genes and proteins that are involved in chondrosenescence and hypertrophy.

Overall, this aim shows that targeting both chondrosenescence and hypertrophy is necessary for improving regeneration by OA cells. RUNX2 drives hypertrophy and is involved in chondrosenescence, presenting a possible role for RUNX2 in driving both phenotypes. This model use lower levels of an inflammatory cytokine and is more physiologically relevant than other models. However, chondrocytes do not proliferate *in vivo* indicating that another method should be used in combination with inflammatory treatments to study chondrosenescence in the future and gain more insight into the phenotype.

5.3 Impact

Strategies to repair cartilage defects in aged patients using autologous cells is still a significant clinical challenge[52,135–137]. There is a need to focus on improving cartilage tissue engineering outcomes using autologous chondrocytes in OA patients since current methods often show subpar results in these patients[52,137]. In this dissertation, I utilized a multidisciplinary approach by combining the fields of synthetic biology and tissue engineering to address these challenges. I demonstrate the application of a synthetic gene circuit that uses auto-regulated RUNX2 suppression in OA chondrocytes to improve regeneration outcomes. In addition, I present models to further investigate the OA phenotype and present other suppression targets that could be used to further overcome the poor outcomes from OA patients.

Auto-regulated RUNX2 suppressing OA chondrocytes have the potential to revolutionize autologous chondrocyte repair. They are able to respond to stimuli without exogenous intervention and improve matrix accumulation and OA cell phenotype, increasing the cells available for clinical procedures. The role of RUNX2 in hypertrophy and chondrosenescence means that autoregulated RUNX2 suppression has the potential to resist hypertrophy and the inflammatory shift seen in chondrosenescence. This shift could help create an environment more conducive to cartilage repair in OA patients **(Figure 5-1).**

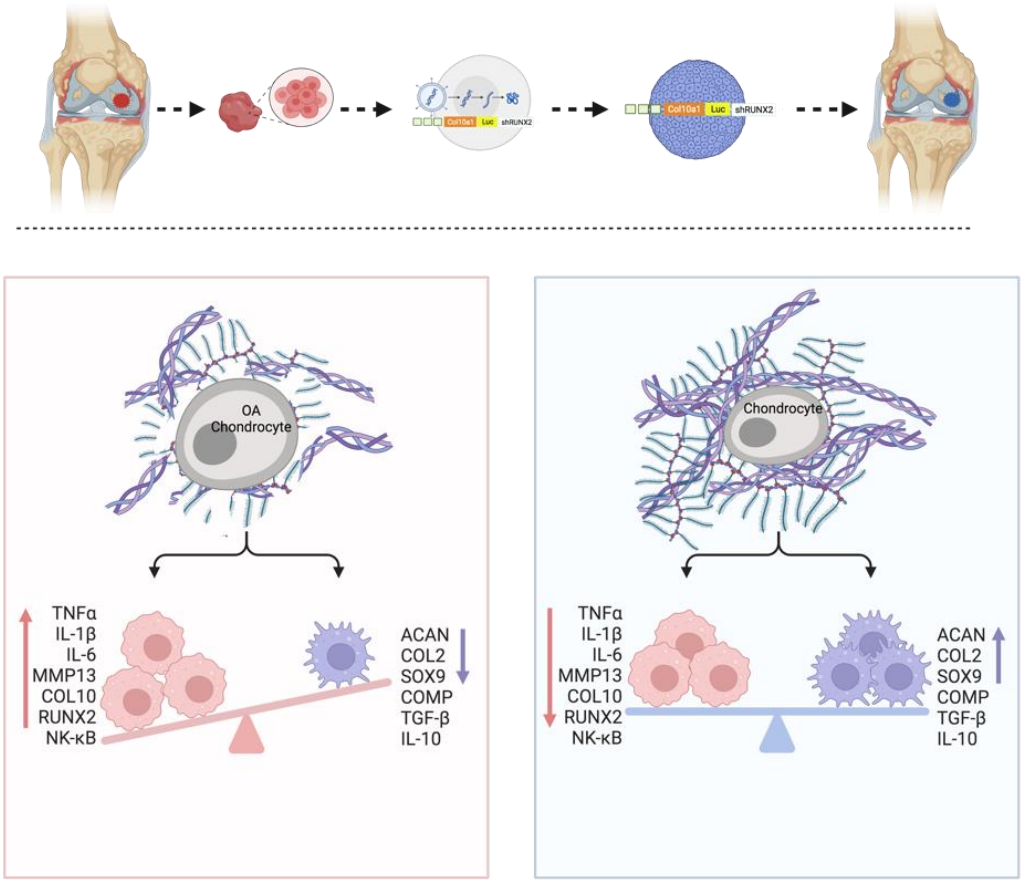

Figure 5-1: Auto-regulated RUNX2 suppression can shift OA phenotype. The pro-inflammatory phenotype seen in OA cells can be shifted with auto-regulated RUNX2 suppression and improve cartilage tissue repair.

5.4 Future Directions

5.4.1 Targeting Chondrosenescent Cells and Other Factors

An obstacle in this thesis and in current clinical strategies is that aged/OA chondrocytes have poor cartilage matrix accumulation. Multiple studies have shown that after the age of 40 increasing age doesn't have an influence on chondrogenic potential[251,252]. This means that the major phenotype is the hypertrophic differentiation seen in OA progression and that aged cells may be exacerbating this progression due to the SASP secreted by chondrosenescent cells[177]. Indeed, Jeon et al. showed that

selective removal of senescent cells from patient-derived OA chondrocytes *in vitro* led to a decrease in senescent and inflammatory markers while increasing expression of cartilage ECM proteins[244]. Combined removal of senescent cells and inhibiting hypertrophic markers in OA cells is a strategy that should be pursued to restore their ability to produce cartilage-like matrix.

Our model induced chondrosenescence with IL-1β treatment, a key inflammatory cytokine involved in inflammaging and OA progression[103,111–113]. IL-1β also activates the NF-κB pathway, which is abnormally active in OA chondrocytes[79] and stimulates the appearance of the SASP[115]. This connection implies that there may be factors that are important to both chondrosenescence and hypertrophy that result in increased OA severity[109]. Based on our data, we're suggesting that RUNX2 is the link between the two phenotypes. We have shown the differences between young and old **(Chapter 2)** and that suppression in OA cells increases matrix production (**Chapter 3).** Additionally, chondrocytes expressing RUNX2 have shown a senescent- like phenotype characterized by flattened morphology and β-galactosidase expression[116,179]. We also show that RUNX2 expression increases with treatment in our model. Coupled with the observations in senescence cells, RUNX2 may play a central role in regulating the cell cycle in response to stress signals and other factors such as inflammaging[179]. The next steps would be to suppress RUNX2 and see the impact on the progression of the chondrosenescent phenotype and on the matrix production of cells from the model.

5.4.2 Using Alternative 3D Culture Methods for Long-Term Culture

Culturing chondrocytes in 3D environments helps them maintain their chondrocyte phenotype *in vitro*. Researchers have used a variety of scaffolds to culture chondrocytes

including agarose[55,147,253], alginate[154], fibrin[254] and synthetic gels[56,255,256]**.** The benefit of using scaffold is that they are similar to the cartilage environment *in vivo* and that it resembles the recently FDA-approved MACI procedure.

Researchers have identified that repairing OA cartilage may require a higher number of cells[183] and scaffold allow for a greater number of cells compared to pellet cultures. Larger pellet sizes than the ones in this thesis are used in literature but can show hypoxia in the center of the pellet indicating that there is a limiting factor of cell number in pellet culture[257–259]. Additionally, scaffolds are often used so that researchers can apply mechanical loads constructs to improve matrix production. This strategy has been effective in early passage chondrocytes, bovine chondrocytes and MdChs[55,61,260,261]. However, these strategies need to be modified for OA cells as high mechanical load is involved in OA pathogenesis and has been shown to induce OA *in vitro*[262,263]. The use of a scaffold and a different mechanical loading scheme, in conjunction with the methods used in this thesis may provide us with the needed stimulus to increase cartilage matrix accumulation.

5.4.3 Identifying Cell Populations within OA Cartilage with Increased Chondrogenic Potential

The use of donor cells in all the strategies results in heterogenous response. Even among young, healthy donors we see varying levels of matrix accumulation when stimulated *in vitro*. OA cells already have a decreased response to chondrogenic growth factors *in vitro* and the varying responses among donors makes it difficult to come up with standardized strategies. We have shown here that many results are similar – but we only explored three donors.

Others have suggested isolating chondroprogenitors from OA cells[264]. Vinod et. al found that chondroprogenitors with low expression of CD34 and high expression of CD166 showed higher glycosaminoglycan and lower calcified matrix deposition[265]. Other MSC markers CD105[266–268], CD146[269], VCAM[270] have also been used to identify this population. This may identify an MSC-like population in cartilage that can be used for cartilage regeneration.

Appendices

Appendix A: Comparison of Chondrogenic Media

Prior to experimentation, we tested different media formulations in both young and aged cells (Chapter 2). We determined that the addition of l-proline and TGF-β enhanced matrix production in both populations.

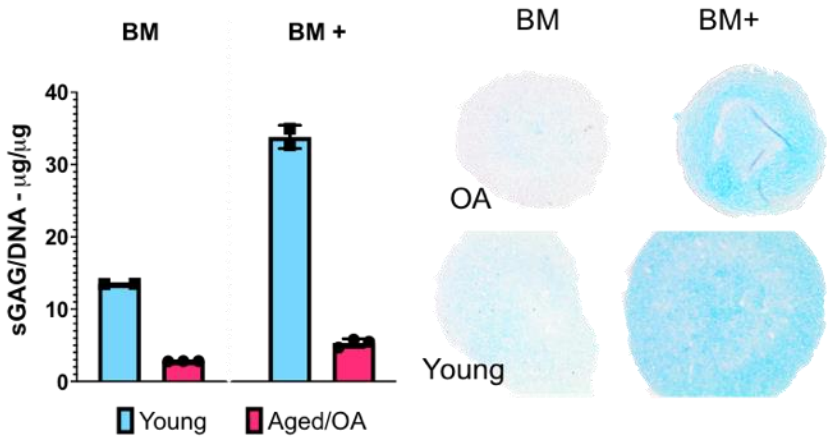

Appendix Figure A-1: Matrix accumulation in different chondrogenic media formulations. (a) sGAG quantification based on biochemical DMMB analysis normalized by DNA (b) Alcian blue stain for cartilage matrix accumulation. Scale = 50 µM

Appendix B: Proliferation in Young and Aged Cells

Young and aged cells differentiated in a similar pattern (Chapter 2), but their growth *in* vitro was different.

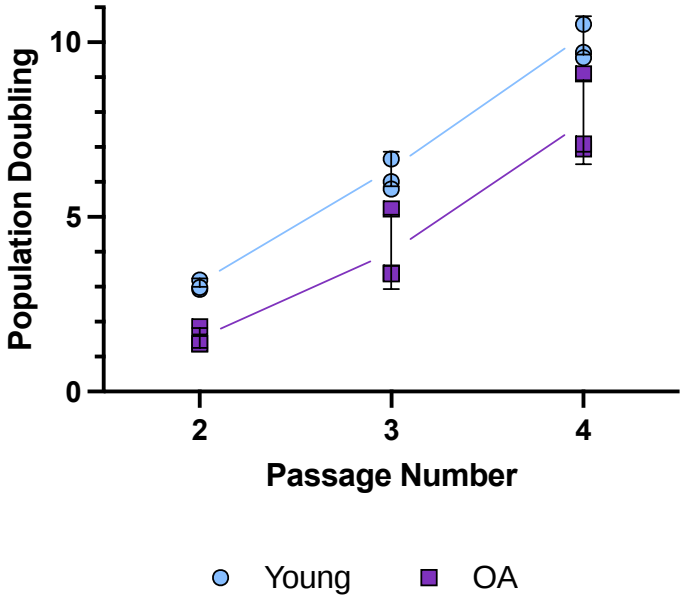

Appendix Figure B-1: Population doubling of young and aged/OA cells. Each donor represents a point on the graph. Overall, young cells proliferated at a higher rate.

Appendix C: Donor Specific qPCR Analysis

qPCR analysis for each donor is presented for both delta CT and delta delta CT analysis in Chapter 2. The averages are shown in the chapters but donor differences can be seen below.

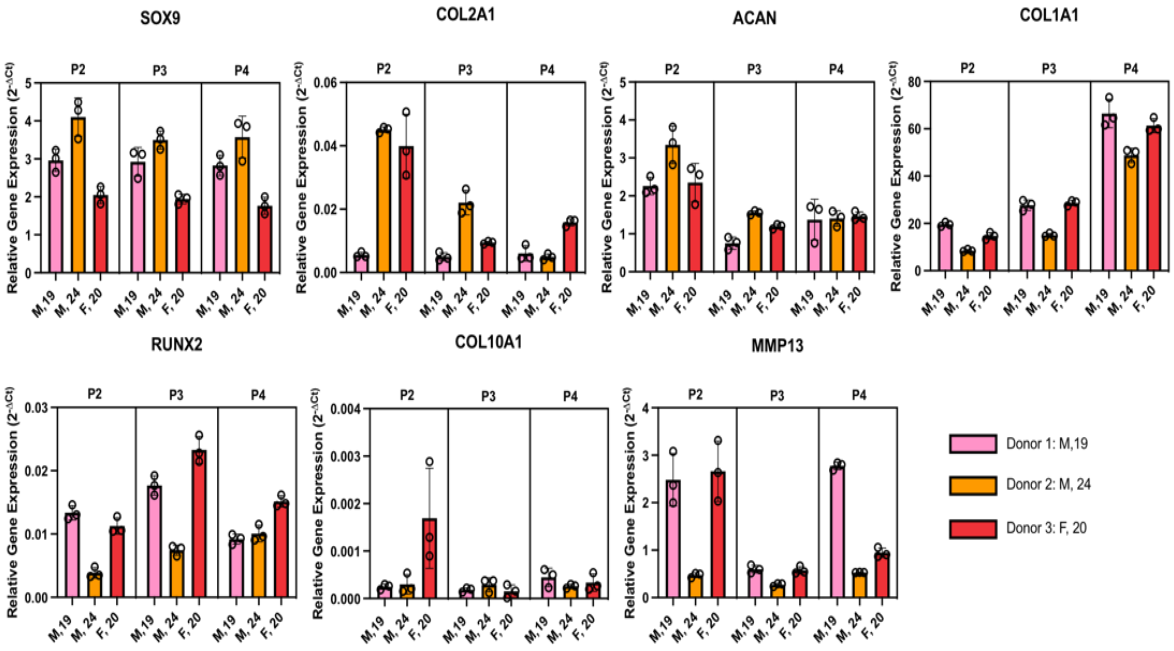

Appendix Figure C-1: Delta CT through each passage separated by donors. qPCR for each young donor is presented at each passage. Each point represents a technical replicate.

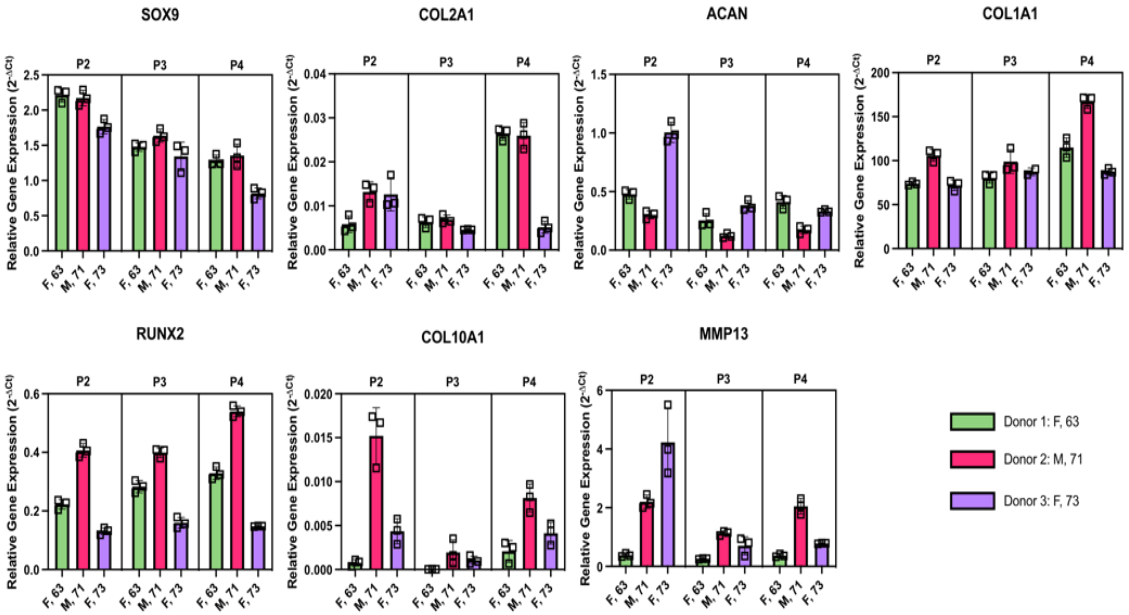

Appendix Figure C-2: Delta CT through each passage separated by donors. qPCR for each aged/OA donor is presented at each passage. Each point represents a technical replicate.

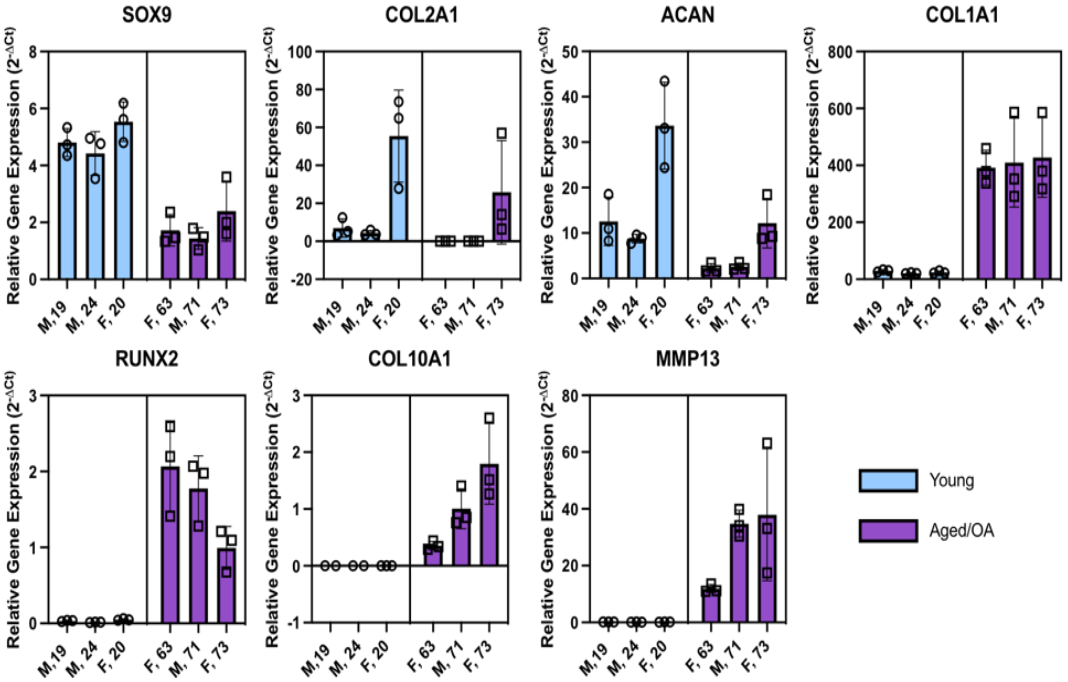

Appendix Figure C-3: Delta delta CT at passage 4 for each donor. qPCR for each young and aged donor is presented at passage 4. Each point represents a technical replicate.

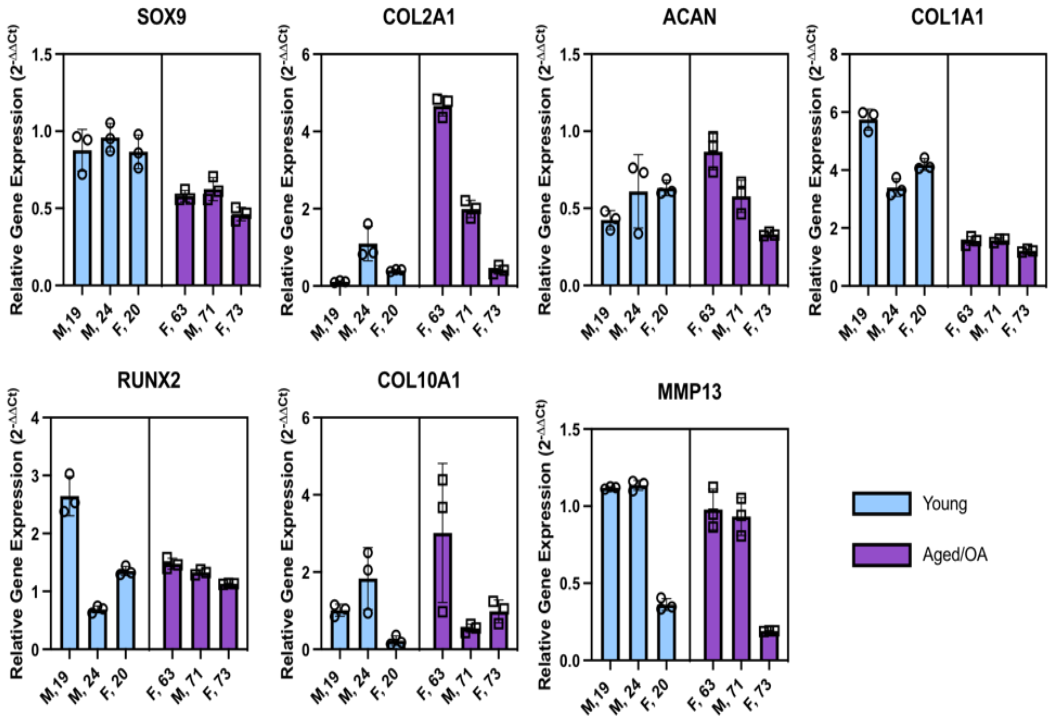

Appendix Figure C-4: Delta delta CT at day 28 for each donor. qPCR for each young and aged donor is presented at day 28. Each point represents a technical replicate.

Appendix D: Experiment Specific qPCR

Experiments with the auto-regulated RUNX2 suppressing circuits resulted in varying qPCR results even in the same donor. The experiment specific qPCR is presented below.

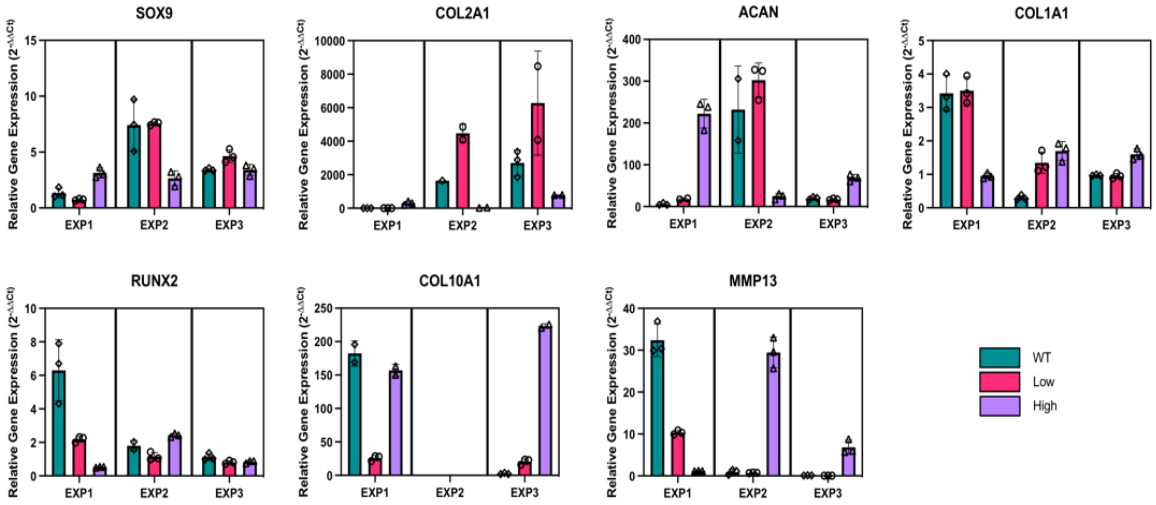

Appendix Figure D-1: Delta delta CT day 28 for each individual experiment testing auto-regulated RUNX2 suppressing circuits. qPCR analysis for each experiment in the same aged donor at day 28. Each point represents a technical replicate. (COL10A1 had no detectable expression.

Appendix E: Additional Luciferase Readings

Preliminary trials of the model indicated that senescence markers were increasing with IL-1β treatment.

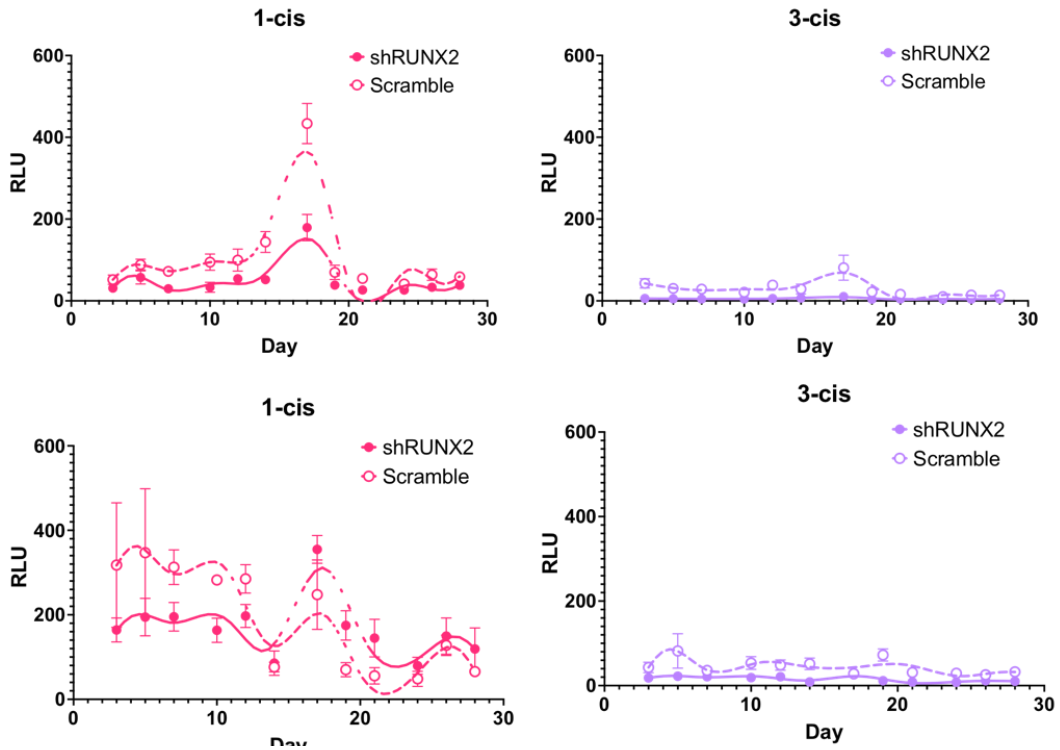

Appendix Figure E-1:Luciferase from additional experiments. Degree of suppression varies but 3-cis-shRUNX2 circuits consistently have low RUNX2 expression compared to 1-cis-shRUNX2 circuits.

Appendix F: Preliminary Chondrosenescence Model

Preliminary trials of the model indicated that senescence markers were increasing with IL-1β treatment.

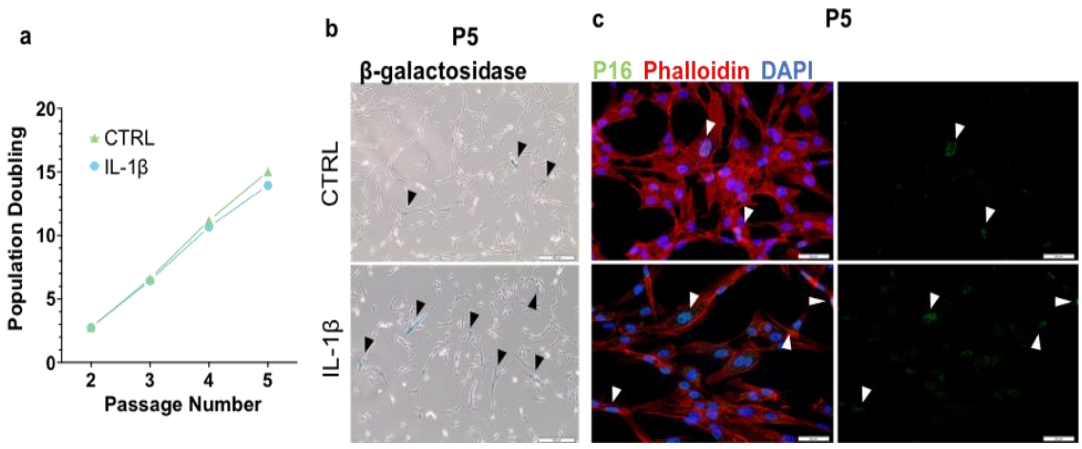

Appendix Figure F-1: Preliminary senescence model. (a) Population doubling of control and il1b treated cells (b) Representative images for staining of senescence marker B-galactosidase. Scale = 100 µM (c) Staining for cell cycle inhibitor P16 shows increased staining in IL1B cells at passage 5. Scale =20 µM.

Bibliography

1. Forster H, Fisher J. The influence of loading time and lubricant on the friction of articular cartilage. Proc Inst Mech Eng H. 1996;210(2):109-119. doi: 10.1243/PIME_PROC_1996_210_399_02. PubMed PMID: 8688115.
2. Tepic S, Macirowski T, Mann RW. Mechanical properties of articular cartilage elucidated by osmotic loading and ultrasound. Proc Natl Acad Sci U S A. 1983;80(11):3331-3333. doi: 10.1073/pnas.80.11.3331. PubMed PMID: 6574487.
3. Chan B, Donzelli PS, Spilker RL. A mixed-penalty biphasic finite element formulation incorporating viscous fluids and material interfaces. Ann Biomed Eng. 2000;28(6):589-597. doi: 10.1114/1.1305529. PubMed PMID: 10983705.
4. Wilson W, van Donkelaar CC, van Rietbergen B, Ito K, Huiskes R. Stresses in the local collagen network of articular cartilage: a poroviscoelastic fibril-reinforced finite element study. J Biomech. 2004;37(3):357-366. doi: 10.1016/s0021-9290(03)00267-7. PubMed PMID: 14757455.
5. Wilson W, van Donkelaar CC, van Rietbergen B, Huiskes R. A fibril-reinforced poroviscoelastic swelling model for articular cartilage. J Biomech. 2005;38(6):1195-1204. doi: 10.1016/j.jbiomech.2004.07.003. PubMed PMID: 15863103.
6. Jones B, Hung CT, Ateshian G. Biphasic Analysis of Cartilage Stresses in the Patellofemoral Joint. J Knee Surg. 2016;29(2):92-98. doi: 10.1055/s-0035-1568989. PubMed PMID: 26641078.
7. Roughley PJ, Mort JS. The role of aggrecan in normal and osteoarthritic cartilage. J Exp Orthop. 2014;1(1):8. doi: 10.1186/s40634-014-0008-7. PubMed PMID: 26914753.
8. Han E, Chen SS, Klisch SM, Sah RL. Contribution of proteoglycan osmotic swelling pressure to the compressive properties of articular cartilage. Biophys J. 2011;101(4):916-924. doi: 10.1016/j.bpj.2011.07.006. PubMed PMID: 21843483.
9. Jiang Y, Tuan RS. Origin and function of cartilage stem/progenitor cells in osteoarthritis. Nat Rev Rheumatol. 2015;11(4):206-212. doi: 10.1038/nrrheum.2014.200. PubMed PMID: 25536487.
10. Hunziker EB, Rosenberg LC. Repair of partial-thickness defects in articular cartilage: cell recruitment from the synovial membrane. J Bone Joint Surg Am. 1996;78(5):721-733. doi: 10.2106/00004623-199605000-00012. PubMed PMID: 8642029.
11. Falah M, Nierenberg G, Soudry M, Hayden M, Volpin G. Treatment of articular cartilage lesions of the knee. Int Orthop. 2010;34(5):621-630. doi: 10.1007/s00264-010-0959-y. PubMed PMID: 20162416.
12. Viswanathan S, Wolfstadt J, Chahal J, Gómez-Aristizábal A. Regenerative Medicine Approaches for Treatment of Osteoarthritis. In: *Osteoarthritis*. Cham: Springer International Publishing; 2015:235-255. doi: 10.1007/978-3-319-19560-

5_12.
13. Honda K, Ohno S, Tanimoto K, Ijuin C, Tanaka N, Doi T, Kato Y, Tanne K. The effects of high magnitude cyclic tensile load on cartilage matrix metabolism in cultured chondrocytes. Eur J Cell Biol. 2000;79(9):601-609. doi: 10.1078/0171-9335-00089. PubMed PMID: 11043401.
14. Fujisawa T, Hattori T, Takahashi K, Kuboki T, Yamashita A, Takigawa M. Cyclic mechanical stress induces extracellular matrix degradation in cultured chondrocytes via gene expression of matrix metalloproteinases and interleukin-1. J Biochem. 1999;125(5):966-975. doi: 10.1093/oxfordjournals.jbchem.a022376. PubMed PMID: 10220591.
15. Ding L, Heying E, Nicholson N, Stroud NJ, Homandberg GA, Buckwalter JA, Guo D, Martin JA. Mechanical impact induces cartilage degradation via mitogen activated protein kinases. Osteoarthr Cartil. 2010;18(11):1509-1517. doi: 10.1016/j.joca.2010.08.014. PubMed PMID: 20813194.
16. Mengshol JA, Vincenti MP, Brinckerhoff CE. IL-1 induces collagenase-3 (MMP-13) promoter activity in stably transfected chondrocytic cells: requirement for Runx-2 and activation by p38 MAPK and JNK pathways. Nucleic Acids Res. 2001;29(21):4361-4372. doi: 10.1093/nar/29.21.4361. PubMed PMID: 11691923.
17. Liacini A, Sylvester J, Li WQ, Huang W, Dehnade F, Ahmad M, Zafarullah M. Induction of matrix metalloproteinase-13 gene expression by TNF-alpha is mediated by MAP kinases, AP-1, and NF-kappaB transcription factors in articular chondrocytes. Exp Cell Res. 2003;288(1):208-217. doi: 10.1016/s0014-4827(03)00180-0. PubMed PMID: 12878172.
18. Raymond L, Eck S, Mollmark J, Hays E, Tomek I, Kantor S, Elliott S, Vincenti M. Interleukin-1 beta induction of matrix metalloproteinase-1 transcription in chondrocytes requires ERK-dependent activation of CCAAT enhancer-binding protein-beta. J Cell Physiol. 2006;207(3):683-688. doi: 10.1002/jcp.20608. PubMed PMID: 16453302.
19. Anderson DD, Chubinskaya S, Guilak F, Martin JA, Oegema TR, Olson SA, Buckwalter JA. Post-traumatic osteoarthritis: improved understanding and opportunities for early intervention. J Orthop Res. 2011;29(6):802-809. doi: 10.1002/jor.21359. PubMed PMID: 21520254.
20. Thomas AC, Hubbard-Turner T, Wikstrom EA, Palmieri-Smith RM. Epidemiology of Posttraumatic Osteoarthritis. J Athl Train. 2017;52(6):491-496. doi: 10.4085/1062-6050-51.5.08. PubMed PMID: 27145096.
21. Buckwalter JA, Anderson DD, Brown TD, Tochigi Y, Martin JA. The Roles of Mechanical Stresses in the Pathogenesis of Osteoarthritis: Implications for Treatment of Joint Injuries. Cartilage. 2013;4(4):286-294. doi: 10.1177/1947603513495889. PubMed PMID: 25067995.
22. Żylińska B, Silmanowicz P, Sobczyńska-Rak A, Jarosz Ł, Szponder T. Treatment of Articular Cartilage Defects: Focus on Tissue Engineering. In Vivo. 2018;32(6):1289-1300. doi: 10.21873/invivo.11379. PubMed PMID: 30348681.
23. Mithoefer K, McAdams T, Williams RJ, Kreuz PC, Mandelbaum BR. Clinical efficacy of the microfracture technique for articular cartilage repair in the knee: an evidence-based systematic analysis. Am J Sports Med. 2009;37(10):2053-2063. doi: 10.1177/0363546508328414. PubMed PMID: 19251676.

24. Kreuz PC, Steinwachs MR, Erggelet C, Krause SJ, Konrad G, Uhl M, Südkamp N. Results after microfracture of full-thickness chondral defects in different compartments in the knee. Osteoarthr Cartil. 2006;14(11):1119-1125. doi: 10.1016/j.joca.2006.05.003. PubMed PMID: 16815714.
25. Kwon H, Brown WE, Lee CA, Wang D, Paschos N, Hu JC, Athanasiou KA. Surgical and tissue engineering strategies for articular cartilage and meniscus repair. Nat Rev Rheumatol. 2019;15(9):550-570. doi: 10.1038/s41584-019-0255-1. PubMed PMID: 31296933.
26. Miller DJ, Smith M V, Matava MJ, Wright RW, Brophy RH. Microfracture and osteochondral autograft transplantation are cost-effective treatments for articular cartilage lesions of the distal femur. Am J Sports Med. 2015;43(9):2175-2181. doi: 10.1177/0363546515591261. PubMed PMID: 26159823.
27. Basad E, Ishaque B, Bachmann G, Stürz H, Steinmeyer J. Matrix-induced autologous chondrocyte implantation versus microfracture in the treatment of cartilage defects of the knee: a 2-year randomised study. Knee Surg Sports Traumatol Arthrosc. 2010;18(4):519-527. doi: 10.1007/s00167-009-1028-1. PubMed PMID: 20062969.
28. Cerynik DL, Lewullis GE, Joves BC, Palmer MP, Tom JA. Outcomes of microfracture in professional basketball players. Knee Surg Sports Traumatol Arthrosc. 2009;17(9):1135-1139. doi: 10.1007/s00167-009-0765-5. PubMed PMID: 19296083.
29. Mithoefer K, Williams RJ, Warren RF, Potter HG, Spock CR, Jones EC, Wickiewicz TL, Marx RG. The Microfracture Technique for the Treatment of Articular Cartilage Lesions in the Knee. J Bone Jt Surg. 2005;87(9):1911-1920. doi: 10.2106/JBJS.D.02846.
30. Mienaltowski MJ, Huang L, Frisbie DD, McIlwraith CW, Stromberg AJ, Bathke AC, Macleod JN. Transcriptional profiling differences for articular cartilage and repair tissue in equine joint surface lesions. BMC Med Genomics. 2009;2:60. doi: 10.1186/1755-8794-2-60. PubMed PMID: 19751507.
31. MIYATA S, TATEISHI T, FURUKAWA K, USHIDA T. Influence of Structure and Composition on Dynamic Viscoelastic Property of Cartilaginous Tissue: Criteria for Classification between Hyaline Cartilage and Fibrocartilage Based on Mechanical Function. JSME Int J Ser C. 2005;48(4):547-554. doi: 10.1299/jsmec.48.547.
32. Bedi A, Feeley BT, Williams RJ. Management of articular cartilage defects of the knee. J Bone Joint Surg Am. 2010;92(4):994-1009. doi: 10.2106/JBJS.I.00895. PubMed PMID: 20360528.
33. Makris EA, Gomoll AH, Malizos KN, Hu JC, Athanasiou KA. Repair and tissue engineering techniques for articular cartilage. Nat Rev Rheumatol. 2015;11(1):21-34. doi: 10.1038/nrrheum.2014.157. PubMed PMID: 25247412.
34. Armiento AR, Alini M, Stoddart MJ. Articular fibrocartilage - Why does hyaline cartilage fail to repair? Adv Drug Deliv Rev. 2019;146:289-305. doi: 10.1016/j.addr.2018.12.015. PubMed PMID: 30605736.
35. Solheim E, Hegna J, Inderhaug E, Øyen J, Harlem T, Strand T. Results at 10-14 years after microfracture treatment of articular cartilage defects in the knee. Knee Surg Sports Traumatol Arthrosc. 2016;24(5):1587-1593. doi: 10.1007/s00167-014-3443-1. PubMed PMID: 25416965.

36. Camp CL, Stuart MJ, Krych AJ. Current concepts of articular cartilage restoration techniques in the knee. Sports Health. 2014;6(3):265-273. doi: 10.1177/1941738113508917. PubMed PMID: 24790697.
37. Buckwalter JA. Articular Cartilage Injuries. Clin Orthop Relat Res. 2002;402:21-37. doi: 10.1097/00003086-200209000-00004.
38. Paul J, Sagstetter A, Kriner M, Imhoff AB, Spang J, Hinterwimmer S. Donor-site morbidity after osteochondral autologous transplantation for lesions of the talus. J Bone Joint Surg Am. 2009;91(7):1683-1688. doi: 10.2106/JBJS.H.00429. PubMed PMID: 19571091.
39. Williams SK, Amiel D, Ball ST, Allen RT, Wong VW, Chen AC, Sah RL, Bugbee WD. Prolonged storage effects on the articular cartilage of fresh human osteochondral allografts. J Bone Joint Surg Am. 2003;85(11):2111-2120. doi: 10.2106/00004623-200311000-00008. PubMed PMID: 14630839.
40. Pallante AL, Görtz S, Chen AC, Healey RM, Chase DC, Ball ST, Amiel D, Sah RL, Bugbee WD. Treatment of articular cartilage defects in the goat with frozen versus fresh osteochondral allografts: effects on cartilage stiffness, zonal composition, and structure at six months. J Bone Joint Surg Am. 2012;94(21):1984-1995. doi: 10.2106/JBJS.K.00439. PubMed PMID: 23138239.
41. Peterson L, Brittberg M, Kiviranta I, Åkerlund EL, Lindahl A. Autologous Chondrocyte Transplantation. Am J Sports Med. 2002;30(1):2-12. doi: 10.1177/03635465020300011601.
42. Gobbi A, Bathan L. Biological approaches for cartilage repair. J Knee Surg. 2009;22(1):36-44. doi: 10.1055/s-0030-1247726. PubMed PMID: 19216352.
43. Brittberg M, Lindahl A, Nilsson A, Ohlsson C, Isaksson O, Peterson L. Treatment of deep cartilage defects in the knee with autologous chondrocyte transplantation. N Engl J Med. 1994;331(14):889-895. doi: 10.1056/NEJM199410063311401. PubMed PMID: 8078550.
44. Kreuz PC, Steinwachs M, Erggelet C, Krause SJ, Ossendorf C, Maier D, Ghanem N, Uhl M, Haag M. Classification of graft hypertrophy after autologous chondrocyte implantation of full-thickness chondral defects in the knee. Osteoarthr Cartil. 2007;15(12):1339-1347. doi: 10.1016/j.joca.2007.04.020. PubMed PMID: 17629514.
45. Ueno T, Kagawa T, Mizukawa N, Nakamura H, Sugahara T, Yamamoto T. Cellular origin of endochondral ossification from grafted periosteum. Anat Rec. 2001;264(4):348-357. doi: 10.1002/ar.10024. PubMed PMID: 11745090.
46. Cherubino P, Grassi FA, Bulgheroni P, Ronga M. Autologous chondrocyte implantation using a bilayer collagen membrane: a preliminary report. J Orthop Surg (Hong Kong). 2003;11(1):10-15. doi: 10.1177/230949900301100104. PubMed PMID: 12810965.
47. Ma B, Leijten JCH, Wu L, Kip M, van Blitterswijk CA, Post JN, Karperien M. Gene expression profiling of dedifferentiated human articular chondrocytes in monolayer culture. Osteoarthr Cartil. 2013;21(4):599-603. doi: 10.1016/j.joca.2013.01.014. PubMed PMID: 23376013.
48. Lin Z, Fitzgerald JB, Xu J, Willers C, Wood D, Grodzinsky AJ, Zheng MH. Gene expression profiles of human chondrocytes during passaged monolayer cultivation. J Orthop Res. 2008;26(9):1230-1237. doi: 10.1002/jor.20523. PubMed PMID:

18404652.
49. Barbero A, Grogan S, Schäfer D, Heberer M, Mainil-Varlet P, Martin I. Age related changes in human articular chondrocyte yield, proliferation and post-expansion chondrogenic capacity. Osteoarthr Cartil. 2004;12(6):476-484. doi: 10.1016/j.joca.2004.02.010. PubMed PMID: 15135144.
50. Loeser RF. Aging and osteoarthritis: the role of chondrocyte senescence and aging changes in the cartilage matrix. Osteoarthr Cartil. 2009;17(8):971-979. doi: 10.1016/j.joca.2009.03.002. PubMed PMID: 19303469.
51. Dozin B, Malpeli M, Camardella L, Cancedda R, Pietrangelo A. Response of young, aged and osteoarthritic human articular chondrocytes to inflammatory cytokines: molecular and cellular aspects. Matrix Biol. 2002;21(5). doi: 10.1016/S0945-053X(02)00028-8.
52. Fan Z, Bau B, Yang H, Soeder S, Aigner T. Freshly isolated osteoarthritic chondrocytes are catabolically more active than normal chondrocytes, but less responsive to catabolic stimulation with interleukin-1beta. Arthritis Rheum. 2005;52(1):136-143. doi: 10.1002/art.20725. PubMed PMID: 15641077.
53. Zhang W, Ouyang H, Dass CR, Xu J. Current research on pharmacologic and regenerative therapies for osteoarthritis. Bone Res. 2016;4:15040. doi: 10.1038/boneres.2015.40. PubMed PMID: 26962464.
54. Tetteh ES, Bajaj S, Ghodadra NS, Cole BJ. Basic science and surgical treatment options for articular cartilage injuries of the knee. J Orthop Sports Phys Ther. 2012;42(3):243-253. doi: 10.2519/jospt.2012.3673.
55. Farrell MJ, Fisher MB, Huang AH, Shin JI, Farrell KM, Mauck RL. Functional properties of bone marrow-derived MSC-based engineered cartilage are unstable with very long-term in vitro culture. J Biomech. 2014;47(9):2173-2182. doi: 10.1016/j.jbiomech.2013.10.030. PubMed PMID: 24239005.
56. Carrion B, Souzanchi MF, Wang VT, Tiruchinapally G, Shikanov A, Putnam AJ, Coleman RM. The Synergistic Effects of Matrix Stiffness and Composition on the Response of Chondroprogenitor Cells in a 3D Precondensation Microenvironment. Adv Healthc Mater. 2016;5(10):1192-1202. doi: 10.1002/adhm.201501017. PubMed PMID: 26959641.
57. Khan WS, Adesida AB, Hardingham TE. Hypoxic conditions increase hypoxia-inducible transcription factor 2alpha and enhance chondrogenesis in stem cells from the infrapatellar fat pad of osteoarthritis patients. Arthritis Res Ther. 2007;9(3):R55. doi: 10.1186/ar2211. PubMed PMID: 17537234.
58. Mackay AM, Beck SC, Murphy JM, Barry FP, Chichester CO, Pittenger MF. Chondrogenic differentiation of cultured human mesenchymal stem cells from marrow. Tissue Eng. 1998;4(4):415-428. doi: 10.1089/ten.1998.4.415. PubMed PMID: 9916173.
59. Johnstone B, Hering TM, Caplan AI, Goldberg VM, Yoo JU. In vitro chondrogenesis of bone marrow-derived mesenchymal progenitor cells. Exp Cell Res. 1998;238(1):265-272. doi: 10.1006/excr.1997.3858. PubMed PMID: 9457080.
60. Prockop, D. J. & Reger RL. *Mesenchymal Stromal Cells*. (Hematti P, Keating A, eds.). New York, NY: Springer New York; 2013. doi: 10.1007/978-1-4614-5711-4.
61. Mansour JM. Biomechanics of Cartilage. Kinesiol Mech pathomechanics Hum Mov. 2009:66–79.

62. Borrelli J, Olson SA, Godbout C, Schemitsch EH, Stannard JP, Giannoudis P V. Understanding Articular Cartilage Injury and Potential Treatments. J Orthop Trauma. 2019;33 Suppl 6:S6-S12. doi: 10.1097/BOT.0000000000001472. PubMed PMID: 31083142.
63. Bhosale AM, Richardson JB. Articular cartilage: structure, injuries and review of management. Br Med Bull. 2008;87(1):77-95. doi: 10.1093/bmb/ldn025.
64. Bian L, Zhai DY, Tous E, Rai R, Mauck RL, Burdick JA. Enhanced MSC chondrogenesis following delivery of TGF-β3 from alginate microspheres within hyaluronic acid hydrogels in vitro and in vivo. Biomaterials. 2011;32(27):6425-6434. doi: 10.1016/j.biomaterials.2011.05.033. PubMed PMID: 21652067.
65. Worster AA, Brower-Toland BD, Fortier LA, Bent SJ, Williams J, Nixon AJ. Chondrocytic differentiation of mesenchymal stem cells sequentially exposed to transforming growth factor-beta1 in monolayer and insulin-like growth factor-I in a three-dimensional matrix. J Orthop Res. 2001;19(4):738-749. doi: 10.1016/S0736-0266(00)00054-1. PubMed PMID: 11518286.
66. Schmitt B, Ringe J, Häupl T, Notter M, Manz R, Burmester G-R, Sittinger M, Kaps C. BMP2 initiates chondrogenic lineage development of adult human mesenchymal stem cells in high-density culture. Differentiation. 2003;71(9-10):567-577. doi: 10.1111/j.1432-0436.2003.07109003.x. PubMed PMID: 14686954.
67. Sekiya I, Colter DC, Prockop DJ. BMP-6 enhances chondrogenesis in a subpopulation of human marrow stromal cells. Biochem Biophys Res Commun. 2001;284(2):411-418. doi: 10.1006/bbrc.2001.4898. PubMed PMID: 11394894.
68. Huang C-YC, Reuben PM, D'Ippolito G, Schiller PC, Cheung HS. Chondrogenesis of human bone marrow-derived mesenchymal stem cells in agarose culture. Anat Rec A Discov Mol Cell Evol Biol. 2004;278(1):428-436. doi: 10.1002/ar.a.20010. PubMed PMID: 15103737.
69. Ma H-L, Hung S-C, Lin S-Y, Chen Y-L, Lo W-H. Chondrogenesis of human mesenchymal stem cells encapsulated in alginate beads. J Biomed Mater Res. 2003;64A(2):273-281. doi: 10.1002/jbm.a.10370.
70. Alves da Silva ML, Martins A, Costa-Pinto AR, Costa P, Faria S, Gomes M, Reis RL, Neves NM. Cartilage tissue engineering using electrospun PCL nanofiber meshes and MSCs. Biomacromolecules. 2010;11(12):3228-3236. doi: 10.1021/bm100476r. PubMed PMID: 21105638.
71. Williams CG, Kim TK, Taboas A, Malik A, Manson P, Elisseeff J. In vitro chondrogenesis of bone marrow-derived mesenchymal stem cells in a photopolymerizing hydrogel. Tissue Eng. 2003;9(4):679-688. doi: 10.1089/107632703768247377. PubMed PMID: 13678446.
72. Xie M, Fritch M, He Y, Fu H, Hong Y, Lin H. Dynamic loading enhances chondrogenesis of human chondrocytes within a biodegradable resilient hydrogel. Biomater Sci. 2021;9(14):5011-5024. doi: 10.1039/d1bm00413a. PubMed PMID: 34109952.
73. Sorrell JM, Somoza RA, Caplan AI. Human mesenchymal stem cells induced to differentiate as chondrocytes follow a biphasic pattern of extracellular matrix production. J Orthop Res. 2018;36(6):1757-1766. doi: 10.1002/jor.23820. PubMed PMID: 29194731.
74. Zha K, Li X, Yang Z, Tian G, Sun Z, Sui X, Dai Y, Liu S, Guo Q. Heterogeneity of

mesenchymal stem cells in cartilage regeneration: from characterization to application. npj Regen Med. 2021;6(1):14. doi: 10.1038/s41536-021-00122-6.
75. Kim J, Adachi T. Cell-fate decision of mesenchymal stem cells toward osteocyte differentiation is committed by spheroid culture. Sci Rep. 2021;11(1):13204. doi: 10.1038/s41598-021-92607-z.
76. Scotti C, Tonnarelli B, Papadimitropoulos A, Scherberich A, Schaeren S, Schauerte A, Lopez-Rios J, Zeller R, Barbero A, Martin I. Recapitulation of endochondral bone formation using human adult mesenchymal stem cells as a paradigm for developmental engineering. Proc Natl Acad Sci U S A. 2010;107(16):7251-7256. doi: 10.1073/pnas.1000302107. PubMed PMID: 20406908.
77. Farrell E, Both SK, Odörfer KI, Koevoet W, Kops N, O'Brien FJ, Baatenburg de Jong RJ, Verhaar JA, Cuijpers V, Jansen J, Erben RG, van Osch GJVM. In-vivo generation of bone via endochondral ossification by in-vitro chondrogenic priming of adult human and rat mesenchymal stem cells. BMC Musculoskelet Disord. 2011;12:31. doi: 10.1186/1471-2474-12-31. PubMed PMID: 21281488.
78. Nishimura R, Hata K, Nakamura E, Murakami T, Takahata Y. Transcriptional network systems in cartilage development and disease. Histochem Cell Biol. 2018;149(4):353-363. doi: 10.1007/s00418-017-1628-7. PubMed PMID: 29308531.
79. Goldring MB, Otero M. Inflammation in osteoarthritis. Curr Opin Rheumatol. 2011;23(5):471-478. doi: 10.1097/BOR.0b013e328349c2b1. PubMed PMID: 21788902.
80. Saito T, Fukai A, Mabuchi A, Ikeda T, Yano F, Ohba S, Nishida N, Akune T, Yoshimura N, Nakagawa T, Nakamura K, Tokunaga K, Chung U-I, Kawaguchi H. Transcriptional regulation of endochondral ossification by HIF-2alpha during skeletal growth and osteoarthritis development. Nat Med. 2010;16(6):678-686. doi: 10.1038/nm.2146. PubMed PMID: 20495570.
81. Zhang W, Ouyang H, Dass CR, Xu J. Current research on pharmacologic and regenerative therapies for osteoarthritis. Bone Res. 2016;4:15040. doi: 10.1038/boneres.2015.40. PubMed PMID: 26962464.
82. Iwasa J, Engebretsen L, Shima Y, Ochi M. Clinical application of scaffolds for cartilage tissue engineering. Knee Surg Sports Traumatol Arthrosc. 2009;17(6):561-577. doi: 10.1007/s00167-008-0663-2. PubMed PMID: 19020862.
83. Kon E, Filardo G, Condello V, Collarile M, Di Martino A, Zorzi C, Marcacci M. Second-generation autologous chondrocyte implantation: results in patients older than 40 years. Am J Sports Med. 2011;39(8):1668-1675. doi: 10.1177/0363546511404675. PubMed PMID: 21596901.
84. Kon E, Filardo G, Berruto M, Benazzo F, Zanon G, Della Villa S, Marcacci M. Articular cartilage treatment in high-level male soccer players: a prospective comparative study of arthroscopic second-generation autologous chondrocyte implantation versus microfracture. Am J Sports Med. 2011;39(12):2549-2557. doi: 10.1177/0363546511420688. PubMed PMID: 21900624.
85. Angele P, Fritz J, Albrecht D, Koh J, Zellner J. Defect type, localization and marker gene expression determines early adverse events of matrix-associated autologous chondrocyte implantation. Injury. 2015;46 Suppl 4:S2-9. doi: 10.1016/S0020-1383(15)30012-7. PubMed PMID: 26542862.

86. Dewan AK, Gibson MA, Elisseeff JH, Trice ME. Evolution of autologous chondrocyte repair and comparison to other cartilage repair techniques. Biomed Res Int. 2014;2014:272481. doi: 10.1155/2014/272481. PubMed PMID: 25210707.
87. Kim D, Rossi J. RNAi mechanisms and applications. Biotechniques. 2008;44(5):613-616. doi: 10.2144/000112792. PubMed PMID: 18474035.
88. Sabariegos R, Giménez-Barcons M, Tàpia N, Clotet B, Martínez MA. Sequence homology required by human immunodeficiency virus type 1 to escape from short interfering RNAs. J Virol. 2006;80(2):571-577. doi: 10.1128/JVI.80.2.571-577.2006. PubMed PMID: 16378959.
89. Ambesajir A, Kaushik A, Kaushik JJ, Petros ST. RNA interference: A futuristic tool and its therapeutic applications. Saudi J Biol Sci. 2012;19(4):395-403. doi: 10.1016/j.sjbs.2012.08.001. PubMed PMID: 23961202.
90. Bianchi A, Guibert M, Cailotto F, Gasser A, Presle N, Mainard D, Netter P, Kempf H, Jouzeau J-Y, Reboul P. Fibroblast Growth Factor 23 drives MMP13 expression in human osteoarthritic chondrocytes in a Klotho-independent manner. Osteoarthr Cartil. 2016;24(11):1961-1969. doi: 10.1016/j.joca.2016.06.003. PubMed PMID: 27307356.
91. Blaney Davidson EN, Remst DFG, Vitters EL, van Beuningen HM, Blom AB, Goumans M-J, van den Berg WB, van der Kraan PM. Increase in ALK1/ALK5 ratio as a cause for elevated MMP-13 expression in osteoarthritis in humans and mice. J Immunol. 2009;182(12):7937-7945. doi: 10.4049/jimmunol.0803991. PubMed PMID: 19494318.
92. Olivotto E, Borzi RM, Vitellozzi R, Pagani S, Facchini A, Battistelli M, Penzo M, Li X, Flamigni F, Li J, Falcieri E, Facchini A, Marcu KB. Differential requirements for IKKalpha and IKKbeta in the differentiation of primary human osteoarthritic chondrocytes. Arthritis Rheum. 2008;58(1):227-239. doi: 10.1002/art.23211. PubMed PMID: 18163512.
93. Borzí RM, Olivotto E, Pagani S, Vitellozzi R, Neri S, Battistelli M, Falcieri E, Facchini A, Flamigni F, Penzo M, Platano D, Santi S, Facchini A, Marcu KB. Matrix metalloproteinase 13 loss associated with impaired extracellular matrix remodeling disrupts chondrocyte differentiation by concerted effects on multiple regulatory factors. Arthritis Rheum. 2010;62(8):2370-2381. doi: 10.1002/art.27512. PubMed PMID: 20506238.
94. Zheng Q, Zhou G, Morello R, Chen Y, Garcia-Rojas X, Lee B. Type X collagen gene regulation by Runx2 contributes directly to its hypertrophic chondrocyte-specific expression in vivo. J Cell Biol. 2003;162(5):833-842. doi: 10.1083/jcb.200211089. PubMed PMID: 12952936.
95. Li F, Lu Y, Ding M, Napierala D, Abbassi S, Chen Y, Duan X, Wang S, Lee B, Zheng Q. Runx2 contributes to murine Col10a1 gene regulation through direct interaction with its cis-enhancer. J Bone Miner Res. 2011;26(12):2899-2910. doi: 10.1002/jbmr.504. PubMed PMID: 21887706.
96. Kaur G, Wu B, Murali S, Lanigan T, Coleman RM. A Synthetic, Closed-Looped Gene Circuit for the Autonomous Regulation of RUNX2 Activity during Chondrogenesis. bioRxiv. 2021.
97. Jakob M, Démarteau O, Schäfer D, Hintermann B, Dick W, Heberer M, Martin I. Specific growth factors during the expansion and redifferentiation of adult human

articular chondrocytes enhance chondrogenesis and cartilaginous tissue formation in vitro. J Cell Biochem. 2001;81(2):368-377. doi: 10.1002/1097-4644(20010501)81:2<368::aid-jcb1051>3.0.co;2-j. PubMed PMID: 11241676.
98. Tominaga T, Shimada R, Okada Y, Kawamata T, Kibayashi K. Senescence-associated-β-galactosidase staining following traumatic brain injury in the mouse cerebrum. PLoS One. 2019;14(3):e0213673. doi: 10.1371/journal.pone.0213673. PubMed PMID: 30856215.
99. Pradhan AD, Manson JE, Rifai N, Buring JE, Ridker PM. C-reactive protein, interleukin 6, and risk of developing type 2 diabetes mellitus. JAMA. 2001;286(3):327-334. doi: 10.1001/jama.286.3.327. PubMed PMID: 11466099.
100. Thorand B, Löwel H, Schneider A, Kolb H, Meisinger C, Fröhlich M, Koenig W. C-reactive protein as a predictor for incident diabetes mellitus among middle-aged men: results from the MONICA Augsburg cohort study, 1984-1998. Arch Intern Med. 2003;163(1):93-99. doi: 10.1001/archinte.163.1.93. PubMed PMID: 12523922.
101. Festa A, D'Agostino R, Tracy RP, Haffner SM, Insulin Resistance Atherosclerosis Study. Elevated levels of acute-phase proteins and plasminogen activator inhibitor-1 predict the development of type 2 diabetes: the insulin resistance atherosclerosis study. Diabetes. 2002;51(4):1131-1137. doi: 10.2337/diabetes.51.4.1131. PubMed PMID: 11916936.
102. Bruunsgaard H, Skinhøj P, Pedersen AN, Schroll M, Pedersen BK. Ageing, tumour necrosis factor-alpha (TNF-alpha) and atherosclerosis. Clin Exp Immunol. 2000;121(2):255-260. doi: 10.1046/j.1365-2249.2000.01281.x. PubMed PMID: 10931139.
103. Greene MA, Loeser RF. Aging-related inflammation in osteoarthritis. Osteoarthr Cartil. 2015;23(11):1966-1971. doi: 10.1016/j.joca.2015.01.008. PubMed PMID: 26521742.
104. Franceschi C, Garagnani P, Vitale G, Capri M, Salvioli S. In fl ammaging and ' Garb-aging .' 2017;28(3):199-212.
105. Zitvogel L, Kepp O, Kroemer G. Decoding cell death signals in inflammation and immunity. Cell. 2010;140(6):798-804. doi: 10.1016/j.cell.2010.02.015. PubMed PMID: 20303871.
106. Cuervo AM, Bergamini E, Brunk UT, Dröge W, Ffrench M, Terman A. Autophagy and aging: the importance of maintaining "clean" cells. Autophagy. 2005;1(3):131-140. doi: 10.4161/auto.1.3.2017. PubMed PMID: 16874025.
107. Brunk UT, Terman A. The mitochondrial-lysosomal axis theory of aging: accumulation of damaged mitochondria as a result of imperfect autophagocytosis. Eur J Biochem. 2002;269(8):1996-2002. doi: 10.1046/j.1432-1033.2002.02869.x. PubMed PMID: 11985575.
108. Caramés B, Taniguchi N, Otsuki S, Blanco FJ, Lotz M. Autophagy is a protective mechanism in normal cartilage, and its aging-related loss is linked with cell death and osteoarthritis. Arthritis Rheum. 2010;62(3):791-801. doi: 10.1002/art.27305. PubMed PMID: 20187128.
109. Vinatier C, Domínguez E, Guicheux J, Caramés B. Role of the inflammation-autophagy-senescence integrative network in Osteoarthritis. Front Physiol. 2018;9(JUN):1-25. doi: 10.3389/fphys.2018.00706.

110. Childs BG, Durik M, Baker DJ, Van Deursen JM. Cellular senescence in aging and age-related disease: From mechanisms to therapy. Nat Med. 2015;21(12):1424-1435. doi: 10.1038/nm.4000. PubMed PMID: 26646499.
111. Page Thomas DP, King B, Stephens T, Dingle JT. In vivo studies of cartilage regeneration after damage induced by catabolin/interleukin-1. Ann Rheum Dis. 1991;50(2):75-80. doi: 10.1136/ard.50.2.75. PubMed PMID: 1998394.
112. van der Kraan PM, van den Berg WB. Anabolic and destructive mediators in osteoarthritis. Curr Opin Clin Nutr Metab Care. 2000;3(3):205-211. doi: 10.1097/00075197-200005000-00007. PubMed PMID: 10871236.
113. Blanco Garcia FJ. Catabolic events in osteoarthritic cartilage. Osteoarthr Cartil. 1999;7(3):308-309. doi: 10.1053/joca.1998.0174. PubMed PMID: 10329308.
114. Lotz M, Loeser RF. Effects of aging on articular cartilage homeostasis. Bone. 2012;51(2):241-248. doi: 10.1016/j.bone.2012.03.023. PubMed PMID: 22487298.
115. Salminen A, Kauppinen A, Kaarniranta K. Emerging role of NF-κB signaling in the induction of senescence-associated secretory phenotype (SASP). Cell Signal. 2012;24(4):835-845. doi: 10.1016/j.cellsig.2011.12.006. PubMed PMID: 22182507.
116. Rim YA, Nam Y, Ju JH. The role of chondrocyte hypertrophy and senescence in osteoarthritis initiation and progression. Int J Mol Sci. 2020;21(7). doi: 10.3390/ijms21072358. PubMed PMID: 32235300.
117. Kawaguchi H. Endochondral ossification signals in cartilage degradation during Osteoarthritis progression in experimental mouse models. Mol Cells. 2008;25(1):1-6. PubMed PMID: 18319608.
118. Ripmeester EGJ, Timur UT, Caron MMJ, Welting TJM. Recent insights into the contribution of the changing hypertrophic chondrocyte phenotype in the development and progression of osteoarthritis. Front Bioeng Biotechnol. 2018;6(MAR). doi: 10.3389/fbioe.2018.00018.
119. Kronenberg HM. Developmental regulation of the growth plate. Nature. 2003;423(6937):332-336. doi: 10.1038/nature01657. PubMed PMID: 12748651.
120. Steinert AF, Proffen B, Kunz M, Hendrich C, Ghivizzani SC, Nöth U, Rethwilm A, Eulert J, Evans CH. Hypertrophy is induced during the in vitro chondrogenic differentiation of human mesenchymal stem cells by bone morphogenetic protein-2 and bone morphogenetic protein-4 gene transfer. Arthritis Res Ther. 2009;11(5):R148. doi: 10.1186/ar2822. PubMed PMID: 19799789.
121. Dong Y-F, Soung DY, Schwarz EM, O'Keefe RJ, Drissi H. Wnt induction of chondrocyte hypertrophy through the Runx2 transcription factor. J Cell Physiol. 2006;208(1):77-86. doi: 10.1002/jcp.20656. PubMed PMID: 16575901.
122. Leboy P, Grasso-Knight G, D'Angelo M, Volk SW, Lian J V, Drissi H, Stein GS, Adams SL. Smad-Runx interactions during chondrocyte maturation. J Bone Joint Surg Am. 2001;83-A Suppl(Pt 1):S15-22. PubMed PMID: 11263661.
123. Yoshida CA, Yamamoto H, Fujita T, Furuichi T, Ito K, Inoue K, Yamana K, Zanma A, Takada K, Ito Y, Komori T. Runx2 and Runx3 are essential for chondrocyte maturation, and Runx2 regulates limb growth through induction of Indian hedgehog. Genes Dev. 2004;18(8):952-963. doi: 10.1101/gad.1174704. PubMed PMID: 15107406.
124. Akiyama H, Chaboissier M-C, Martin JF, Schedl A, de Crombrugghe B. The transcription factor Sox9 has essential roles in successive steps of the chondrocyte

differentiation pathway and is required for expression of Sox5 and Sox6. Genes Dev. 2002;16(21):2813-2828. doi: 10.1101/gad.1017802. PubMed PMID: 12414734.
125. Vimalraj S, Arumugam B, Miranda PJ, Selvamurugan N. Runx2: Structure, function, and phosphorylation in osteoblast differentiation. Int J Biol Macromol. 2015;78:202-208. doi: 10.1016/j.ijbiomac.2015.04.008.
126. Wang X, Manner PA, Horner A, Shum L, Tuan RS, Nuckolls GH. Regulation of MMP-13 expression by RUNX2 and FGF2 in osteoarthritic cartilage. Osteoarthr Cartil. 2004;12(12):963-973. doi: 10.1016/j.joca.2004.08.008. PubMed PMID: 15564063.
127. Nishimura R, Wakabayashi M, Hata K, Matsubara T, Honma S, Wakisaka S, Kiyonari H, Shioi G, Yamaguchi A, Tsumaki N, Akiyama H, Yoneda T. Osterix regulates calcification and degradation of chondrogenic matrices through matrix metalloproteinase 13 (MMP13) expression in association with transcription factor Runx2 during endochondral ossification. J Biol Chem. 2012;287(40):33179-33190. doi: 10.1074/jbc.M111.337063. PubMed PMID: 22869368.
128. Fosang AJ, Last K, Knäuper V, Murphy G, Neame PJ. Degradation of cartilage aggrecan by collagenase-3 (MMP-13). FEBS Lett. 1996;380(1-2):17-20. doi: 10.1016/0014-5793(95)01539-6. PubMed PMID: 8603731.
129. Mitchell PG, Magna HA, Reeves LM, Lopresti-Morrow LL, Yocum SA, Rosner PJ, Geoghegan KF, Hambor JE. Cloning, expression, and type II collagenolytic activity of matrix metalloproteinase-13 from human osteoarthritic cartilage. J Clin Invest. 1996;97(3):761-768. doi: 10.1172/JCI118475. PubMed PMID: 8609233.
130. Lu Y, Ding M, Li N, Wang Q, Li J, Li X, Gu J, Im H-J, Lei G, Zheng Q. Col10a1-Runx2 transgenic mice with delayed chondrocyte maturation are less susceptible to developing osteoarthritis. Am J Transl Res. 2014;6(6):736-745. PubMed PMID: 25628784.
131. Ding M, Lu Y, Abbassi S, Li F, Li X, Song Y, Geoffroy V, Im H-J, Zheng Q. Targeting Runx2 expression in hypertrophic chondrocytes impairs endochondral ossification during early skeletal development. J Cell Physiol. 2012;227(10):3446-3456. doi: 10.1002/jcp.24045. PubMed PMID: 22223437.
132. Liao L, Zhang S, Gu J, Takarada T, Yoneda Y, Huang J, Zhao L, Oh C, Li J, Wang B, Wang M, Chen D. Deletion of Runx2 in Articular Chondrocytes Decelerates the Progression of DMM-Induced Osteoarthritis in Adult Mice. Sci Rep. 2017;7(1):2371. doi: 10.1038/s41598-017-02490-w. PubMed PMID: 28539595.
133. Li H, Davison N, Moroni L, Feng F, Crist J, Salter E, Bingham CO, Elisseeff J. Evaluating Osteoarthritic Chondrocytes through a Novel 3-Dimensional In Vitro System for Cartilage Tissue Engineering and Regeneration. Cartilage. 2012;3(2):128-140. doi: 10.1177/1947603511429698.
134. Martin JA, Buckwalter JA. Telomere erosion and senescence in human articular cartilage chondrocytes. Journals Gerontol - Ser A Biol Sci Med Sci. 2001;56(4):172-179. doi: 10.1093/gerona/56.4.B172. PubMed PMID: 11283188.
135. Olson SA, Furman BD, Kraus VB, Huebner JL, Guilak F. Therapeutic opportunities to prevent post-traumatic arthritis: Lessons from the natural history of arthritis after articular fracture. J Orthop Res. 2015;33(9):1266-1277. doi: 10.1002/jor.22940. PubMed PMID: 25939531.

136. Caldwell KL, Wang J. Cell-based articular cartilage repair: the link between development and regeneration. Osteoarthr Cartil. 2015;23(3):351-362. doi: 10.1016/j.joca.2014.11.004. PubMed PMID: 25450846.
137. Brittberg M, Gomoll AH, Canseco JA, Far J, Lind M, Hui J. Cartilage repair in the degenerative ageing knee. Acta Orthop. 2016;87(sup363):26-38. doi: 10.1080/17453674.2016.1265877. PubMed PMID: 27910738.
138. Mor A, Grijota M, Nørgaard M, Munthe J, Lind M, Déruaz A, Pedersen AB. Trends in arthroscopy-documented cartilage injuries of the knee and repair procedures among 15-60-year-old patients. Scand J Med Sci Sports. 2015;25(4):e400-7. doi: 10.1111/sms.12330. PubMed PMID: 25262959.
139. Martin JA, Buckwalter JA. Aging, articular cartilage chondrocyte senescence and osteoarthritis. Biogerontology. 2002;3(5):257-264. doi: 10.1023/A:1020185404126. PubMed PMID: 12237562.
140. Chao PH, Roy R, Mauck RL, Liu W, Valhmu WB, Hung CT. Chondrocyte translocation response to direct current electric fields. J Biomech Eng. 2000;122(3):261-267. doi: 10.1115/1.429661. PubMed PMID: 10923294.
141. Chao P-HG, Lu HH, Hung CT, Nicoll SB, Bulinski JC. Effects of applied DC electric field on ligament fibroblast migration and wound healing. Connect Tissue Res. 2007;48(4):188-197. doi: 10.1080/03008200701424451. PubMed PMID: 17653975.
142. Nwachukwu BU, Bozic KJ, Schairer WW, Bernstein JL, Jevsevar DS, Marx RG, Padgett DE. Current status of cost utility analyses in total joint arthroplasty: a systematic review. Clin Orthop Relat Res. 2015;473(5):1815-1827. doi: 10.1007/s11999-014-3964-4. PubMed PMID: 25267271.
143. Curl WW, Krome J, Gordon ES, Rushing J, Smith BP, Poehling GG. Cartilage injuries: a review of 31,516 knee arthroscopies. Arthroscopy. 1997;13(4):456-460. doi: 10.1016/s0749-8063(97)90124-9. PubMed PMID: 9276052.
144. Arøen A, Løken S, Heir S, Alvik E, Ekeland A, Granlund OG, Engebretsen L. Articular cartilage lesions in 993 consecutive knee arthroscopies. Am J Sports Med. 2004;32(1):211-215. doi: 10.1177/0363546503259345. PubMed PMID: 14754746.
145. van der Kraan PM, Blaney Davidson EN, van den Berg WB. A role for age-related changes in TGFbeta signaling in aberrant chondrocyte differentiation and osteoarthritis. Arthritis Res Ther. 2010;12(1):201. doi: 10.1186/ar2896. PubMed PMID: 20156325.
146. van der Kraan PM, Blaney Davidson EN, Blom A, van den Berg WB. TGF-beta signaling in chondrocyte terminal differentiation and osteoarthritis: modulation and integration of signaling pathways through receptor-Smads. Osteoarthr Cartil. 2009;17(12):1539-1545. doi: 10.1016/j.joca.2009.06.008. PubMed PMID: 19583961.
147. O'Connell GD, Tan AR, Cui V, Bulinski JC, Cook JL, Attur M, Abramson SB, Ateshian GA, Hung CT. Human chondrocyte migration behaviour to guide the development of engineered cartilage. J Tissue Eng Regen Med. 2017;11(3):877-886. doi: 10.1002/term.1988. PubMed PMID: 25627968.
148. Barbero A, Martin I. Human articular chondrocytes culture. Methods Mol Med. 2007;140:237-247. doi: 10.1007/978-1-59745-443-8_13. PubMed PMID: 18085212.

149. Heywood HK, Nalesso G, Lee DA, Dell'accio F. Culture expansion in low-glucose conditions preserves chondrocyte differentiation and enhances their subsequent capacity to form cartilage tissue in three-dimensional culture. Biores Open Access. 2014;3(1):9-18. doi: 10.1089/biores.2013.0051. PubMed PMID: 24570841.
150. Coleman RM, Case ND, Guldberg RE. Hydrogel effects on bone marrow stromal cell response to chondrogenic growth factors. Biomaterials. 2007;28(12):2077-2086. doi: 10.1016/j.biomaterials.2007.01.010. PubMed PMID: 17257670.
151. Coleman RM, Schwartz Z, Boyan BD, Guldberg RE. The therapeutic effect of bone marrow-derived stem cell implantation after epiphyseal plate injury is abrogated by chondrogenic predifferentiation. Tissue Eng Part A. 2013;19(3-4):475-483. doi: 10.1089/ten.TEA.2012.0125. PubMed PMID: 22920855.
152. Wu B, Durisin EK, Decker JT, Ural EE, Shea LD, Coleman RM. Phosphate regulates chondrogenesis in a biphasic and maturation-dependent manner. Differentiation. 2017;95:54-62. doi: 10.1016/j.diff.2017.04.002. PubMed PMID: 28511052.
153. Wilfinger WW, Mackey K, Chomczynski P. Effect of pH and ionic strength on the spectrophotometric assessment of nucleic acid purity. Biotechniques. 1997;22(3):474-476, 478-481. doi: 10.2144/97223st01. PubMed PMID: 9067025.
154. Caron MMJ, Emans PJ, Coolsen MME, Voss L, Surtel DAM, Cremers A, van Rhijn LW, Welting TJM. Redifferentiation of dedifferentiated human articular chondrocytes: comparison of 2D and 3D cultures. Osteoarthr Cartil. 2012;20(10):1170-1178. doi: 10.1016/j.joca.2012.06.016.
155. Tew SR, Murdoch AD, Rauchenberg RP, Hardingham TE. Cellular methods in cartilage research: primary human chondrocytes in culture and chondrogenesis in human bone marrow stem cells. Methods. 2008;45(1):2-9. doi: 10.1016/j.ymeth.2008.01.006. PubMed PMID: 18442700.
156. Pei M, He F, Vunjak-Novakovic G. Synovium-derived stem cell-based chondrogenesis. Differentiation. 2008;76(10):1044-1056. doi: 10.1111/j.1432-0436.2008.00299.x. PubMed PMID: 18637024.
157. Sampat SR, O'Connell GD, Fong J V, Alegre-Aguarón E, Ateshian GA, Hung CT. Growth factor priming of synovium-derived stem cells for cartilage tissue engineering. Tissue Eng Part A. 2011;17(17-18):2259-2265. doi: 10.1089/ten.TEA.2011.0155. PubMed PMID: 21542714.
158. Cao C, Zhang Y, Ye Y, Sun T. Effects of cell phenotype and seeding density on the chondrogenic capacity of human osteoarthritic chondrocytes in type i collagen scaffolds. J Orthop Surg Res. 2020;15(1):1-11. doi: 10.1186/s13018-020-01617-6. PubMed PMID: 32228637.
159. Ono Y, Sakai T, Hiraiwa H, Hamada T, Omachi T, Nakashima M, Ishizuka S, Matsukawa T, Knudson W, Knudson CB, Ishiguro N. Chondrogenic capacity and alterations in hyaluronan synthesis of cultured human osteoarthritic chondrocytes. Biochem Biophys Res Commun. 2013;435(4):733-739. doi: 10.1016/j.bbrc.2013.05.052. PubMed PMID: 23702485.
160. Orfanidou T, Iliopoulos D, Malizos KN, Tsezou A. Involvement of SOX-9 and FGF-23 in RUNX-2 regulation in osteoarthritic chondrocytes. J Cell Mol Med. 2009;13(9 B):3186-3194. doi: 10.1111/j.1582-4934.2009.00678.x. PubMed PMID: 20196777.
161. Liu H, Zhao Z, Clarke RB, Gao J, Garrett IR, Margerrison EEC. Enhanced tissue

regeneration potential of juvenile articular cartilage. Am J Sports Med. 2013;41(11):2658-2667. doi: 10.1177/0363546513502945. PubMed PMID: 24043472.
162. Xu J, Wang W, Ludeman M, Cheng K, Hayami T, Lotz JC, Kapila S. Chondrogenic differentiation of human mesenchymal stem cells in three-dimensional alginate gels. Tissue Eng Part A. 2008;14(5):667-680. doi: 10.1089/tea.2007.0272. PubMed PMID: 18377198.
163. Kamekura S, Hoshi K, Shimoaka T, Chung U, Chikuda H, Yamada T, Uchida M, Ogata N, Seichi A, Nakamura K, Kawaguchi H. Osteoarthritis development in novel experimental mouse models induced by knee joint instability. Osteoarthr Cartil. 2005;13(7):632-641. doi: 10.1016/j.joca.2005.03.004. PubMed PMID: 15896985.
164. Kamekura S, Kawasaki Y, Hoshi K, Shimoaka T, Chikuda H, Maruyama Z, Komori T, Sato S, Takeda S, Karsenty G, Nakamura K, Chung U Il, Kawaguchi H. Contribution of runt-related transcription factor 2 to the pathogenesis of osteoarthritis in mice after induction of knee joint instability. Arthritis Rheum. 2006;54(8):2462-2470. doi: 10.1002/art.22041. PubMed PMID: 16868966.
165. van der Kraan PM. The changing role of TGFβ in healthy, ageing and osteoarthritic joints. Nat Rev Rheumatol. 2017;13(3):155-163. doi: 10.1038/nrrheum.2016.219. PubMed PMID: 28148919.
166. Papathanasiou I, Malizos KN, Tsezou A. Bone morphogenetic protein-2-induced Wnt/β-catenin signaling pathway activation through enhanced low-density-lipoprotein receptor-related protein 5 catabolic activity contributes to hypertrophy in osteoarthritic chondrocytes. Arthritis Res Ther. 2012;14(2):R82. doi: 10.1186/ar3805. PubMed PMID: 22513174.
167. Papathanasiou I, Kostopoulou F, Malizos KN, Tsezou A. DNA methylation regulates sclerostin (SOST) expression in osteoarthritic chondrocytes by bone morphogenetic protein 2 (BMP-2) induced changes in Smads binding affinity to the CpG region of SOST promoter. Arthritis Res Ther. 2015;17(1):160. doi: 10.1186/s13075-015-0674-6. PubMed PMID: 26071314.
168. Dehne T, Karlsson C, Ringe J, Sittinger M, Lindahl A. Chondrogenic differentiation potential of osteoarthritic chondrocytes and their possible use in matrix-associated autologous chondrocyte transplantation. Arthritis Res Ther. 2009;11(5):1-14. doi: 10.1186/ar2800. PubMed PMID: 19723327.
169. Praemer A, Furner S RD. Musculoskeletal Conditions in the United States. Am Acad Orthop Surg. 1999.
170. Buckwalter JA, Martin J, Mankin HJ. Synovial joint degeneration and the syndrome of osteoarthritis. Instr Course Lect. 2000;49:481-489. PubMed PMID: 10829201.
171. Buckwalter JA, Stanish WD, Rosier RN, Schenck RC DD and CR. The increasing need for nonoperative treatment of osteoarthritis. Clin Ortho Rel Res. 2001;385:36-45.
172. Mazor M, Lespessailles E, Best TM, Ali M, Toumi H. Gene Expression and Chondrogenic Potential of Cartilage Cells: Osteoarthritis Grade Differences. Int J Mol Sci. 2022;23(18):1-15. doi: 10.3390/ijms231810610. PubMed PMID: 36142513.
173. Schrobback K, Klein TJ, Schuetz M, Upton Z, Leavesley DI, Malda J. Adult human articular chondrocytes in a microcarrier-based culture system: expansion and

redifferentiation. J Orthop Res. 2011;29(4):539-546. doi: 10.1002/jor.21264. PubMed PMID: 20957734.
174. Kafienah W, Jakob M, Démarteau O, Frazer A, Barker MD, Martin I, Hollander AP. Three-dimensional tissue engineering of hyaline cartilage: comparison of adult nasal and articular chondrocytes. Tissue Eng. 2002;8(5):817-826. doi: 10.1089/10763270260424178. PubMed PMID: 12459060.
175. Katopodi T, Tew SR, Clegg PD, Hardingham TE. The influence of donor and hypoxic conditions on the assembly of cartilage matrix by osteoarthritic human articular chondrocytes on Hyalograft matrices. Biomaterials. 2009;30(4):535-540. doi: 10.1016/j.biomaterials.2008.09.064. PubMed PMID: 18990440.
176. Martin JA, Buckwalter JA. Aging, articular cartilage chondrocyte senescence and osteoarthritis. Biogerontology. 2002;3(5):257-264. doi: 10.1023/a:1020185404126. PubMed PMID: 12237562.
177. Mobasheri A, Matta C, Zákány R, Musumeci G. Chondrosenescence: Definition, hallmarks and potential role in the pathogenesis of osteoarthritis. Maturitas. 2015;80(3):237-244. doi: 10.1016/j.maturitas.2014.12.003. PubMed PMID: 25637957.
178. Riegger J, Brenner RE. Pathomechanisms of posttraumatic osteoarthritis: Chondrocyte behavior and fate in a precarious environment. Int J Mol Sci. 2020;21(5). doi: 10.3390/ijms21051560. PubMed PMID: 32106481.
179. Kilbey A, Blyth K, Wotton S, Terry A, Jenkins A, Bell M, Hanlon L, Cameron ER, Neil JC. Runx2 disruption promotes immortalization and confers resistance to oncogene-induced senescence in primary murine fibroblasts. Cancer Res. 2007;67(23):11263-11271. doi: 10.1158/0008-5472.CAN-07-3016. PubMed PMID: 18056452.
180. Guilak F, Pferdehirt L, Ross AK, Choi Y-R, Collins K, Nims RJ, Katz DB, Klimak M, Tabbaa S, Pham CTN. Designer Stem Cells: Genome Engineering and the Next Generation of Cell-Based Therapies. J Orthop Res. 2019;37(6):1287-1293. doi: 10.1002/jor.24304. PubMed PMID: 30977548.
181. Meerbrey KL, Hu G, Kessler JD, et al. The pINDUCER lentiviral toolkit for inducible RNA interference in vitro and in vivo. Proc Natl Acad Sci U S A. 2011;108(9):3665-3670. doi: 10.1073/pnas.1019736108. PubMed PMID: 21307310.
182. Hsieh-Bonassera ND, Wu I, Lin JK, Schumacher BL, Chen AC, Masuda K, Bugbee WD, Sah RL. Expansion and redifferentiation of chondrocytes from osteoarthritic cartilage: cells for human cartilage tissue engineering. Tissue Eng Part A. 2009;15(11):3513-3523. doi: 10.1089/ten.TEA.2008.0628. PubMed PMID: 19456239.
183. Stoop R, Albrecht D, Gaissmaier C, Fritz J, Felka T, Rudert M, Aicher WK. Comparison of marker gene expression in chondrocytes from patients receiving autologous chondrocyte transplantation versus osteoarthritis patients. Arthritis Res Ther. 2007;9(3):R60. doi: 10.1186/ar2218. PubMed PMID: 17596264.
184. Catheline SE, Hoak D, Chang M, Ketz JP, Hilton MJ, Zuscik MJ, Jonason JH. Chondrocyte-Specific RUNX2 Overexpression Accelerates Post-traumatic Osteoarthritis Progression in Adult Mice. J Bone Miner Res. 2019;34(9):1676-1689. doi: 10.1002/jbmr.3737. PubMed PMID: 31189030.
185. Takeda S, Bonnamy JP, Owen MJ, Ducy P, Karsenty G. Continuous expression of

Cbfa1 in nonhypertrophic chondrocytes uncovers its ability to induce hypertrophic chondrocyte differentiation and partially rescues Cbfa1-deficient mice. Genes Dev. 2001;15(4):467-481. doi: 10.1101/gad.845101. PubMed PMID: 11230154.
186. Ito Y, Miyazono K. RUNX transcription factors as key targets of TGF-β superfamily signaling. Curr Opin Genet Dev. 2003;13(1):43-47. doi: 10.1016/S0959-437X(03)00007-8.
187. van Caam A, Madej W, Garcia de Vinuesa A, Goumans M-J, Ten Dijke P, Blaney Davidson E, van der Kraan P. TGFβ1-induced SMAD2/3 and SMAD1/5 phosphorylation are both ALK5-kinase-dependent in primary chondrocytes and mediated by TAK1 kinase activity. Arthritis Res Ther. 2017;19(1):112. doi: 10.1186/s13075-017-1302-4. PubMed PMID: 28569204.
188. Wu M, Chen G, Li Y-P. TGF-β and BMP signaling in osteoblast, skeletal development, and bone formation, homeostasis and disease. Bone Res. 2016;4(1):16009. doi: 10.1038/boneres.2016.9.
189. Farahat MN, Yanni G, Poston R, Panayi GS. Cytokine expression in synovial membranes of patients with rheumatoid arthritis and osteoarthritis. Ann Rheum Dis. 1993;52(12):870-875. doi: 10.1136/ard.52.12.870. PubMed PMID: 8311538.
190. Smith MD, Triantafillou S, Parker A, Youssef PP, Coleman M. Synovial membrane inflammation and cytokine production in patients with early osteoarthritis. J Rheumatol. 1997;24(2):365-371. PubMed PMID: 9034998.
191. Fahy N, de Vries-van Melle ML, Lehmann J, Wei W, Grotenhuis N, Farrell E, van der Kraan PM, Murphy JM, Bastiaansen-Jenniskens YM, van Osch GJVM. Human osteoarthritic synovium impacts chondrogenic differentiation of mesenchymal stem cells via macrophage polarisation state. Osteoarthr Cartil. 2014;22(8):1167-1175. doi: 10.1016/j.joca.2014.05.021. PubMed PMID: 24911520.
192. Vincenti MP, Brinckerhoff CE. Transcriptional regulation of collagenase (MMP-1, MMP-13) genes in arthritis: integration of complex signaling pathways for the recruitment of gene-specific transcription factors. Arthritis Res. 2002;4(3):157-164. doi: 10.1186/ar401. PubMed PMID: 12010565.
193. Takada S, Nakamura E, Sabanai K, Tsukamoto M, Otomo H, Kanoh S, Murai T, Fukuda H, Okada Y, Uchida S, Sakai A. Attenuation of Post-Traumatic Osteoarthritis After Anterior Cruciate Ligament Injury Via Inhibition of Hedgehog Signaling. J Orthop Res. 2020;38(3):609-619. doi: 10.1002/jor.24494. PubMed PMID: 31608494.
194. Takahata Y, Nakamura E, Hata K, Wakabayashi M, Murakami T, Wakamori K, Yoshikawa H, Matsuda A, Fukui N, Nishimura R. Sox4 is involved in osteoarthritic cartilage deterioration through induction of ADAMTS4 and ADAMTS5. FASEB J. 2019;33(1):619-630. doi: 10.1096/fj.201800259R. PubMed PMID: 30016600.
195. Hashimoto K, Otero M, Imagawa K, de Andrés MC, Coico JM, Roach HI, Oreffo ROC, Marcu KB, Goldring MB. Regulated transcription of human matrix metalloproteinase 13 (MMP13) and interleukin-1β (IL1B) genes in chondrocytes depends on methylation of specific proximal promoter CpG sites. J Biol Chem. 2013;288(14):10061-10072. doi: 10.1074/jbc.M112.421156. PubMed PMID: 23417678.
196. Oliviero A, Della Porta G, Peretti GM, Maffulli N. MicroRNA in osteoarthritis: physiopathology, diagnosis and therapeutic challenge. Br Med Bull.

2019;130(1):137-147. doi: 10.1093/bmb/ldz015. PubMed PMID: 31066454.
197. Zheng L, Zhang Z, Sheng P, Mobasheri A. The role of metabolism in chondrocyte dysfunction and the progression of osteoarthritis. Ageing Res Rev. 2021;66. doi: 10.1016/j.arr.2020.101249. PubMed PMID: 33383189.
198. Martin JA, Buckwalter JA. *Telomere Erosion and Senescence in Human Articular Cartilage Chondrocytes*. Vol 56.; 2001.
199. Dai SM, Shan ZZ, Nakamura H, Masuko-Hongo K, Kato T, Nishioka K, Yudoh K. Catabolic stress induces features of chondrocyte senescence through overexpression of caveolin 1: Possible involvement of caveolin 1-induced down-regulation of articular chondrocytes in the pathogenesis of osteoarthritis. Arthritis Rheum. 2006;54(3):818-831. doi: 10.1002/art.21639.
200. Philipot D, Guérit D, Platano D, Chuchana P, Olivotto E, Espinoza F, Dorandeu A, Pers Y-M, Piette J, Borzi R, Jorgensen C, Noel D, Brondello J-M. p16INK4a and its regulator miR-24 link senescence and chondrocyte terminal differentiation-associated matrix remodeling in osteoarthritis. Arthritis Res Ther. 2014;16(1):R58. doi: 10.1186/ar4494. PubMed PMID: 24572376.
201. Lou C, Deng A, Zheng H, Sun G, Zhao H, Li A, Liu Q, Li Y, Lv Z. Pinitol suppresses TNF-α-induced chondrocyte senescence. Cytokine. 2020;130:155047. doi: 10.1016/j.cyto.2020.155047.
202. Hong E-H, Lee S-J, Kim J-S, Lee K-H, Um H-D, Kim J-H, Kim S-J, Kim J-I, Hwang S-G. Ionizing Radiation Induces Cellular Senescence of Articular Chondrocytes via Negative Regulation of SIRT1 by p38 Kinase. J Biol Chem. 2010;285(2):1283-1295. doi: 10.1074/jbc.M109.058628.
203. Kim D, Langmead B, Salzberg SL. HISAT: a fast spliced aligner with low memory requirements. Nat Methods. 2015;12(4):357-360. doi: 10.1038/nmeth.3317.
204. Pertea M, Pertea GM, Antonescu CM, Chang T-C, Mendell JT, Salzberg SL. StringTie enables improved reconstruction of a transcriptome from RNA-seq reads. Nat Biotechnol. 2015;33(3):290-295. doi: 10.1038/nbt.3122.
205. Marini F, Binder H. pcaExplorer: an R/Bioconductor package for interacting with RNA-seq principal components. BMC Bioinformatics. 2019;20(1):331. doi: 10.1186/s12859-019-2879-1.
206. Love MI, Huber W, Anders S. Moderated estimation of fold change and dispersion for RNA-seq data with DESeq2. Genome Biol. 2014;15(12):550. doi: 10.1186/s13059-014-0550-8.
207. Thomas PD, Campbell MJ, Kejariwal A, Mi H, Karlak B, Daverman R, Diemer K, Muruganujan A, Narechania A. PANTHER: a library of protein families and subfamilies indexed by function. Genome Res. 2003;13(9):2129-2141. doi: 10.1101/gr.772403. PubMed PMID: 12952881.
208. Thomas PD, Kejariwal A, Guo N, Mi H, Campbell MJ, Muruganujan A, Lazareva-Ulitsky B. Applications for protein sequence-function evolution data: mRNA/protein expression analysis and coding SNP scoring tools. Nucleic Acids Res. 2006;34(Web Server issue):W645-50. doi: 10.1093/nar/gkl229. PubMed PMID: 16912992.
209. Ilic MZ, Handley CJ, Robinson HC, Mok MT. Mechanism of catabolism of aggrecan by articular cartilage. Arch Biochem Biophys. 1992;294(1):115-122. doi: 10.1016/0003-9861(92)90144-l. PubMed PMID: 1550337.

210. Pospelova T V, Demidenko ZN, Bukreeva EI, Pospelov VA, Gudkov A V, Blagosklonny M V. Pseudo-DNA damage response in senescent cells. Cell Cycle. 2009;8(24):4112-4118. doi: 10.4161/cc.8.24.10215. PubMed PMID: 19946210.
211. Paull TT, Rogakou EP, Yamazaki V, Kirchgessner CU, Gellert M, Bonner WM. A critical role for histone H2AX in recruitment of repair factors to nuclear foci after DNA damage. Curr Biol. 10(15):886-895. doi: 10.1016/s0960-9822(00)00610-2. PubMed PMID: 10959836.
212. Sulli G, Di Micco R, d'Adda di Fagagna F. Crosstalk between chromatin state and DNA damage response in cellular senescence and cancer. Nat Rev Cancer. 2012;12(10):709-720. doi: 10.1038/nrc3344. PubMed PMID: 22952011.
213. Knook DL, Sleyster EC, van Noord MJ. Changes in lysosomes during ageing of parenchymal and nonparenchymal liver cells. Adv Exp Med Biol. 1975;53:155-169. doi: 10.1007/978-1-4757-0731-1_12. PubMed PMID: 235190.
214. Gerland L-M, Peyrol S, Lallemand C, Branche R, Magaud J-P, Ffrench M. Association of increased autophagic inclusions labeled for beta-galactosidase with fibroblastic aging. Exp Gerontol. 2003;38(8):887-895. doi: 10.1016/s0531-5565(03)00132-3. PubMed PMID: 12915210.
215. Bosmann HB, Guthell RL, Case KR. Loss of a critical neutral protease in ageing WI-38 cells. Nature. 1976;261(5560):499-501. doi: 10.1038/261499a0. PubMed PMID: 934284.
216. Cristofalo VJ, Kabakjian J. Lysosomal enzymes and aging in vitro: subcellular enzyme distribution and effect of hydrocortisone on cell life-span. Mech Ageing Dev. 1975;4(1):19-28. doi: 10.1016/0047-6374(75)90004-4. PubMed PMID: 1142849.
217. Brunk U, Ericsson JL, Ponten J, Westermark B. Residual bodies and "aging" in cultured human glia cells. Effect of entrance into phase 3 and prolonged periods of confluence. Exp Cell Res. 1973;79(1):1-14. PubMed PMID: 4591931.
218. Sánchez-Martín MM, Cabezas JA. Evaluation of the activities of eight lysosomal hydrolases in sera of humans, rats and pigs of different ages. Mech Ageing Dev. 1997;99(2):95-107. doi: 10.1016/s0047-6374(97)00093-6. PubMed PMID: 9483485.
219. Lee BY, Han JA, Im JS, Morrone A, Johung K, Goodwin EC, Kleijer WJ, DiMaio D, Hwang ES. Senescence-associated beta-galactosidase is lysosomal beta-galactosidase. Aging Cell. 2006;5(2):187-195. doi: 10.1111/j.1474-9726.2006.00199.x. PubMed PMID: 16626397.
220. Catterall JB, Stabler T V, Flannery CR, Kraus VB. Changes in serum and synovial fluid biomarkers after acute injury (NCT00332254). Arthritis Res Ther. 2010;12(6):R229. doi: 10.1186/ar3216. PubMed PMID: 21194441.
221. Kokebie R, Aggarwal R, Lidder S, Hakimiyan AA, Rueger DC, Block JA, Chubinskaya S. The role of synovial fluid markers of catabolism and anabolism in osteoarthritis, rheumatoid arthritis and asymptomatic organ donors. Arthritis Res Ther. 2011;13(2):R50. doi: 10.1186/ar3293. PubMed PMID: 21435227.
222. Westacott CI, Whicher JT, Barnes IC, Thompson D, Swan AJ, Dieppe PA. Synovial fluid concentration of five different cytokines in rheumatic diseases. Ann Rheum Dis. 1990;49(9). doi: 10.1136/ard.49.9.676.
223. Bigoni M, Sacerdote P, Turati M, Franchi S, Gandolla M, Gaddi D, Moretti S,

Munegato D, Augusti CA, Bresciani E, Omeljaniuk RJ, Locatelli V, Torsello A. Acute and late changes in intraarticular cytokine levels following anterior cruciate ligament injury. J Orthop Res. 2013;31(2):315-321. doi: 10.1002/jor.22208. PubMed PMID: 22886741.

224. Kahle P, Saal JG, Schaudt K, Zacher J, Fritz P, Pawelec G. Determination of cytokines in synovial fluids: correlation with diagnosis and histomorphological characteristics of synovial tissue. Ann Rheum Dis. 1992;51(6):731-734. doi: 10.1136/ard.51.6.731. PubMed PMID: 1616355.
225. Li L, Li Z, Li Y, Hu X, Zhang Y, Fan P. Profiling of inflammatory mediators in the synovial fluid related to pain in knee osteoarthritis. BMC Musculoskelet Disord. 2020;21(1):99. doi: 10.1186/s12891-020-3120-0. PubMed PMID: 32059658.
226. Santos Savio A, Machado Diaz AC, Chico Capote A, Miranda Navarro J, Rodríguez Alvarez Y, Bringas Pérez R, Estévez del Toro M, Guillen Nieto GE. Differential expression of pro-inflammatory cytokines IL-15Ralpha, IL-15, IL-6 and TNFalpha in synovial fluid from rheumatoid arthritis patients. BMC Musculoskelet Disord. 2015;16:51. doi: 10.1186/s12891-015-0516-3. PubMed PMID: 25879761.
227. Leung YY, Huebner JL, Haaland B, Wong SBS, Kraus VB. Synovial fluid pro-inflammatory profile differs according to the characteristics of knee pain. Osteoarthr Cartil. 2017;25(9):1420-1427. doi: 10.1016/j.joca.2017.04.001. PubMed PMID: 28433814.
228. McCulloch K, Litherland GJ, Rai TS. Cellular senescence in osteoarthritis pathology. Aging Cell. 2017;16(2):210-218. doi: 10.1111/acel.12562. PubMed PMID: 28124466.
229. Coryell PR, Diekman BO, Loeser RF. Mechanisms and therapeutic implications of cellular senescence in osteoarthritis. Nat Rev Rheumatol. 2021;17(1):47-57. doi: 10.1038/s41584-020-00533-7. PubMed PMID: 33208917.
230. Hayflick L, Moorhead PS. The serial cultivation of human diploid cell strains. Exp Cell Res. 1961;25(3). doi: 10.1016/0014-4827(61)90192-6.
231. Blanco FJ, Geng Y, Lotz M. Differentiation-dependent effects of IL-1 and TGF-beta on human articular chondrocyte proliferation are related to inducible nitric oxide synthase expression. J Immunol. 1995;154(8):4018-4026. PubMed PMID: 7535818.
232. Chin JE, Lin YA. Effects of recombinant human interleukin-1 beta on rabbit articular chondrocytes. Stimulation of prostanoid release and inhibition of cell growth. Arthritis Rheum. 1988;31(10):1290-1296. doi: 10.1002/art.1780311011. PubMed PMID: 3263134.
233. Guerne PA, Sublet A, Lotz M. Growth factor responsiveness of human articular chondrocytes: distinct profiles in primary chondrocytes, subcultured chondrocytes, and fibroblasts. J Cell Physiol. 1994;158(3):476-484. doi: 10.1002/jcp.1041580312. PubMed PMID: 8126071.
234. Kumkumian GK, Lafyatis R, Remmers EF, Case JP, Kim SJ, Wilder RL. Platelet-derived growth factor and IL-1 interactions in rheumatoid arthritis. Regulation of synoviocyte proliferation, prostaglandin production, and collagenase transcription. J Immunol. 1989;143(3):833-837. PubMed PMID: 2545778.
235. Ashraf S, Cha B-H, Kim J-S, Ahn J, Han I, Park H, Lee S-H. Regulation of senescence associated signaling mechanisms in chondrocytes for cartilage tissue

regeneration. Osteoarthr Cartil. 2016;24(2):196-205. doi: 10.1016/j.joca.2015.07.008. PubMed PMID: 26190795.
236. Zhao X, Huang P, Li G, Feng Y, Zhendong L, Zhou C, Hu G, Xu Q. Overexpression of Pitx1 attenuates the senescence of chondrocytes from osteoarthritis degeneration cartilage-A self-controlled model for studying the etiology and treatment of osteoarthritis. Bone. 2020;131:115177. doi: 10.1016/j.bone.2019.115177. PubMed PMID: 31783149.
237. Sharpless NE, Sherr CJ. Forging a signature of in vivo senescence. Nat Rev Cancer. 2015;15(7):397-408. doi: 10.1038/nrc3960. PubMed PMID: 26105537.
238. Blackburn EH. Structure and function of telomeres. Nature. 1991;350(6319):569-573. doi: 10.1038/350569a0. PubMed PMID: 1708110.
239. Allsopp RC, Chang E, Kashefi-Aazam M, Rogaev EI, Piatyszek MA, Shay JW, Harley CB. Telomere shortening is associated with cell division in vitro and in vivo. Exp Cell Res. 1995;220(1):194-200. doi: 10.1006/excr.1995.1306. PubMed PMID: 7664836.
240. Levy MZ, Allsopp RC, Futcher AB, Greider CW, Harley CB. Telomere end-replication problem and cell aging. J Mol Biol. 1992;225(4):951-960. doi: 10.1016/0022-2836(92)90096-3. PubMed PMID: 1613801.
241. Allsopp RC, Harley CB. Evidence for a critical telomere length in senescent human fibroblasts. Exp Cell Res. 1995;219(1):130-136. doi: 10.1006/excr.1995.1213. PubMed PMID: 7628529.
242. Allsopp RC, Vaziri H, Patterson C, Goldstein S, Younglai E V, Futcher AB, Greider CW, Harley CB. Telomere length predicts replicative capacity of human fibroblasts. Proc Natl Acad Sci U S A. 1992;89(21):10114-10118. doi: 10.1073/pnas.89.21.10114. PubMed PMID: 1438199.
243. Kim HJ, Park SR, Park HJ, Choi BH, Min B-H. Potential predictive markers for proliferative capacity of cultured human articular chondrocytes: PCNA and p21. Artif Organs. 2005;29(5):393-398. doi: 10.1111/j.1525-1594.2005.29066.x. PubMed PMID: 15854215.
244. Jeon OH, Kim C, Laberge RM, Demaria M, Rathod S, Vasserot AP, Chung JW, Kim DH, Poon Y, David N, Baker DJ, Van Deursen JM, Campisi J, Elisseeff JH. Local clearance of senescent cells attenuates the development of post-traumatic osteoarthritis and creates a pro-regenerative environment. Nat Med. 2017. doi: 10.1038/nm.4324. PubMed PMID: 28436958.
245. Diekman BO, Sessions GA, Collins JA, Knecht AK, Strum SL, Mitin NK, Carlson CS, Loeser RF, Sharpless NE. Expression of p16INK4a is a biomarker of chondrocyte aging but does not cause osteoarthritis. Aging Cell. 2018;17(4):e12771. doi: 10.1111/acel.12771. PubMed PMID: 29744983.
246. Baker DJ, Childs BG, Durik M, Wijers ME, Sieben CJ, Zhong J, Saltness RA, Jeganathan KB, Verzosa GC, Pezeshki A, Khazaie K, Miller JD, van Deursen JM. Naturally occurring p16(Ink4a)-positive cells shorten healthy lifespan. Nature. 2016;530(7589):184-189. doi: 10.1038/nature16932. PubMed PMID: 26840489.
247. Rowland CR, Glass KA, Ettyreddy AR, Gloss CC, Matthews JRL, Huynh NPT, Guilak F. Regulation of decellularized tissue remodeling via scaffold-mediated lentiviral delivery in anatomically-shaped osteochondral constructs. Biomaterials. 2018;177:161-175. doi: 10.1016/j.biomaterials.2018.04.049. PubMed PMID:

29894913.
248. Ross AK, Coutinho de Almeida R, Ramos YFM, Li J, Meulenbelt I, Guilak F. The miRNA-mRNA interactome of murine induced pluripotent stem cell-derived chondrocytes in response to inflammatory cytokines. FASEB J. 2020;34(9):11546-11561. doi: 10.1096/fj.202000889R. PubMed PMID: 32767602.
249. Ji Q, Xu X, Zhang Q, Kang L, Xu Y, Zhang K, Li L, Liang Y, Hong T, Ye Q, Wang Y. The IL-1β/AP-1/miR-30a/ADAMTS-5 axis regulates cartilage matrix degradation in human osteoarthritis. J Mol Med (Berl). 2016;94(7):771-785. doi: 10.1007/s00109-016-1418-z. PubMed PMID: 27067395.
250. Tang J, Cui W, Song F, Zhai C, Hu H, Zuo Q, Fan W. Effects of mesenchymal stem cells on interleukin-1β-treated chondrocytes and cartilage in a rat osteoarthritic model. Mol Med Rep. 2015;12(2):1753-1760. doi: 10.3892/mmr.2015.3645. PubMed PMID: 25892273.
251. Hunziker EB, Shintani N, Haspl M, Lippuner K, Vögelin E, Keel MJB. The Synovium of Human Osteoarthritic Joints Retains Its Chondrogenic Potential Irrespective of Age. Tissue Eng Part A. 2022;28(5-6):283-295. doi: 10.1089/ten.TEA.2021.0105. PubMed PMID: 34693739.
252. Laganà M, Arrigoni C, Lopa S, Sansone V, Zagra L, Moretti M, Raimondi MT. Characterization of articular chondrocytes isolated from 211 osteoarthritic patients. Cell Tissue Bank. 2014;15(1):59-66. doi: 10.1007/s10561-013-9371-3. PubMed PMID: 23549979.
253. Hung CT, Lima EG, Mauck RL, Taki E, LeRoux MA, Lu HH, Stark RG, Guo XE, Ateshian GA. Anatomically shaped osteochondral constructs for articular cartilage repair. J Biomech. 2003;36(12):1853-1864. doi: 10.1016/S0021-9290(03)00213-6.
254. Perka C, Schultz O, Lindenhayn K, Spitzer RS, Muschik M, Sittinger M, Burmester GR. Joint cartilage repair with transplantation of embryonic chondrocytes embedded in collagen-fibrin matrices. Clin Exp Rheumatol. 2000;18(1):13-22. PubMed PMID: 10728439.
255. Li W-J, Danielson KG, Alexander PG, Tuan RS. Biological response of chondrocytes cultured in three-dimensional nanofibrous poly(epsilon-caprolactone) scaffolds. J Biomed Mater Res A. 2003;67(4):1105-1114. doi: 10.1002/jbm.a.10101. PubMed PMID: 14624495.
256. Hsu S-H, Chang S-H, Yen H-J, Whu SW, Tsai C-L, Chen DC. Evaluation of biodegradable polyesters modified by type II collagen and Arg-Gly-Asp as tissue engineering scaffolding materials for cartilage regeneration. Artif Organs. 2006;30(1):42-55. doi: 10.1111/j.1525-1594.2006.00179.x. PubMed PMID: 16409397.
257. Tare RS, Howard D, Pound JC, Roach HI, Oreffo ROC. Tissue engineering strategies for cartilage generation—Micromass and three dimensional cultures using human chondrocytes and a continuous cell line. Biochem Biophys Res Commun. 2005;333(2):609-621. doi: 10.1016/j.bbrc.2005.05.117.
258. Lovati AB, Colombini A, Recordati C, Ceriani C, Zagra L, Berzero G, Moretti M. Chondrogenic capability of osteoarthritic chondrocytes from the trapeziometacarpal and hip joints. Cell Tissue Bank. 2016;17(1):171-177. doi: 10.1007/s10561-015-9519-4. PubMed PMID: 26150189.
259. Giovannini S, Diaz-Romero J, Aigner T, Heini P, Mainil-Varlet P, Nesic D.

Micromass co-culture of human articular chondrocytes and human bone marrow mesenchymal stem cells to investigate stable neocartilage tissue formation in vitro. Eur Cells Mater. 2010;20:245-259. doi: 10.22203/eCM.v020a20.
260. Mauck RL, Yuan X, Tuan RS. Chondrogenic differentiation and functional maturation of bovine mesenchymal stem cells in long-term agarose culture. Osteoarthr Cartil. 2006;14(2):179-189. doi: 10.1016/j.joca.2005.09.002.
261. Das RHJ, Jahr H, Verhaar JAN, van der Linden JC, van Osch GJVM, Weinans H. In vitro expansion affects the response of chondrocytes to mechanical stimulation. Osteoarthr Cartil. 2008;16(3):385-391. doi: 10.1016/j.joca.2007.07.014.
262. Chang SH, Mori D, Kobayashi H, et al. Excessive mechanical loading promotes osteoarthritis through the gremlin-1-NF-κB pathway. Nat Commun. 2019;10(1):1442. doi: 10.1038/s41467-019-09491-5. PubMed PMID: 30926814.
263. Occhetta P, Mainardi A, Votta E, Vallmajo-Martin Q, Ehrbar M, Martin I, Barbero A, Rasponi M. Hyperphysiological compression of articular cartilage induces an osteoarthritic phenotype in a cartilage-on-a-chip model. Nat Biomed Eng. 2019;3(7):545-557. doi: 10.1038/s41551-019-0406-3. PubMed PMID: 31160722.
264. Fickert S, Fiedler J, Brenner RE. Identification of subpopulations with characteristics of mesenchymal progenitor cells from human osteoarthritic cartilage using triple staining for cell surface markers. Arthritis Res Ther. 2004;6(5):R422-32. doi: 10.1186/ar1210. PubMed PMID: 15380042.
265. Vinod E, Kachroo U, Rebekah G, Yadav BK, Ramasamy B. Characterization of human articular chondrocytes and chondroprogenitors derived from non-diseased and osteoarthritic knee joints to assess superiority for cell-based therapy. Acta Histochem. 2020;122(6):151588. doi: 10.1016/j.acthis.2020.151588. PubMed PMID: 32778244.
266. Zhang K, Shi J, Li Y, Jiang Y, Tao T, Li W, Gui J. Chondrogenic cells respond to partial-thickness defects of articular cartilage in adult rats: an in vivo study. J Mol Histol. 2016;47(3):249-258. doi: 10.1007/s10735-016-9668-1. PubMed PMID: 26956364.
267. Tao T, Li Y, Gui C, Ma Y, Ge Y, Dai H, Zhang K, Du J, Guo Y, Jiang Y, Gui J. Fibronectin Enhances Cartilage Repair by Activating Progenitor Cells Through Integrin α5β1 Receptor. Tissue Eng Part A. 2018;24(13-14):1112-1124. doi: 10.1089/ten.TEA.2017.0322. PubMed PMID: 29343182.
268. Walsh SK, Schneider SE, Amundson LA, Neu CP, Henak CR. Maturity-dependent cartilage cell plasticity and sensitivity to external perturbation. J Mech Behav Biomed Mater. 2020;106:103732. doi: 10.1016/j.jmbbm.2020.103732. PubMed PMID: 32321631.
269. Su X, Zuo W, Wu Z, Chen J, Wu N, Ma P, Xia Z, Jiang C, Ye Z, Liu S, Liu J, Zhou G, Wan C, Qiu G. CD146 as a new marker for an increased chondroprogenitor cell sub-population in the later stages of osteoarthritis. J Orthop Res. 2015;33(1):84-91. doi: 10.1002/jor.22731. PubMed PMID: 25266708.
270. Grogan SP, Miyaki S, Asahara H, D'Lima DD, Lotz MK. Mesenchymal progenitor cell markers in human articular cartilage: normal distribution and changes in osteoarthritis. Arthritis Res Ther. 2009;11(3):R85. doi: 10.1186/ar2719. PubMed PMID: 19500336.